



# Options and Limitations in Clinical Investigation of Bacterial Biofilms

Maria Magana,<sup>a</sup> Christina Sereti,<sup>a,b</sup> Anastasios Ioannidis,<sup>a,c</sup> Courtney A. Mitchell,<sup>d</sup> Anthony R. Ball,<sup>e,f</sup> Emmanouil Magiorkinis,<sup>g</sup> Stylianos Chatzipanagiotou,<sup>a</sup>  Michael R. Hamblin,<sup>h,i,j</sup> Maria Hadjifrangiskou,<sup>k</sup> George P. Tegos<sup>e,f</sup>

<sup>a</sup>Department of Clinical Microbiology, Athens Medical School, Aeginition Hospital, Athens, Greece

<sup>b</sup>Department of Microbiology, Thriassio General Hospital, Attiki, Greece

<sup>c</sup>Department of Nursing, Faculty of Human Movement and Quality of Life Sciences, University of Peloponnese, Sparta, Greece

<sup>d</sup>Department of Chemical and Biomolecular Engineering, Vanderbilt University, Nashville, Tennessee, USA

<sup>e</sup>Gliese 623b, Mendon, Massachusetts, USA

<sup>f</sup>GAMA Therapeutics LLC, Pepperell, Massachusetts, USA

<sup>g</sup>Department of Hygiene, Epidemiology and Medical Statistics, Medical School, University of Athens, Athens-Goudi, Greece

<sup>h</sup>Harvard-MIT Division of Health Science and Technology, Cambridge, Massachusetts, USA

<sup>i</sup>Department of Dermatology, Harvard Medical School, Boston, Massachusetts, USA

<sup>j</sup>Wellman Center for Photomedicine, Massachusetts General Hospital, Boston, Massachusetts, USA

<sup>k</sup>Department of Pathology, Microbiology and Immunology, Vanderbilt University Medical Center, Nashville, Tennessee, USA

<b>SUMMARY</b> .....	<b>1</b>
<b>INTRODUCTION</b> .....	<b>2</b>
<b>MULTIDIMENSIONAL ARCHITECTURE OF BIOFILMS</b> .....	<b>3</b>
Surface-Associated Biofilms and Importance of the Substratum .....	<b>3</b>
Submerged Biofilms .....	<b>4</b>
Roots of Biofilm Phenotypic Resistance .....	<b>5</b>
<b>LABORATORY SETUPS</b> .....	<b>6</b>
Culturing Biofilms under Static Conditions .....	<b>6</b>
Culturing Biofilms under Flow Conditions .....	<b>8</b>
<b>QUANTITATION AND VIABILITY ASSAYS</b> .....	<b>11</b>
<b>“GRIND AND FIND” APPROACH VIA MOLECULAR ANALYSIS</b> .....	<b>17</b>
<b>IMAGING MODALITIES TO VISUALIZE COMMUNITY ARCHITECTURE</b> .....	<b>20</b>
Optical Microscopy .....	<b>20</b>
Electron and X-Ray Microscopy .....	<b>21</b>
Scanning Probe Microscopy and Imaging Mass Spectrometry .....	<b>21</b>
<b>MODELING BIOFILMS EX VIVO</b> .....	<b>22</b>
<b>DISSECTING BIOFILMS IN VIVO</b> .....	<b>23</b>
Nonvertebrate Animal Models .....	<b>23</b>
Vertebrate Animal Models .....	<b>26</b>
<b>IN VIVO IMAGING TOOLS</b> .....	<b>28</b>
<b>SHAPING UP THE METHODOLOGICAL PIPELINE</b> .....	<b>29</b>
Literature Search on Method Implementation .....	<b>29</b>
State-of-the-Art Methodologies in Biofilm Investigation .....	<b>31</b>
Extending beyond Commonplace Platforms .....	<b>32</b>
<b>CONCLUDING REMARKS</b> .....	<b>33</b>
<b>ACKNOWLEDGMENTS</b> .....	<b>34</b>
<b>REFERENCES</b> .....	<b>34</b>
<b>AUTHOR BIOS</b> .....	<b>48</b>

Published 4 April 2018

**Citation** Magana M, Sereti C, Ioannidis A, Mitchell CA, Ball AR, Magiorkinis E, Chatzipanagiotou S, Hamblin MR, Hadjifrangiskou M, Tegos GP. 2018. Options and limitations in clinical investigation of bacterial biofilms. *Clin Microbiol Rev* 31:e00084-16. <https://doi.org/10.1128/CMR.00084-16>.

**Copyright** © 2018 American Society for Microbiology. All Rights Reserved.

Address correspondence to George P. Tegos, [gtegos@gmail.com](mailto:gtegos@gmail.com).

M.M. and C.S. contributed equally to this article.

**SUMMARY** Bacteria can form single- and multispecies biofilms exhibiting diverse features based upon the microbial composition of their community and microenvironment. The study of bacterial biofilm development has received great interest in the past 20 years and is motivated by the elegant complexity characteristic of these

multicellular communities and their role in infectious diseases. Biofilms can thrive on virtually any surface and can be beneficial or detrimental based upon the community's interplay and the surface. Advances in the understanding of structural and functional variations and the roles that biofilms play in disease and host-pathogen interactions have been addressed through comprehensive literature searches. In this review article, a synopsis of the methodological landscape of biofilm analysis is provided, including an evaluation of the current trends in methodological research. We deem this worthwhile because a keyword-oriented bibliographical search reveals that less than 5% of the biofilm literature is devoted to methodology. In this report, we (i) summarize current methodologies for biofilm characterization, monitoring, and quantification; (ii) discuss advances in the discovery of effective imaging and sensing tools and modalities; (iii) provide an overview of tailored animal models that assess features of biofilm infections; and (iv) make recommendations defining the most appropriate methodological tools for clinical settings.

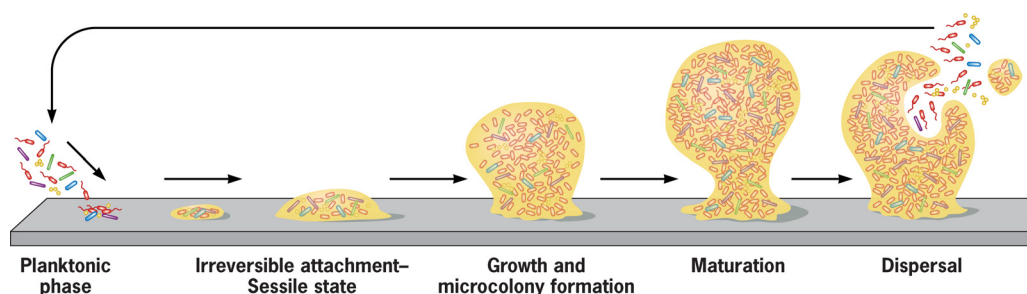
**KEYWORDS** animal host models, biofilms, flow cells, imaging, quantification

## INTRODUCTION

**B**iofilms are multidimensional communities in which resident bacteria coexist within the self-derived extracellular matrix (ECM) (1, 2). Although the developmental stages leading to biofilm formation appear to be conserved (Fig. 1), every species (or consortium of species in the case of polymicrobial biofilms) forms a unique multicellular community (3, 4). This protected network possesses the ability to evade environmental threats, such as antimicrobials and host defense mechanisms (5).

Biofilms account for 80% of chronic microbial human infections, leading to increased rates of hospitalization, elevated health care costs, and increased mortality and morbidity rates (6). Upper and lower respiratory tract diseases, native valve endocarditis, chronic otitis media, eye infections, chronic wounds, diabetic foot ulcers, urinary tract infections (UTIs), and periodontitis are all biofilm-associated diseases (7–12). Biofilms can also develop on abiotic surfaces, including medical devices such as orthopedic prostheses, artificial cardiac valves, coronary stents, intravascular and urinary catheters, neurosurgical, cochlear, and breast implants, dentures, and ventricular-assist and ocular devices (13).

Since the term “biofilm” was introduced in 1978, the intrigue and excitement surrounding a new microbiological field of study have produced opportunities of environmental, industrial, and clinical importance (14). Biofilms made a global impact in the literature, and their study continues to generate more questions. Because of the mechanical, physicochemical, microbiological, and medical components of biofilms, different disciplines view biofilms from different perspectives: chemists focus on organized chemicals, physicists deal with thermodynamics, and biologists examine the microbial physiology that affects biofilm formation and also unravel resistance patterns, yet all are left with the question of how all these components comprise the biofilm-associated threat. The unique nature of biofilm communities within the context of infection makes the constant development of new strategies acting against biofilms, as well as architectural and behavioral investigations, an evolving necessity (15). The last decade has seen a multitude of diverse methodological tools and enabled a context for comparative use and analysis that follows the rationale that biofilms thrive on living and inanimate surfaces by adaptation and survival. Their versatile behavior leads to extended (by design) experimental diversity and subsequently confounds efforts to evaluate biofilm-specific *in vitro* antimicrobial susceptibility. For the methodological piece alone, it should be noted that the risk of erroneous data acquisition is significant and that limited accuracy and reproducibility of viability assays have been recorded (16, 17). This description fails to capture the inconvenient reality. Dye aggregates will not bind stoichiometrically to complex communities (18). Microscopic enumerations, by default, provide indirect population assessments. Conventional colony formation assays



**FIG 1** Developmental stages in biofilm formation. One or more planktonic bacterial species adhere to a biotic/abiotic surface. Attached bacteria grow as a multicellular community, forming microcolonies in which they multiply and mature. This microbial infrastructure results in the development of a mature biofilm. Eventually, biofilms serve as bacterial reservoirs that are transmitted back to the environment through biofilm dispersal and then colonize new surfaces. (The concept of this figure was inspired by reference 71.)

have limited value, as the attempt to “normalize” these communities in test tubes often requires processes that disturb the members.

In this review, we (i) emphasize classical approaches for biofilm monitoring and quantification, (ii) highlight the evolution of imaging tools for architectural analysis of biofilm communities, and (iii) provide examples of methodological applications, including apparatuses to trace clinical biofilms. Despite the wealth of research approaches, there is an unmet need to filter the most interesting contribution per methodological group. We present here an understanding of the advantages and disadvantages of each group to help guide current research in this field of study.

### MULTIDIMENSIONAL ARCHITECTURE OF BIOFILMS

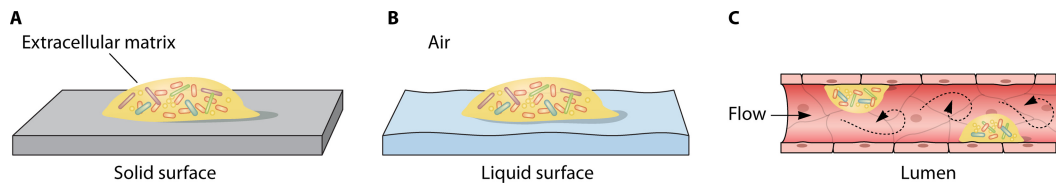
The ECM typically includes some type(s) of polysaccharides, proteins, and/or DNA (19). However, the ECM structure differentiates according to (i) the species or strains comprising the biofilm (20, 21); (ii) the conditions during development, and in turn the expression of bacterial factors (22); and (iii) the spatial location sampled within any given biofilm (23, 24). The ECM components affect structure, physiology, interactions with the surrounding environment, resistance toward antibiotics, and host defense mechanisms (25–28).

Biofilm architecture is highly variable. Bacteria can build exposed or submerged biofilms on either biotic or abiotic surfaces and under static or shear-flow conditions or, alternatively, coalesce directly in the host, as seen in intracellular bacterial communities (IBCs) involving uropathogenic *Escherichia coli* (UPEC) and *Klebsiella pneumoniae* (29–33). Another example of complex biofilm architecture is that of sputum-encased endobronchial *Pseudomonas aeruginosa* biofilms, which form aggregated clusters of bacterial cells surrounded by polymorphonuclear leukocytes (PMNs), the PMN-released enzymes elastase and collagenase, and oxygen radicals in the cystic fibrosis (CF) lung (34).

Differences among biofilm communities are also created in response to incoming signals and have importance in bacterial dispersal triggered by nutrient availability modifications (35). D-Amino acids, for example, have been reported to act individually or synergistically to trigger disassembly of biofilms and to inhibit pellicle formation by *Bacillus subtilis* and other species (36). The process happens through D-amino acid internalization in the bacterial cell wall affecting the anchoring of the amyloid-like protein TasA (37). Likewise, the cyclic diguanylate monophosphate (c-di-GMP) concentration affects matrix and structural component production, motility, cell attachment, and eventually biofilm formation in a number of species (38–41).

### Surface-Associated Biofilms and Importance of the Substratum

Surface-attached biofilms forming colonies are valuable for studying bacterial community architecture on a solid surface (Fig. 2A). Interestingly, different gene expression patterns are observed by comparing biofilms attached to solid surfaces and planktonic



**FIG 2** Biofilm types. (A) Surface-attached biofilms form colonies on a solid surface and are highly dependent on the substratum material. (B) Pellicles are formed in the air-liquid interface of fluids in nature or in the lab. Cells are bound together, forming a distinct macroscopic floating infrastructure. Thick pellicle formation requires the presence of exopolysaccharides (EPS). (C) Submerged biofilms develop under flow conditions. Biofilm formation under flow conditions is achieved in either indwelling catheters or suitably adapted lab devices.

bacteria grown in liquid cultures (42–47). Surface-associated biofilms are highly dependent on the substratum material and may or may not be exposed to air. Among the most common materials that promote biofilm formation on abiotic substrata are polyvinyl chloride (PVC), silicone, polystyrene, and metal (48–50). In microbial keratitis, for example, *P. aeruginosa* exhibits preferential adhesion to polymeric contact lenses (51), while in urinary catheters bacteria are preferably adherent to silicone and PVC biomaterials (52). As far as air exposure is concerned, the acquisition of antimicrobial resistance (AMR) and tolerance to xenobiotics has been attributed to (i) adequate oxygenation required for bacterial metabolism and (ii) facilitated DNA exchange due to the juxtaposed distribution of the bacterial cells in the well-organized biofilm cluster at the air-liquid interface (53).

Apart from surface composition, surface coatings can also play a role in biofilm formation. Blood components (fibrin, laminin, collagen, fibronectin, and immunoglobulins) compose the fibrin sheath that fosters the adherent growth mode around and into the air-deprived lumen of central venous catheters (CVC). Although results from both *in vitro* and *in vivo* studies regarding fibrin sheath-coated surfaces are inconsistent, reports of enhanced incidence of persistent bacteremia confirm the biofilm formation attributed to fibrin coating for some species (54).

Biofilms that take up nutrients directly from the surface to which they adhere (such as bacterial colonies on agar plates) are highly dependent on the substratum material (55, 56). In this case, the community grows outwards from the center of the colony, and architectural complexity most likely increases in response to nutrient and other environmental gradients that are created over time (45, 55, 56). Among these biofilms are the type called pellicles, which have been described as floating biofilms formed on a liquid surface (Fig. 2B) (42). Examples of bacteria that form liquid surface-associated pellicles include different strains of *E. coli* and *Salmonella* spp. (23, 57–59). This type of biofilm exhibits various degrees of meniscus growth, strength, and structure and possesses matrix-embedding, host-derived extracellular polymeric substance (EPS) components, laying the foundation for involvement in clinically relevant conditions (29, 60, 61). The liquid substratum provides the primary source of nutrients for the growing community. The term “pellicle” has also been used for dental diseases caused by biofilms formed from multicellular aggregates that require saliva proteins for attachment (62, 63).

### Submerged Biofilms

In addition to surface-associated biofilms, bacteria can form submerged biofilms under both static and shear-flow conditions. These types of biofilms are perhaps the most relevant in most chronic infectious disease states, as most of the device-associated infections involve the formation of submerged biofilms. Pathogenic biofilms formed on all types of catheters, including urinary and central/peripheral venous access lines, endotracheal and nasogastric tubes, and cerebrospinal fluid shunts, as well as on artificial cardiac valves, are examples of multicellular communities developing under variable-flow conditions (Fig. 2C) (64, 65). In catheters of all types, bacteria are introduced from the outside environment into the catheter lumen during catheter insertion

and can swim or are carried by normal fluid flow. Bacteria then attach to the abiotic material by using adhesive fibers. Host biomolecules, such as fibrinogen, laminin, collagen, and fibronectin, also serve as platforms for bacterial adherence, as they become deposited on the surface in both central venous and urinary catheters shortly after insertion of the device (62, 66). Bacterial expansion upon adherence leads to the formation of the biofilm community, a process known as maturation.

Laminar/semilaminar flow (implicated in biofilm formation in blood vessels), turbulent fluid mechanics (characterizing prosthetic valves), and discontinuous trickle (referring to catheter-associated UTIs [CAUTIs]) are several examples of fluid flow dynamics (67–69). For each condition, suitably adapted lab devices that contain simultaneous growth medium supply and waste removal are developed. These flow systems create optimal conditions for the generation of mature biofilms. Culture preparation, surface conditioning, and adjusted methods provide lab substrates mimicking clinical conditions. A characteristic example involves the evaluation of four CVC *Staphylococcus epidermidis* biofilm infection models that differ in material type (glass versus polymer) and nutrient presentation (static versus continuous flow) (70).

### Roots of Biofilm Phenotypic Resistance

The biofilm life cycle ends with the dispersal of bacterial cells stemming from the biomass after maturation (71). The dissemination and colonization of new target sites explain recalcitrant chronic infections within the host; biofilm-originating cells form bacterial niches with resistance phenotypes at the newly colonized sites. The biofilm dispersal process is controlled by environmental signals (oxygen, nutrients, temperature, and signaling molecules), intracellular reduction of the concentration of c-di-GMP, and upregulation of motility or quorum sensing (QS) genes, though many bacterial dispersal signals remain cryptic (13, 72, 73).

A single clonal population alters the growth rate and turns on adaptive pathways due to multiple environmental signals. The study of this complex yet distinct adaptation process elucidates changes in chronicity that contribute to fitness without being limited to specialized cells and signals (74). Since the environmental gradients surrounding the microbial community influence biofilm composition, phenotypically distinct subpopulations arise, including extracellular matrix producers, adhesive fiber producers, motile bacteria, and metabolically quiescent and/or antibiotic-tolerant bacteria (23, 24, 75, 76). Persisters emerge through diverse cellular and molecular phenomena, including biofilm matrix protection against the host immune system, redundant toxin-antitoxin (TA) modules induced by DNA damage (SOS response), nutrient elimination, the age of the inoculum, and the downregulation of genes related to motility, cell division, and protein synthesis (77–79). The quiescent phenotype is actively present in chronic and recalcitrant infections surviving under antibiotic pressure. For example, the reversible overexpression of the HipA and RelE toxins has been implicated in the interruption of cellular functional processes in *E. coli* under stress. Hence, persisters prevail without multiplying or being killed, exhibiting tolerance but not resistance, and therefore do not qualify as mutants (80, 81). The slow-growing small-colony variant (SCV) subpopulation is another equally puzzling phenotype that complicates biofilm formation as well as treatment and diagnosis of biofilm-related disease. The contribution of SCVs to biofilm formation has been studied for a rather small number of bacterial pathogens despite the huge clinical significance of persistent infections evading detection and complicating treatment (82, 83). In combination, these different phenotypes within microbial communities give rise to an extremely resilient community that can withstand many stressors and shield the resident bacteria from eradication.

Adaptive and phenotypic biofilm variations generate hurdles for the overall investigation and understanding of infection mechanisms. The partitioning of one or many different bacterial species is an additional unknown in this equation. Multispecies populations generate dynamic consortia with unique interactions [pathogen(s)-pathogen(s), pathogen(s)-commensal, and pathogen(s)-host], metabolic requirements,

and phenotypes, setting investigative limitations with respect to the *in vivo* clinical setup, infection pathogenicity, and response to treatment; on the other hand, mono-species biofilms constitute a minute fraction of both acute and chronic infections (84). Inter- and intraspecies interactions based on species-specific virulence traits set the stage for a complex microenvironment in which bacteria can exchange genetic markers and compete or cooperate for resources. The interplay among multiple pathogenic species enhances horizontal gene transfer of clinically prevailing phenotypic resistance elements. A fundamental trait of pluralism in biofilm composition is based upon the presence and content of nonbacterial elements. Examples of bacterial-fungal cooperation within the protected environment of a biofilm include that in wounds, the oral cavity, and urinary tract infections. This evolutionary tactic provides a stable survival equilibrium among kingdoms (85, 86). Therefore, explaining the rationale for the clinical relevance of multispecies biofilms is not trivial. While multispecies biofilms are the most clinically relevant infections, their study has been the most limited due to the complexity of each community, the lack of knowledge regarding the identity and abundance of each biofilm resident, and the technical limitations associated with different biofilm setups. Examples include *Haemophilus influenzae* competing with *Streptococcus pneumoniae*, but not with *Moraxella catarrhalis*, in ear infections; *Staphylococcus aureus* and *P. aeruginosa* cooperating for survival in chronic wound infections; group B streptococci promoting survival of UPEC in UTIs; and *Porphyromonas gingivalis* and *Treponema denticola* exhibiting synergy in biofilm formation involved in periodontal disease (87–92).

Since the onset of the first biofilm studies, several technological advancements have greatly enhanced our ability to molecularly dissect biofilm architecture and characteristics both temporally and spatially. Below is a comprehensive review of the methodological landscape used for the study of biofilms, presenting a blend of classical and more recent technologies.

## LABORATORY SETUPS

Cutting-edge points regarding technical information are discussed and the strengths and limitations of the most popular laboratory devices are provided in Table 1. All biofilm species are not created equal, so they often require specific experimental conditions matching the developed methodological tools. Some tools are more practical and relevant than others, covering adherence, life in a “turbulent flow habitat,” or the effect of coaggregation and flagellation on all types of bacteria.

### Culturing Biofilms under Static Conditions

The complexity of colony biofilms on agar plates was overlooked for decades due to the lack of advanced methodologies to probe architecture differences (Fig. 3A). This method generates a stable structure and limits the possibility of cell detachment, ensuring that observed differences in cell numbers are due to cell death rather than detachment (93).

Microtiter plate-based assays were first described in 1985 for assessing staphylococcal adherence to plastic tissue culture plates (94) (Fig. 3B). Bacterial inocula with standardized concentrations are placed in a 96-well microtiter plate made of PVC, polystyrene, or other material and incubated aerobically at 37°C for designated time frames (1 to 4 h for initial attachment and ~20 h for biofilm formation, depending on the species). Planktonic cells are removed by gentle washing, and the adherent cells are stained with crystal violet (CV) and quantified by spectrophotometry (95, 96). Studies concerning biofilm-forming isolates have exhibited that motile bacteria, including flagellated *E. coli*, *P. aeruginosa*, *Vibrio cholerae*, and *Salmonella enterica*, tend to coaggregate at the air-liquid interface. In contrast, the nonmotile cocci, including enterococci (with the exception of the motile organisms *Enterococcus casseliflavus* and *Enterococcus gallinarum*) and staphylococci, form aggregates at the microtiter plate base (97–102). Microtiter plates with removable silicone or polystyrene disks at the

**TABLE 1** Assays and lab devices used for biofilm formation evaluation

Assay or device	Advantage(s)	Disadvantage(s)	Reference(s)
Static conditions			
Agar plating	Stable structure	Difficulties in handling colonies due to increased growth rate	93, 435
Microtiter plate assay	Low possibility of cell detachment	Variations in bacterial strain motility rate	436, 437
	Simple	Difficulties in mature biofilm generation due to lack of nutrient supply	
Air-liquid assay	Rapid	Poor attachment to abiotic surfaces by several clinical strains	93, 95
	Highly reproducible	Limited substratum options	
	Antimicrobial susceptibility assay	Inability to test biofilms with flow viability validation	
BRT	Simple	Visualization of early-stage biofilms only	105, 108
	Direct microscopy	Planktonic cells may hinder biofilm observation	
	Coverslips can be used in the absence of an inverted microscope	Washing and staining steps required	
BRT	Stained coverslips do not require immediate microscopy (can wait ~1 wk)	No biofilm viability validation	105, 108
	Accurate, automated, reproducible, and rapid	Specified software and biofilm index provide the result	
	Amenable for high-throughput screening	Inability to test biofilms under flow	
No need for staining or washing steps			
Flow conditions			
Kadouri system	Large biomass generation	Planktonic cells may not be discarded due to low flow	93
	Applies to various growth demands	Wells overflow	
DNA microarray assay facilitation		Close monitoring required to avoid waste tube blocking and drying of the wells	95, 126
	Proteomics facilitation		
	Mature biofilm formation		
Drip-flow cell reactor	Large biomass produced	Limitations in confocal microscopy visualization	95, 126
	Viable cell enumeration	No nutrient laminar flow	
	Medical material surface antibiofilm testing		
Molecular study facilitation			119, 438
	Antimicrobial susceptibility assay facilitation		
Microsensor monitoring study			
Robbins device	Structural integrity conserved	Limited <i>in situ</i> biofilm visualization	119, 438
Modified Robbins device	Study of biofilm physiology	Biofilm destruction during sampling for quantitative analysis	
Biofilm-related bacterial metabolic product investigation			126, 127, 128, 439
	Investigation of immune response to biofilm-associated bacteria		
	Allows aseptic sampling and plug handling		
Surface material-associated study		Limitations in confocal microscopy visualization	126, 127, 128, 439
	Biofilm growth rate study	For antimicrobial compound testing, coupons need transfer into 96-well plates	
Biomass structure investigation			436, 440
	Antimicrobial susceptibility testing		
	Identical biofilm production		
Calgary device	Antimicrobial susceptibility assay	Sonication may lead to erroneous results	436, 440
	3D imaging facilitates structural analysis	Time-consuming	
Viability assay facilitation		Specific fluorophores required for CLSM	441
		Sample destruction due to fixation required for microscopy	
Microfermentors	Genetic and biochemistry analysis facilitation		441
	Study of biofilm adherence and formation		
	Multi- or monospecies biofilm evaluation		
Mature biofilm formation			

(Continued on next page)

TABLE 1 (Continued)

Assay or device	Advantage(s)	Disadvantage(s)	Reference(s)
Microfluidics-based device	Noninvasive technique Continuous biofilm formation assessment Enhanced physiological relevance of live-cell assays due to shear flow Simplicity of usage Host-bacterium interaction analysis Real-time visualization of biofilm growth	No metabolic products obtained (closed system)	

bottom can serve as platforms to facilitate microscopic and molecular examinations (97).

An air-liquid assay enables qualitative analysis of biofilm formation through direct phase-contrast microscopic visualization of the early-stage bacterial aggregates in flat-bottomed wells (Fig. 3C). Bacterial inocula placed in a 24-well flat-bottomed plate are incubated at an angle or coverslips are placed at an angle into wells for the appropriate incubation time; coverslips are washed and stained with crystal violet or with a fluorescent antibody against a species-specific antigen or a protein of choice. A conventional or fluorescence microscope can be used for biofilm visualization (93). The *sad* (surface attachment defective)-associated reversible and irreversible attachment of *P. aeruginosa* was investigated by this assay to decipher the pseudomonal developmental shift from the planktonic to the biofilm state in the CF lung (103). Biofilm formation on epithelial cells, assessed by the air-liquid method, served as an *in vitro* model of chronic rhinosinusitis due to *P. aeruginosa* PAO1 (104).

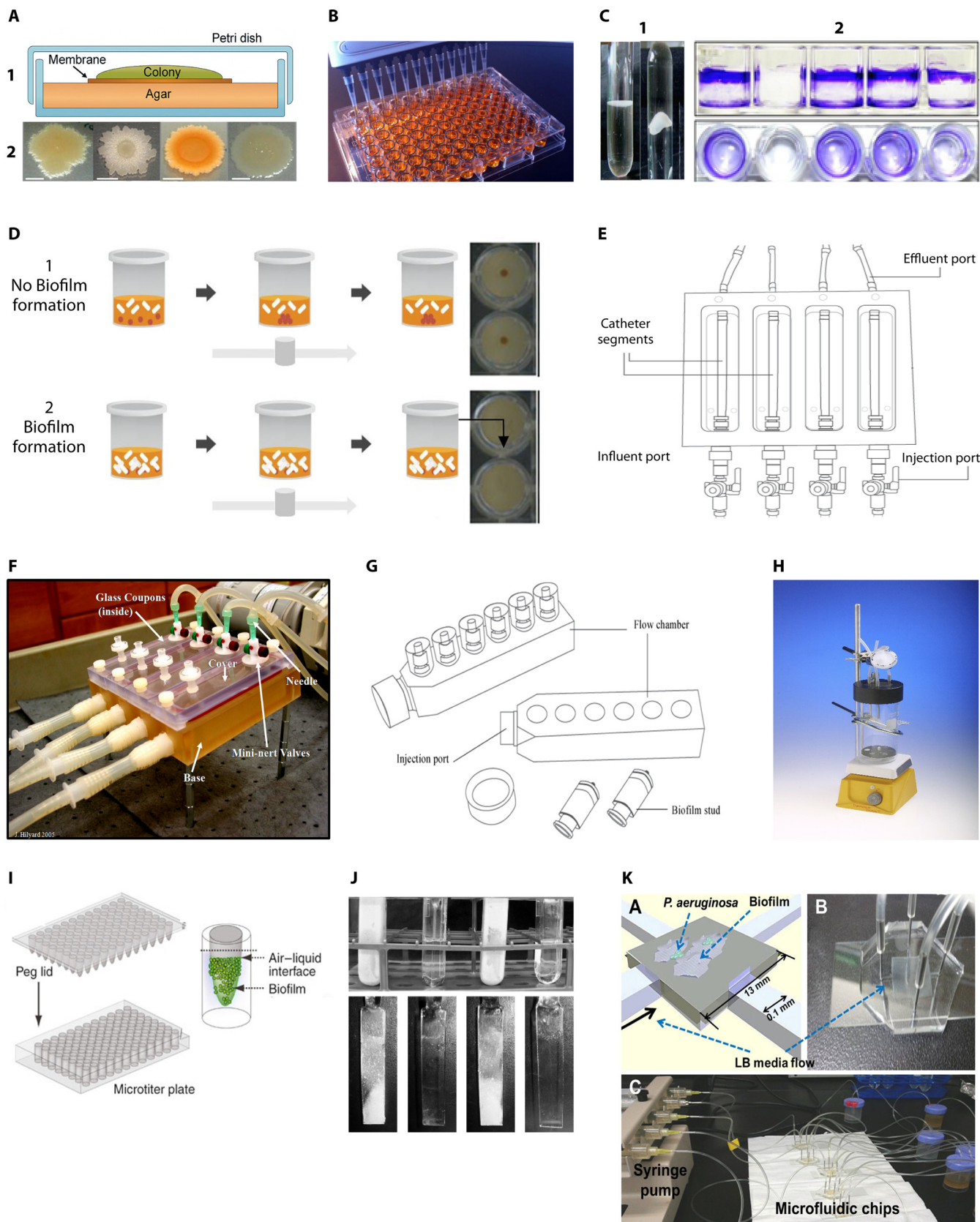
The BioFilm ring test (BRT) is a newly available tool for the study of biofilm formation kinetics that was developed in the last decade. It detects biofilm formation in modified 96-well polystyrene microtiter plates by use of magnetic microbeads and a scanning plate reader (105) (Fig. 3D). Biofilm-associated adherence is determined when beads remain scattered after the application of a magnetic field; in contrast, beads are immobilized in the center of the well bottom in the presence of planktonic cells (105, 106). Examples of BRT biofilm formation kinetics include those of (i) the nontypeable *H. influenzae* (NTHi) strains isolated from body fluids (blood, sputum, and pleural and cerebrospinal fluid) of individuals with nonbacteremic, community-acquired pneumonia and chronic obstructive pulmonary disease (COPD) and from middle ear fluid of patients with otitis media; (ii) the *S. aureus* and *S. epidermidis* strains from acute and chronic osteomyelitis and infectious arthritis cases; and (iii) the *P. aeruginosa* strains from CF patient sputum samples (107–110). A recent extension of BRT is Antibiofilmogram, which is used for susceptibility profile testing of bone and joint infection-related *S. aureus* biofilms with 11 widely used antibiotics. This method aims to facilitate therapeutic choices by narrowing the window of truly efficient antibiofilm treatment options (111).

### Culturing Biofilms under Flow Conditions

Continuous-flow cultures enable the formation of mature biofilms in chambers covered with coverslips or on silicone or latex tubes fitted to a peristaltic or syringe pump. The peristaltic pump facilitates flow of fresh growth medium, whereas planktonic cells and waste are removed. The biofilm formed is monitored microscopically after introducing fluorescent proteins or reporter genes (112). Reporter genes are informative for the stage-specific physiological changes that occur under dynamic conditions and differentiate biofilms from their planktonic counterparts (21, 23, 113). Green fluorescent protein (GFP) serves as an example of the reporter signals associated with the *csgBA* genes, which have been used extensively in biofilm interventions for UPEC (23).

Among the advantages of continuous-flow models is the ability to compare the effects that different media, oxygen concentrations, temperature shifts, and substances exert on a biofilm at all developmental phases. These models also offer evaluation of





**FIG 3** Laboratory setups. (A) Colony biofilms on agar plates. (1) Schematic diagram of a colony biofilm. (2) Various types of macrocolonies grown on agar medium. (Panel 1 reprinted from reference 427 with permission of the publisher; panel 2 reprinted from reference 428.) (B) Microtiter plate. (Photograph taken and kindly provided by Alex Hall.) (C) Air-liquid biofilms. (1) Pellicle formation at the air-liquid surface. (2) Crystal violet staining was performed to assess (Continued on next page)

the effects that transiently occurring molecules, such as antibiotics or adherence inhibitors, have on biofilms. However, the technical disadvantages of continuous-flow biofilms include increased experimental complexity as well as possible formation/trapping of air bubbles in the setup tubing. This can perturb proper medium flow, affect the architecture, and put the system at risk for contamination (114, 115).

The Kadouri system is an intermediate system between static biofilms and low-flow cells (Fig. 3E). The major difference from static assays is that the wells are part of a closed system with two outputs, one for the continuous fresh medium supply via an adjusted pump and one for the removal of waste and planktonic cells, while the difference from flow-cell systems lies in the minimal shear forces (93, 116).

Drip-flow cell reactors enable biofilm formation in the air-liquid interface at low shear forces (117) (Fig. 3F). A biofilm is formed in channels (mainly silicon tubes) containing glass coupons or catheters, and a large biomass is produced (20, 22, 61). An *in vitro* model has been applied for bacteriophage-based bacterial biofilm inhibition on medical device surfaces. This model involved *S. epidermidis* biofilms on hydrogel-coated urinary and central venous catheters with a modified drip-flow biofilm reactor; the modification was a shift from drip to constant flow (118).

The Robbins device (RD) generates submerged biofilms growing in aqueous systems that can be used for the interrogation of multispecies communities (119, 120). Culturing multispecies biofilms *in vitro* can become complex regarding the microenvironment simulations. At present, multispecies biofilms are formed either by coculture of different preacquired clinical strains or by transfer of a mixed environmental population into the experimental setup (121). So far, the most commonly applied device is the modified Robbins device (MRD) (Fig. 3G), involving mono- or multispecies biofilm formation on catheter segments of various materials under flow conditions. Thus, MRD enables real-life biofilm simulation on catheter surfaces and is considered amenable for *in vivo* evaluation of implanted devices and catheters (14, 122, 123). This setup has been applied for biofilm therapeutic interventions, including pharmaceutical preparations, such as minocycline and EDTA (M-EDTA), as well as the maintenance of catheter lumen patency and bacteriophage therapy for biofilm-related infections in CF patients (124, 125).

Rotating-disk reactors, including the CDC biofilm reactor, facilitate growth under controlled moderate shear stress and continuous-medium-flow conditions (126) (Fig. 3H). The reactor consists of a disk that rotates over a magnetic base and coupons of various materials that promote biofilm growth. A glass reactor vessel enables medium supply and waste removal; coupon removal at desired intervals is feasible (126). An alternative method involves concentric reaction chambers with cylinders enabling biofilm formation. Modifications in speed or the cylinder's diameter affect the cell density and biofilm structure (127, 128). Rotating-disk reactors enable antimicrobial agent and antifouling material efficacy, and the removable disks serve as testing surfaces for antibiofilm compounds (21).

The peg lid Calgary biofilm device (CBD) generates biofilms on the bottoms of 96 pegs fitted in a polystyrene microplate lid or a multichannel tray containing a bacterial inoculum of a standardized optical density (Fig. 3I). Pegs are then sealed and incubated on a rocking table that creates shear forces at a specific temperature for a specific time. Planktonic cells are rinsed off, and biofilms are detached from the pegs by sonication and then placed into sterile 96-well microtiter plates with specific dilutions of the tested biocide to estimate the minimum biofilm eradication concentration (MBEC) after 24 h

### FIG 3 Legend (Continued)

air-liquid biofilm formation on abiotic surfaces. (Panel 1 reprinted from reference 429; panel 2 reprinted from reference 430.) (D) BioFilm ring test. Photos of scanning microplates were taken with a plate reader after magnetization and show no biofilm formation (1) and biofilm formation (2). (Photos reprinted from reference 108.) (E) Kadouri biofilm system for flow biofilm study. (Reprinted from reference 431.) (F) Drip-flow reactor and various components. (Photograph kindly provided by the Center for Biofilm Engineering, MSU-Bozeman; see reference 117 for further details.) (G) Modified Robbins device. (Reprinted from reference 431.) (H) Rotating-disk reactor. (Photograph kindly provided by BioSurface Technologies Corp.) (I) Peg lid Calgary device. (Adapted from reference 432 with permission from Macmillan Publishers Ltd.) (J) Biofilm growth in microfermentors. (Reprinted from reference 433.) (K) Microfluidic device and experimental setup for biofilm formation (Reprinted from reference 434 with permission.)

of incubation (129, 130). The study of sputum biofilm-forming *P. aeruginosa* strains isolated from CF patients is one example of CBD being used to compare the efficacies of multiple antibiotic combinations (131, 132).

Microfermentors use slides of various materials as the substrate to form bacterial communities, while a constant medium flow and sterile air supply are provided (5, 133, 134) (Fig. 3J). The large mass of biofilm generated through this assay provides information not only about the biofilm-forming ability of the tested strains but also about the antimicrobial susceptibility profile (5, 134). Methicillin-resistant *S. aureus* (MRSA) strains appear to switch between proteinaceous and exopolysaccharidic biofilm matrices according to the provided substrate and environmental conditions in microfermentors (135).

Microfluidics-based devices, including the relatively recent BioFlux device, are fully integrated platforms consisting of modified 96-well plates with laminar flow chambers, a shear-flow control system, an imaging system, and advanced software for data collection and analysis (Fig. 3K). Microfluidic channels enable fresh medium movement due to pneumatic pressure at a controlled flow rate, rolling velocity, and time. Antimicrobial agents can be delivered to the flow biofilms from the inlet to the outlet well. In high-throughput (HT) flow-cell biofilm viability assays, viable cells are quantified by epifluorescence microscopy coupled with chemical or genetic color coding; high-quality images are attributed to coverslip glass at the bottom of the wells (136). Modifications involving protocol adaptations (temperature, medium type, and concentrations) and supplemental accessories (software packages and modules) extend microfluidic applications by facilitating complex assays and multiple experiments (137). Examples of the use of microfluidics-based devices adapted for coculturing eukaryotic cell lines with bacterial aggregates include the study of HeLa cells with enterohemorrhagic *E. coli* (EHEC) and commensal biofilms to demonstrate the developmental events in a gastrointestinal (GI) tract infection (138). Another example provided real-time monitoring of osteoblast adhesion and viability on the Ti alloy surfaces of orthopedic implants infected with *S. epidermidis* (139).

Most of the existing lab setups for monospecies or multispecies bacterial biofilm formation also serve for biofilm-mammalian cell coculture systems. Both static and flow coculture biofilm model systems have been applied to study biofilm formation on biotic surfaces as well as the responses to various therapeutic approaches (140). These models aim to reflect the infectious process in real time and offer the advantage of examining the host-pathogen interaction. Various culture systems have been employed in biofilm-mammalian cell coculture models, including (i) human airway epithelial cells (CFBE cells) and human bronchial epithelial cells (BEAS-2B) cocultured with *P. aeruginosa* (140–142); (ii) a human oral keratinocyte cell line cocultured with multispecies oral biofilms involving *P. gingivalis*, *Fusobacterium nucleatum*, *Aggregatibacter actinomycetemcomitans*, *Streptococcus mitis*, *Streptococcus oralis*, *Streptococcus intermedius*, *Veillonella dispar*, *Actinomyces naeslundii*, and *Prevotella intermedia* (143, 144); (iii) intestinal epithelial cells cocultured with *E. coli* O157:H7 (145); and (iv) human osteoblasts cocultured with *Staphylococcus epidermidis* (146).

### QUANTITATION AND VIABILITY ASSAYS

Static experimental conditions and a discontinuous nutrient supply are limiting factors in assessing mature biofilms in a lab setting (147). Monitoring the viable bacteria within a biofilm can be achieved through (i) cultivation, (ii) metabolic activity detection, and (iii) membrane integrity evaluation. Conventional CFU enumeration fails to generate reproducibly reliable results for most biofilm quantification due to the presence of cell aggregates hampering distinct colony development as well as individual-species resolution, in the case of multispecies biofilms. Furthermore, vortexing or sonication before plating may lead to sample structure destruction or air bubble entrapment and erroneous results due to partial cell detachment (2, 148).

The crystal violet (CV) assay, one of the most commonly used *in vitro* biofilm-associated techniques (Table 2), enables optical visualization of biofilm thickness and

**TABLE 2** Assays applied for biofilm quantification and viability determination<sup>a</sup>

Assay or reagent	Quantification ability	Assay combination	Advantage(s)	Disadvantage(s)	Reference(s)
Fluorescent dyes					
CV	Biofilm matrix biomass		Easy Inexpensive Wide applicability	Dependent on absorption of the dye into the biomass Nonspecific to multispecies biofilms No dimensional information Sample destruction Poor reproducibility Low accuracy for biofilm visual analysis	110, 124, 162
Congo red	Biofilm matrix biomass		Easy	Low accuracy for biofilm visual analysis	149, 442
DMMB	Biofilm matrix biomass	Resazurin, XTT, BTA, FDA	Inexpensive Strain specific ( <i>S. aureus</i> ) Cell viability assessment	pH-dependent binding ability Reagent instability Expensive	154, 162 443, 444
Live/Dead BacLight (Syto 9 and PI)	Semiquantitative	CLSM			
AO	Apoptotic quantification	Ethidium bromide, epifluorescence microscopy	Time efficient	Intermediate “unknown” population Underestimation of living cells Large no. of samples required Lab safety requirements due to high mutagenicity	157, 445
DAPI	Live-cell biomass	CTC	DNA and RNA labeling Detects apoptotic phenomena Feasible combination with other probes Nuclear integrity	Used only for fixed cells	200, 446
XTT	Counts metabolically active cells		Cell viability assessment Reproducible	High concn is required for live-cell staining	162, 437
AB/resazurin	Counts metabolically active cells		Nondestructive Cell viability assessment Reproducible	Requires highly respirative bacteria Variations due to biofilm heterogeneity Time-consuming Large no. of samples required Heat and light sensitive	447, 448
CTC	Counts metabolically active cells	DAPI, epifluorescence microscopy	Cell viability assessment Bright red fluorescence	Detects only highly metabolically active cells Toxicity	166, 449–451
BTA (with phenol red and resazurin)	Counts living cells in biofilm		Discrimination between active cells and abiotic parts Cell viability assessment Inexpensive	Solute-associated inhibition Challenging for multispecies biofilm evaluation	167, 452
FDA	Semiquantitative		No sample manipulation required Cell viability assessment Easy Inexpensive High repeatability Independent of growth conditions	Unsuitable for mature biofilms Impaired by biofilm thickness	162, 437
ATP	Live-cell biomass			Standard needed to ensure quantification accuracy	453

(Continued on next page)

**TABLE 2** (Continued)

Assay or reagent	Quantification ability	Assay combination	Advantage(s)	Disadvantage(s)	Reference(s)
SYBR Green I	Multispecies biofilm cell quantification Can synthesize DNA in real time	Real-time PCR	Detects bacteria with low metabolic activity Cell viability assessment Reliable and reproducible No specific probes required Cell viability assessment	Risk of sample contamination	454, 455
Genetic/molecular approaches RT-PCR	Multispecies biofilm cell quantification	Gel electrophoresis (DGGE)	Detects uncultivable or challenging-to-culture species, live and dead cells, matrix components DGGE detects predominant species, gives early clinical diagnosis Easy, rapid, reliable, and reproducible High sensitivity	Risk of sample contamination Expensive and complex procedure	456
Real-time PCR	Can synthesize DNA in real time Counts cells in multispecies biofilms	SYBR green I	Cell viability assessment High sensitivity	Risk of sample contamination	455, 457
Next-generation sequencing (NGS)	Quantification of genomic sequences	PCR, RT-PCR <sup>e</sup>	Entire transcriptome available in a single analysis (RNA-seq) <sup>e</sup> Biofilm phenotype, protein profile determinant, and resistance pattern analysis	Expensive	458
Proteomic analysis	ECM protein component	Mass spectroscopy/NMR	Independent of growth conditions Applicable to multispecies biofilms Detects all viable microorganisms Visualization and spatial distribution Simple procedure	Protein expression variations in multispecies biofilms	187, 190
Microscopy FISH	Semiquantitative	CLSM		Low permeability of DNA probes	175, 200, 459, 460
IF	Antibody-antigen complexes	Fluorescently labeled antibodies		Low sensitivity Hybridization between complementary PNA probes Expensive and lengthy multistep procedure Less flexible procedure Costly Risk of cross-reaction in multilabeling Complex, with low sensitivity and specificity due to cross-reactions Little reagent standardization and laboratory variations	461

(Continued on next page)

**TABLE 2** (Continued)

Assay or reagent	Quantification ability	Assay combination	Advantage(s)	Disadvantage(s)	Reference(s)
CLSM	Quantitative imaging	Fluorescence assay, FISH, FCS	Nondestructive	Probe efficacy dependent on biofilm EPS complexity	162, 204, 205, 462, 463
SIM	Live-cell biomass imaging	Fluorescent probes	3D imaging Cell and EPS spatial distribution Applicable to thick sample 3D imaging of living cells	Special equipment required	210, 211, 464
OCT	Biomass, structure, and porosity identification	Ultra-broad-bandwidth lasers	Enhanced resolution Computational amplification Imaging of thick samples Real-time 3D imaging	No cell-level resolution	216, 465–467
TEM	Total biofilm matrix biomass imaging		Speedy measurements Noninvasive Label-free High resolution	Limited penetration depth	204, 468, 469
SEM <sup>a</sup>	Synergy with focus ion beam for inner biofilm study	EDS <sup>b</sup>	Surface visualization <sup>a</sup>	Special equipment required Risk of sample distortion due to dehydration <sup>a</sup>	162, 220, 223, 227, 470, 471
ESEM <sup>b</sup> Cryo-SEM <sup>c</sup> ASEM <sup>d</sup>			Detailed 3D visualization <sup>a</sup> No structural damage <sup>b</sup> No sample prep <sup>b</sup> Imaging of EPS <sup>b</sup> No dehydration required <sup>c</sup> Nonconductive surfaces <sup>c</sup> Time efficient <sup>c</sup> Nanostructure biofilm surface visualization in liquids <sup>d</sup> Macromolecule distribution	Low resolution <sup>b</sup> Artifacts due to sample prep <sup>c</sup> Low resolution <sup>c</sup> Multiple labeling <sup>d</sup>	
STXM	Total biofilm biomass	X-ray fluorescence	Visualization of biological and environmental components and spatial distribution Real-time 3D imaging	Applicable to thin samples	162, 204, 224, 472, 473
AFM	Chemical biofilm components Chemical biofilm component imaging		Little/no sample prep Performed in both air and water Elucidation of molecular interactions High resolution Visualizes cellular interactions	Special equipment required Artifacts and sample damage due to incorrect tip elections Deformation of soft samples Poor image quality in water Special equipment required	227, 228, 474–476

(Continued on next page)

**TABLE 2** (Continued)

Assay or reagent	Quantification ability	Assay combination	Advantage(s)	Disadvantage(s)	Reference(s)
CRM			High spatial resolution	Low resolution at boundary separation Limited penetration depth	231, 477
MALDI-IMS	Biofilm biomass Chemical biofilm component quantification		Species identification Molecular detection Label-free Spatial distribution information Chemical identity definition	Ion imaging artifacts Chemical modification of sample surface required	24, 232, 233
SIMS	Biofilm molecular composition identification		Subpopulation discrimination Host-pathogen interaction imaging Differentiation between similar molecules with different masses Imaging over wide mass range Molecular identification	Limited mass range	234, 235, 478

<sup>a</sup>Characteristics referring to SEM.

<sup>b</sup>Characteristics referring to ESEM.

<sup>c</sup>Characteristics referring to cryo-SEM.

<sup>d</sup>Characteristics referring to ASEM.

<sup>e</sup>Characteristics referring to RT-PCR.

<sup>f</sup>CV, crystal violet; DMMB, dimethylmethylene blue; PI, propidium iodine; AO, acridine orange; DAPI, 4',6-diamidino-2-phenylindole; XTT, 2,3-bis(2-methoxy-4-nitro-5-sulphophenyl)-5-[(phenylamino)carbonyl]-2H-tetrazolium hydroxide; AB, alamarBlue; CTC, oxidized 5-cyano-2,3-dithioly tetrazolium chloride; BTA, biotimer assay; FDA, fluorescein diacetate; RT-PCR, reverse transcription-PCR; DGGE, denaturing gradient gel electrophoresis; FISH, fluorescence *in situ* hybridization; PNA, peptide nucleic acids; IF, immunofluorescence; CLSM, confocal laser scanning microscopy; FCS, fluorescence correlation spectroscopy; SIM, structured illumination microscopy; OCT, optical computed tomography; TEM, transmission electron microscopy; SEM, scanning electron microscopy; ESEM, environmental scanning electron microscopy; ASEM, atmospheric scanning electron microscopy; EDS, energy-dispersive X-ray spectroscopy; EPS, extracellular polymeric substances; STXM, scanning transmission X-ray microscopy; AFM, atomic force microscopy; CRM, confocal resonance microscopy; MALDI-IMS, matrix-assisted laser desorption ionization-imaging mass spectrometry; SIMS, secondary ion mass spectrometry.

total biofilm biomass quantification, especially in the initial stages, but is not accurate for calculating cell viability (24). Additionally, CV lacks sensitivity and specificity due to high variability when the dye (i) binds unspecifically to negatively charged molecules or (ii) is unevenly extracted by ethanol. The Congo red agar method investigates coagulase-negative staphylococcus (CoNS) strains for the production of slime and qualitatively scores cellulose and amyloid fiber production by Gram-negative bacteria (tested predominantly in *E. coli*, *P. aeruginosa*, and *Salmonella*) (149–153). Dimethylmethylene blue (DMMB) binds to glycosaminoglycans (GAG) and polysaccharide intercellular adhesins (PIA). This is a species-specific method targeting *S. aureus* biofilms, restraining the diagnostic range of the technique to this PIA-related biofilm matrix-possessing species (154).

The Live/Dead BacLight assay uses double staining with the fluorescent nucleic acid dyes Syto 9 and propidium iodide (PI). Syto 9 fluoresces green and penetrates both damaged and intact cell membranes, providing total cell counts, while PI fluoresces red and crosses only damaged cell membranes. The dual presence of the dyes enables multimodal measurements, including microplate readings, flow cytometry analysis, and even microscopy. Indeed, in flow cytometry studies addressing antimicrobial agent testing for MIC determination, the dual usage of Syto 9 and PI required no preparatory stages. Drawbacks of the green fluorophore, including bleaching, ranging binding affinities (as in the case of Gram-negative bacteria), and background cross-signals, undermine the utility of Syto 9, thus welcoming the combination with PI. Additionally, the pronounced ability of PI to intercalate with DNA results in enhanced fluorescence, displacing Syto 9 and interfering with cell viability testing (155). The large sample requirement makes the method time-consuming and unfit for HT assays (147). Fluorescence-activated cell sorting (FACS) has been investigated intensively for the separation of biofilm subpopulations in the lab, with the potential to be deployed for quantification; reliable single-cell isolation of bacterial cells, on a scale orders of magnitude smaller than what mammalian cell flow systems are commonly designed to provide, remains a confounding factor in many cases (156).

Other nucleic acid-binding dyes applied for fluorescence microscopy include acridine orange (AO), a cell-permeating dye that enables total counts of cells within the biomass; ethidium bromide (EB), which stains nucleic acids red when the integrity of the cell membrane is lost; and the DNA-specific probe DAPI (4',6-diamidino-2-phenylindole), which stains cells with intact membranes (157–159). The concept of dual-dye flow cytometric cell determination was introduced by use of a customized lab-built device employing a violet diode laser (397 nm) that excites fluorescence of both DAPI and Hoechst dyes in permeabilized and intact cells. Despite the fluorophore complications, flow cytometry is unique for the study of heterogeneous subpopulations (160). A high DAPI concentration is indicative of a thicker biofilm; therefore, it can be used for biofilm extracellular matrix component detection and visualization. Such an example of DAPI implementation is the matrix analysis of *Salmonella enterica* serovar Typhi- and *S. Typhimurium*-associated gallstones (161).

2,3-Bis(2-methoxy-4-nitro-5-sulfophenyl)-5-[(phenylamino)carbonyl]-2H-tetrazolium hydroxide (XTT) is used to spectrophotometrically identify metabolically active cells that reduce XTT to water-soluble formazan (162). However, it requires bacteria with high levels of aerobic metabolism and exhibits intra- and interspecies variability due to biofilm heterogeneity (30). The resazurin dye, also known as alamarBlue (AB), fluoresces and can be measured via spectrophotometry. In fact, resazurin is a nonfluorescent blue redox indicator that is reduced to the pink fluorescent compound resorufin through cellular respiration (163, 164).

Oxidized 5-cyano-2,3-ditolyl tetrazolium chloride (CTC) dissolves in water, and the electron transport chain of metabolically active cells reduces CTC to fluorescent formazan crystals (165). The incubation time and the CTC concentration affect the number of detectable cells, so this method is suitable only for estimating the number of highly metabolically active cells and only for aerobic or microaerophilic systems (166).

The biotimer assay (BTA) measures metabolism by estimating the time needed for



the visualized color change of specific indicators (phenol red and resazurin) with respect to the initial bacterial concentration according to correlation curves for planktonic bacteria (167). The BTA is a rather simple and convenient colorimetric tool for biofilm susceptibility determination without requiring particular lab equipment. Fluorescein diacetate (FDA) emits yellow fluorescence once it is hydrolyzed by esterases. Although it is used to reproducibly measure microbial activity and biofilm biomass, it is unable to reach deep into thick biofilms (162, 168).

### “GRIND AND FIND” APPROACH VIA MOLECULAR ANALYSIS

Multispecies biofilm interrogation requires advanced molecular methodologies that enable species discrimination and strain-specific probes highlighting spatial distribution through advanced microscopy (Table 2). Additionally, surface cell attachment and phenotypic variation are initiated and influenced by specific on/off switch genes. Wild-type strains, isogenic mutants, and plasmids are constructed and studied with molecular assays to further specify and recognize genetic factors involved in biofilm formation. For example, the *ica* gene cluster was found to mediate PIA production, whereas the reversible insertion/excision of the IS256 sequence element has a strong correlation with phase variation/phenotypic switching of staphylococcal strains (169–173).

PCR-based approaches as well as transcriptional and proteomic profiling can be used to interrogate gene expression differences occurring among free-living and sessile species. Genetic virulence traits are associated with phenotypic shifts contributing to the pathogenesis of clinically relevant strains. Genome sequences for adhesion proteins, tissue-penetrating enzymes, and toxins have been studied extensively for human biofilm-forming colonizers, such as MRSA, enterococcal, *Acinetobacter baumannii*, and *K. pneumoniae* strains (174). Alterations in the expression of transmissibility, QS, and oxidative stress regulatory genes affect the survival of pseudomonal strains in CF patients, and genetic modifications affecting the biofilm-associated pneumococcal phenotype lead to a shift from asymptomatic carriage to nasopharyngeal pathogenesis (175).

Early microarray analysis revealed that during the formation of *E. coli* biofilms and subsequent colonization, 38% of genes were modified, resulting in the altered expression of 600 genes (176). Similar to microarray analyses, quantitative real-time PCR (qPCR) examines a subset of genes from biofilm-isolated cells, while multiplex PCR detects multiple target sequences and is a useful tool for genetic analysis of polymicrobial/multispecies communities or gene polymorphisms (177–179) (Table 3). PCR product detection and quantification are based on probe chemistry.

RNA sequencing (RNA-seq) analyses based on next-generation sequencing (NGS) are now replacing conventional microarrays and provide higher sensitivity and information pertaining to small noncoding RNAs actively participating in oral pathogen dysbiotic processes (180). Additionally, RNA-seq-based transcriptomic analyses have provided a multitude of genes associated with biofilm formation by both Gram-positive and Gram-negative bacterial species (such as MRSA, *Enterococcus faecalis*, and *P. aeruginosa*) in clinical entities, including otitis media, CF, chronic wounds, and endodontic and indwelling device infections (181, 182). NGS platforms provide massive parallel sequencing of DNA segments physically or artificially produced from a single sample. This allows time-efficient reading of entire genomes (whole-genome sequencing [WGS]) as well as identification and quantification of genomic sequences in a sample at the level of a single molecule (target sequencing or sequencing of multiple bacterial species and subpopulations).

NGS in combination with reverse transcription-PCR (RT-PCR) (whole-exome sequencing or RNA-seq) provides evidence for a sample transcriptome. This combinatorial approach does not require genetic sequences, thus worthily replacing microarrays. RNA-seq analyses revealed the proportion of the dormant cell subpopulation within the bacterial biomass of *S. epidermidis* and the coexistence of unknown bacterial species in oral cavity pathogenesis (183–186).

**TABLE 3** Biofilm-related gene detection<sup>a</sup>

Method	Species	Gene(s)	Function	Reference(s)	
PCR	<i>Staphylococcus</i> spp.	<i>ica</i> gene cluster	Biosynthesis of PIA, cell accumulation, biofilm formation	444, 479	
		MSCRAMM genes	10 genes encoding surface components, involved in recognition of adhesive matrix molecules	480, 481	
	<i>Enterococcus</i> spp.	<i>esp</i> , <i>ace</i> , <i>agg</i> , <i>empfm</i> operon	<i>esp</i> encodes extracellular surface protein (Esp), involved in adhesion and facilitation of colonization and persistence	482, 483	
			<i>ace</i> encodes collagen adhesion protein (Ace), which regulates interaction with host matrix proteins (collagens I and IV, laminin)	483	
			<i>agg</i> encodes aggregation substance (Agg), involved in conjugation mediation, adhesion to eukaryotic cells, and cellular aggregation	483	
	<i>Escherichia coli</i>	<i>fimA</i> , <i>papC</i> , <i>hly</i> , <i>ecpA</i>	<i>empfm</i> operon is involved in biofilm formation <i>fim</i> encodes type I fimbriae <i>pap</i> encodes P-fimbriae <i>hly</i> encodes pilin structure	484 485	
	<i>Salmonella</i> spp.	<i>adrA</i> , <i>csgD</i> , <i>csgA</i> , <i>gcpA</i> , <i>spiA</i>	<i>adrA</i> is involved in cyclic di-GMP level control, cellulose production, biofilm formation	486	
			<i>csgD</i> is involved in biofilm formation		
			<i>csgA</i> and <i>adrA</i> are involved in curli and cellulose expression <i>gcpA</i> is involved in cellulose production, biofilm formation		
	<i>Acinetobacter baumannii</i> <i>Pseudomonas aeruginosa</i>	<i>bla</i> <sub>PER-1</sub>	Cell adhesion, drug resistance	487, 489	
		<i>psl</i> gene cluster ( <i>pslA</i> to -F)	Involved in biofilm formation, protection against aminoglycoside antibiotics	25, 490	
	<i>Klebsiella pneumoniae</i>	<i>pel</i> genes	Seven genes involved in pellicle matrix formation	25	
			QS genes ( <i>lasIR</i> , <i>rhIIIR</i> )	Cell-to-cell communication enhancement, coding for AHL synthase, biofilm formation, resistance, motility	491, 492
			TA genes ( <i>mazEF</i> , <i>relBE</i> , <i>hipBA</i> , <i>ccdAB</i> , <i>mqsR</i> )	Biofilm formation, virulence, "genetic competence"	492
		<i>ecpA</i>	Encodes major pilin subunit	493	
<i>fimA</i> , <i>fimH</i>			<i>fimA</i> and <i>mrkA</i> encode fimbrial subunits	493	
<i>mrkA</i> , <i>mrkD</i>			<i>fimH</i> and <i>mrkD</i> encode minor tip adhesion	493	
<i>Yersinia pestis</i>		<i>hmsT</i> , <i>hmsP</i> (*)	Regulatory genes, involved in biofilm formation on biotic and abiotic surfaces (*)	494	
<i>Vibrio cholerae</i>		<i>flaA</i> , <i>fliH</i> , <i>fliN</i> , <i>flgH</i> , <i>flgL</i> , <i>pomA</i>	Encode flagellar proteins for cellular motility		
		<i>cpsF</i> , <i>epsD</i> , <i>epsF</i> , <i>rfaD</i>	Encode cell wall components (EPS, LPS)		
		<i>lacl</i>	Encodes a transcriptional regulation protein		
RT-PCR	<i>Streptococcus pneumoniae</i>	CSP receptor gene <i>comD</i>	Encodes a QS peptide for competence system induction, biofilm formation, virulence enhancement	495	
Quantitative RT-PCR	<i>Streptococcus mutans</i>	<i>brpA</i> , <i>comDE</i> , <i>vicR</i>	Encode regulatory proteins	496	
		<i>gbpB</i> , <i>spaP</i>	Adhesion facilitation		
		<i>ftf</i> , <i>gtfB</i> , <i>gtfC</i>	Polysaccharide synthesis		
		<i>relA</i>	Acid stress tolerance		
		<i>smu0630</i>	Biofilm formation in both presence and absence of sucrose		
		<i>A. baumannii</i>	<i>pgaABC</i> gene cluster		Extracellular matrix production and biofilm thickness increase
<i>Y. pestis</i>	<i>hmsT</i>	Regulatory gene, biofilm formation on biotic/abiotic surfaces	498		
<i>P. aeruginosa</i>	<i>psl</i> , <i>pel</i> (*)	Biofilm formation, protection against aminoglycoside antibiotics (*)	25		
<i>Salmonella</i> spp.	<i>spiA</i> , <i>qseB</i>	<i>spiA</i> is involved in biofilm formation and virulence	487, 499		

(Continued on next page)

TABLE 3 (Continued)

Method	Species	Gene(s)	Function	Reference(s)
			<i>qseBC</i> are involved in fimbria regulation, biofilm formation, quorum sensing, virulence	
Multiplex PCR	CoNS	<i>ica</i> gene cluster	PIA biosynthesis, cell accumulation, biofilm formation	500
Quantitative multiplex PCR		<i>mecA</i> , <i>agrA</i> , <i>sarA</i> , <i>atlE</i> , <i>divIVA</i> (**)	<i>mecA</i> is involved in resistance to methicillin <i>agr</i> locus is involved in cell wall and extracellular protein synthesis <i>sarA</i> is involved in hemolysin production <i>atlE</i> is involved in initial adherence <i>divIVA</i> is involved in cell division, is unique to <i>S. epidermidis</i> (**)	501
	MRSA	<i>sea</i> , <i>seb</i> , <i>sec</i> , <i>sed</i> , <i>see</i> , <i>seg</i> , <i>seh</i> , <i>sei</i> , <i>sej</i> <i>eta</i> , <i>etb</i> , <i>etd</i> , <i>cna</i> , <i>atl</i> , <i>fnbA</i> , <i>fnbB</i> , <i>cap5HK</i> , <i>cap8HK</i>	Staphylococcal enterotoxin genes <i>eta</i> , <i>etb</i> , and <i>etd</i> are exfoliate toxin genes <i>cna</i> , <i>atl</i> , <i>fnbA</i> , and <i>fnbB</i> are adhesion genes Surface-associated genes	502
Real-time PCR	<i>E. faecalis</i> <i>S. epidermidis</i>	<i>gelE</i> (***) <i>sarA</i> , <i>arlRS</i>	Gelatinase production, virulence factor Encode staphylococcal regulators	503 504
Quantitative real-time PCR	<i>S. aureus</i> <i>P. aeruginosa</i>	<i>icaC</i> , <i>fnbA</i> , <i>fnbB</i> , <i>clfB</i> QS genes ( <i>lasR</i> , <i>rhIR</i> ) (***)	Adhesion genes Production of autoinducer molecules important for cell-to-cell communication, coding for acyl homoserine lactone (AHL) synthase, biofilm formation, resistance, motility (***)	505 506, 507

<sup>a</sup>PIA, polysaccharide intercellular adhesion; TA, toxin-antitoxin system; AHL, acyl homoserine lactone; QS, quorum sensing; EPS, extracellular polymeric substances; LPS, lipopolysaccharides; CoNS, coagulase-negative staphylococci. Some genes were studied by use of more than one technique, as follows: \*, studied with RT-PCR; \*\*, studied with multiplex PCR; and \*\*\*, studied with real-time PCR.

The heterogeneous, noncrystalline, and insoluble biofilm extracellular matrix is a rather perplexing assembly. Proteomics has provided deeper knowledge by (i) giving insights into the protein profile determinants that regulate host-pathogen interactions as well as the virulence and pathogenicity traits of the menacing bacteria; (ii) answering substantial questions regarding the biofilm antimicrobial resistance phenotype, offering potential alternatives for rational drug design; and (iii) underpinning physiological differences from planktonic species (187–189). Indeed, the use of proteomics has been substantiated by mass spectrometry (MS) to extend its utility beyond research in the field of diagnostics to clinically oriented infectious disease investigation, with particular emphasis on host-pathogen interactions (190, 191). The coupled use of proteomics with MS was an amenable mapping approach in a landmark study of the microbial proteome and the human microbiome (192). Moving one step further, metaproteomics constitutes a cutting-edge tool for the study of multispecies community interactions by means of cooperation and competitiveness and the ways that these relationships shape the microbial consortium. Metaproteomics also offers the ability to elucidate the metabolic signatures of multispecies biofilms, even for the unculturable bacteria that reside within biofilms but cannot be cultivated by classic microbiological means, potentially providing novel tools for drug design (189, 193, 194).

Hydrogen nuclear magnetic resonance (<sup>1</sup>H-NMR) has been deployed for proteomic chemical compositional biofilm analysis and exhibits wide applicability to single- and multispecies communities. A “sum-of-the-parts” method to examine *E. coli* amyloid-integrated biofilms aimed to determine the pristine biofilm ECM composition. NMR also allows principal chemical component analysis, supporting the identification of key features between methicillin-susceptible *S. aureus* (MSSA) planktonic and biofilm species. The phenotypic differences were attributed to the uptake of specific amino acids, lipid catabolism, fermentation of butanediol, and metabolism alterations ranging from the production of energy to the accumulation of cellular components

(195). Structural and morphological properties are also characterized by  $^{13}\text{C}$ -NMR, which groups carbon pools from a single intact ECM sample. This approach defined the chemical composition and protein content of *Vibrio cholerae* biofilms (196, 197). Proteome-wide tagging and labeling of bacterial proteins allow state-selective analysis and were applied to determine differences in predetermined proteins for planktonic and sessile bacterial species (198). Another example of NMR-based applications for diverse systems involves total correlation spectroscopy (TOCSY)-NMR for the detection of solution and carbohydrate polymer components in *S. epidermidis* biofilms (199). Although NMR is a good choice for biofilm compositional study, in the case of full matrix analysis and determination of the actual composition of biofilm carbohydrate components MS is usually applied due to the need for derivatization into monosaccharides.

## IMAGING MODALITIES TO VISUALIZE COMMUNITY ARCHITECTURE

Evolving imaging modalities have contributed to significant improvements in spatial and temporal characterization of biofilms themselves and the signaling factors that alter bacterial behavior within the host-biofilm microenvironment (Table 2).

### Optical Microscopy

Fluorescence *in situ* hybridization (FISH) utilizes nucleic acid probes that bind to cRNA or DNA sequences within individual bacterial cells, enabling visualization of the spatial distribution of multispecies biofilms by use of specific probes (16S or 23S rRNA) along with epifluorescence microscopy. The targets are independent of cell metabolism levels, so FISH detects all viable microorganisms, including unculturable ones (200). Peptide nucleic acids (PNA) exhibit higher target specificity and better hybridization kinetics. PNA FISH is versatile in clinical microbiology and biofilm investigations, in combination with confocal laser scanning microscopy (CLSM), offering species identification, spatial information, and bacterial load determination within mixed-species biofilms in chronic wound specimens and CF sputum (201, 202). On the other hand, immunofluorescence (IF) assay employs fluorescently labeled antibodies that bind to specific target antigens and detect cell types or cellular subcomponents defining expression at biofilm developmental stages (203).

The use of specific fluorescent probes has enhanced the specificity of CLSM for protein quantification and localization within colony biofilms. The structural complexity of the microbial polysaccharides confers a significant limitation on the use of labeled probes (45, 204, 205). Fluorescent probes (dextrans, rhodamines, and Oregon Green) and fluorescence correlation spectroscopy (FCS) combined with CLSM enable biofilm diffusion quantification and thickness evaluation. These provide information on factors affecting antibiotic and biocide transportation within the biofilm microenvironment (206). CLSM in combination with computational software can be extended to a multi-spectral and three-dimensional (3D) biofilm imaging and quantification technique. Digital analysis has replaced conventional qualitative and semiquantitative techniques with more accurate and sensitive procedures. Computer programs and software packages for biofilm visualization, quantification, and deconvolution (Imaris, COMSTAT, Amira, Volocity, ISA3D, ImageJ, and Fiji), containing structural variables including porosity, thickness and roughness coefficients, fractal dimension, and homogeneity, have been launched or belong in the public domain, thus providing analysis options (207–209).

Structured illumination microscopy (SIM) enhances fluorescence abilities for 3D imaging of living cells (210). Computational removal of out-of-focus light leads to true optical sectioning via exclusion of the associated blurred images (211–213). 3D-SIM visualizes macromolecules interacting within the surrounding cellular environment.

Optical coherence tomography (OCT) offers real-time, 3D *in vivo* biofilm imaging ideal for biomass structure development and porosity identification. OCT enables nondestructive *in situ* biofilm analysis for chronic middle ear infection and dental

biofilm growth monitoring (214, 215). Doppler OCT imaging can be employed for quantitative biofilm dynamics analysis during the biofilm formation stages (216).

### Electron and X-Ray Microscopy

Transmission electron microscopy (TEM) offers a high resolution for visualizing specific structural components, such as polysaccharide fibrils and extracellular DNA. Combined with ruthenium red staining, TEM reveals the morphological features of bacterial cells within a fibrous matrix; such an example is the confirmation of the presence of *P. aeruginosa* biofilm in a burn wound animal model (204). Scanning electron microscopy (SEM) is applied for biofilm structure and function (morphology, glycocalyx density, and layer thickness) analysis on living surfaces or inanimate materials. Compared to TEM, it is considered the optimal imaging tool, offering detailed, high-resolution 3D biofilm visualization (217). *Staphylococcus lugdunensis* and *Propionibacterium acnes* causing implant-related osteomyelitis in an *in vivo* animal model were visualized by SEM analysis when present in intercellular aggregates within the bone marrow but not when localized intracellularly (218).

Unlike SEM and TEM, environmental SEM (ESEM) retains visualization ability without laborious sample preparation and facilitates imaging of external cell polymers, though the spatial resolution is reduced compared to that of traditional SEM techniques (217, 219). ESEM combined with energy-dispersive X-ray spectroscopy (EDS) has been employed for determination of the *Proteus mirabilis* biofilm composition on infected urinary catheters (219). Finally, cryo-SEM is optimal for fragile, fully hydrated samples, offering ultrafast freezing as an optimal method of nonsolid specimen fixation (220). When biofilms from diabetic foot wounds were investigated using SEM, a high level of resolution and detail was obtained, but the exopolymer matrix was destroyed during sample preparation. This limitation was overcome by the application of ESEM or cryo-SEM due to preservation of the biofilm hydrated state (221).

The recent discovery that ionic liquids provide clear SEM-based visualization of biofilms from fully hydrated biological samples has opened new ways for broad SEM utilization (222). Additionally, the method of immersed atmospheric SEM (ASEM), combining heavy metal labeling, charged nanogold labeling, and immunolabeling, enabled visualization of nanostructures of the biofilm-surface interface in liquids (223).

Scanning transmission X-ray microscopy (STXM) provides data on spatial distribution as well as quantitative and qualitative analyses of biofilm components, thus dissecting the heterogeneity of microbial communities (224). For example, multispecies microbial consortia have been investigated by STXM for the analysis of selenium particle biotransformation (225). In another application, a CLSM-STXM combination was used on pseudomonal biofilms tested with antimicrobial agents, such as chlorhexidine dihydrochloride, benzalkonium chloride, triclosan, and trisodium phosphate, to detect differences in cell density, spatial distribution, and membrane integrity (226).

### Scanning Probe Microscopy and Imaging Mass Spectrometry

Atomic force microscopy (AFM) has gained increased attention due to its microbial cell surface structural and physical probing ability (227, 228). AFM applications involve visualization of the biofilm structure and detection of the physicochemical interactions (van der Waals and electrostatic forces) between microbial cells and various surfaces (229). For example, an AFM-mediated investigation of *P. aeruginosa* biofilm formation and adhesion on surface substrates, including sheets of aluminum, steel, rubber, and polypropylene, indicated that the polypropylene substrate's rough surface exhibited enhanced bacterial adherence compared to that on steel (230). Confocal resonance microscopy (CRM) determines chemical differences among bacterial species. This technique can be used to map distributions of biomass, EPS, chemical components, and molecular compounds (231).

Matrix-assisted laser desorption ionization–imaging mass spectrometry (MALDI-IMS) provides the spatial molecular distribution for each identified molecule within the biomass (24). IMS generates a wealth of data for developing “chemical fingerprint”

databases that enable chemical definition of colonies between bacterial species as well as discrimination of the subpopulations within biofilms (50, 232, 233). MALDI-IMS was used on single-species UPEC biofilms in order to analyze differences in the spatial proteome of adhesive fibers that confer virulence and biomass growth. Phase variation of the promoter of *fim*, encoding type 1 pili, was found to be under the control of oxygen availability (24).

Secondary ion mass spectrometry (SIMS) constitutes a label-free imaging methodology providing the highest depth and spatial resolution (234, 235). Unlike MALDI-IMS, SIMS does not require the use of a matrix to get spatial information. When complemented with MALDI and CRM, this method provides identification and specific locations of proteins and other chemical species, macroscopic and cell-level chemical differences, mass-based discrimination of similar molecules, and the spatiotemporal distribution of metabolites and signaling molecules, even for multispecies biofilms (234–236). For example, the chemical heterogeneity and secondary metabolites, such as rhamnolipids or quinolones, participating in biofilm growth and cellular signaling of a *P. aeruginosa* wild-type strain and an isogenic QS mutant were investigated by MALDI-SIMS, providing *in situ* chemical mapping (234).

The future of biofilm visualization requires (i) *in situ* imaging of fully hydrated biological specimens, with avoidance of biofilm-destructive procedures; (ii) defined probes that enable a combination of imaging techniques for better resolution and 3D structure and/or microscopy that does not require probes (OCT or magnetic resonance imaging [MRI]); and (iii) updated software tools to meet the demands for enhanced digital biofilm imaging analyses (209).

### MODELING BIOFILMS EX VIVO

*Ex vivo* models involve biofilm growth on natural tissue in a minimally altered environment, offering more strictly controlled experimental conditions for extensive research than those of *in vivo* models (5). They facilitate the study of the association between biofilm formation and virulence or determinants of pathogenicity. These models contribute to the development of effective imaging tools that can monitor tissue-specific bacterial establishment. For example, porcine skin explants infected with *S. aureus* and *P. aeruginosa* have been used for the growth of mature biofilms that mimic chronic skin wounds and provide a way to assess antibiofilm antibiotic efficacy (237).

Implants and medical devices enable biofilm formation that results in chronic infection. An *ex vivo* whole-blood model of *S. epidermidis* prosthetic joint infection was employed to elucidate the association between complement C5a levels and PIA-related biofilms as one of the main components of biofilm accumulation (238). An *ex vivo* model of MG63 human osteoblasts cocultured with *S. epidermidis* strains was used to examine whether infection-related isolates exhibit adherence and internalization abilities different from those of commensal isolates. Flow cytometry, BRT, and CV assays were combined to test this hypothesis, which showed no statistically significant difference compared to studies on the harboring and expression of virulence factors that efficiently discriminate invasive strains from commensals (110, 239).

*Ex vivo* models are also useful for assessing therapeutic windows of antibiofilm experimental treatments. A 3-day tolerant *S. aureus* biofilm grown on a porcine skin explant model was no longer detectable after treatment with a surfactant-based wound dressing, whereas biofilms wiped with moistened gauze reoccurred (240). In a similar model, biofilms formed within the first 24 h were found to be more susceptible to antibiotics than mature formations, validating current therapeutic strategies that aim at early wound prophylaxis (241). Similarly, porcine skin models have been used to test the effect of negative-pressure wound therapy with instillation on *P. aeruginosa* biofilms as well as the influence of tetracycline release of a zein and poly- $\epsilon$ -caprolactone (zein/PCL) fibrous dressing on *S. aureus* biofilms (242, 243). The comparative efficacy of glycine and tricalcium phosphate (TCP) over that of glycine or sodium bicarbonate in biofilm removal was examined by use of an *ex vivo* model using biofilms grown on

titanium (Ti) and zirconium (Zr) implant surfaces (244). The effects of topical treatments and commonly used antimicrobial dressings on biofilms of different maturation levels were also tested (237, 245).

Cardiac valves constitute a substratum for *in vivo* clinical biofilms, highlighting the need for an *ex vivo* study model. An *ex vivo* model of porcine cardiac valve tissue combined with electron microscopy was used to examine the effects of the aggregation substance (Asc10) protein of *E. faecalis* on biofilm formation and persistence in endocarditis. It was found that Asc10 increased cell aggregation, leading to accelerated biofilm formation (246).

The murine respiratory pathogen *Mycoplasma pulmonis* was recently used for biofilm development of a tracheal epithelium organ-mounting system that can be scanned with a fluorescence microscope, resulting in the observation that *in vitro* and *ex vivo* biofilms share common structural features and characteristics (247). In a similar way, an *ex vivo* pig model of bronchiolar tissue infected with *P. aeruginosa*, resembling the CF lung mucus environment, provides a realistic and replicable HT assay to study the structure as well as virulence and physicochemical traits present in chronic biofilm-associated lung infections (248).

The otitis, nasal, and throat mucosal biofilm formation models are further substrates for *ex vivo* biofilm model applications (249). An *ex vivo* model of stainless steel tympanostomy tubes inoculated with *P. aeruginosa* and *S. pneumoniae* combined with SEM was used to examine biofilms formed on clearance of mucoid plugs after ofloxacin challenge (250). Moreover, consecutive lavage samples of otitis media biofilms revealed the presence of NTHi subpopulations with different growth rates and gene expression modes (251). In the case of the oral cavity, an *ex vivo* root canal model was applied to test the parameters influencing the efficacy of irrigation in biofilm removal, utilizing marketed fibronectin- and collagen-based films (252, 253).

In a GI biofilm study, the pathogenicity of *Aeromonas caviae* strains isolated from human feces was investigated by use of an *ex vivo* rabbit ileal and colonic mucosa model. Cultured tissue was used for adhesion assessment of *A. caviae* strains (incubated with colonic and ileal intestinal fragments), whereas microscopy generated information regarding colonic and ileal mucosa colonization and biofilm formation (254).

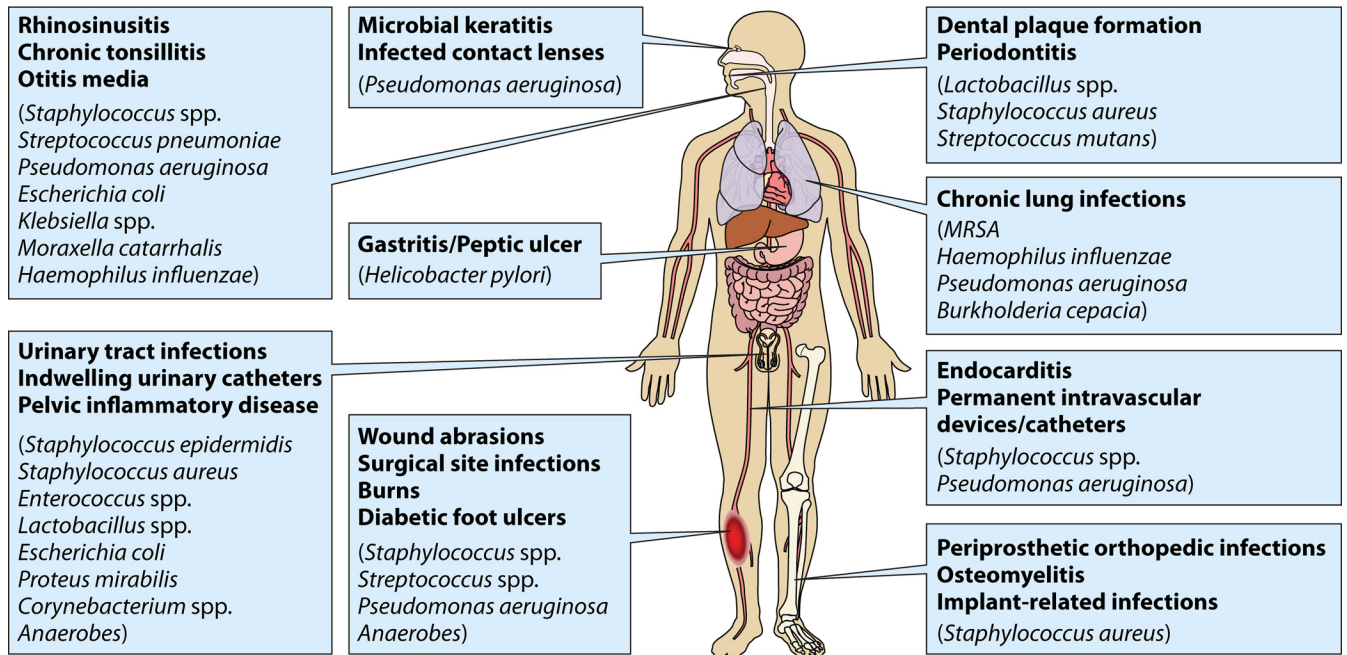
A porcine vaginal mucosal model (PVM) aimed to investigate the interactions among the commensal vaginal *Lactobacillus* spp., the anaerobic species *Gardnerella vaginalis*, and the sexually transmitted organism *Neisseria gonorrhoeae*, as well as the mechanisms of biofilm formation. The model quantified and unraveled different profiles for the effects of pH, acids, and *Lactobacillus crispatus* on *G. vaginalis* and *N. gonorrhoeae* growth when a live vaginal mucosal surface was used (255).


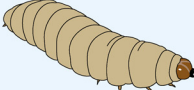
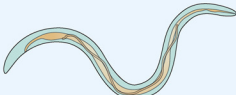


## DISSECTING BIOFILMS *IN VIVO*

The urgent need to investigate biofilm-associated infections and develop effective therapeutic strategies gave birth to translational approaches that allow the dissection of virulence and pathogenicity determinants and the identification of novel therapeutic targets. The widespread host-based models simulating biofilm-related mammalian diseases (Fig. 4) are discussed below.

### Nonvertebrate Animal Models

Exploiting nonvertebrate animal models has provided an important solution to the need for investigations of biofilm-associated infections. The fruit fly (*Drosophila melanogaster*), the wax moth (*Galleria mellonella*), and the nematode worm (*Caenorhabditis elegans*) have historically been used to evaluate microbial virulence traits involved in mammalian infections and to test the efficacy of antimicrobial compounds (256–262). These studies have elucidated factors affecting virulence, pathogenicity, and host immune responses by altering gene expression, studying efflux systems, toxins, or QS compounds, and allowing easy measurement of the host mortality (263–270). The majority of pathogenic assays using these invertebrate models, by design, detect



	Model organisms	Pathogen tested	Associated infections
<b>Non-vertebrate animal models</b>	 Fruit fly	<i>Pseudomonas</i> spp. <i>Providencia sneebia</i> <i>Yersinia pestis</i>	Epithelial/Wound/Gut infection
	 Wax moth	<i>Pseudomonas aeruginosa</i> <i>Acinetobacter baumannii</i> <i>Burkholderia cepacia</i> <i>Burkholderia multivorans</i> <i>Campylobacter</i> spp.	Sepsis Visceral invasion
	 Nematode	<i>Pseudomonas aeruginosa</i> <i>Escherichia coli</i> <i>Burkholderia pseudomallei</i> <i>Burkholderia cepacia</i> (Bcc) <i>Yersinia pseudotuberculosis</i>	Pulmonary infection
<b>Mammalian Animal models</b>	 Zebrafish	<i>Streptococcus suis</i> <i>Mycobacterium haemophilum</i> <i>Pseudomonas aeruginosa</i> <i>Vibrio parahaemolyticus</i>	Meningitis Septicemia Visceral organ granulomatosis Chronic inflammation Gut infection
	 Rat/ Mouse	<i>Staphylococcus aureus</i> <i>Staphylococcus epidermidis</i> <i>Enterococcus</i> spp. <i>Mycobacterium bovis</i> <i>Pseudomonas aeruginosa</i> <i>Escherichia coli</i> <i>Vibrio vulnificus</i> <i>Acinetobacter baumannii</i> <i>Porphyromonas gingivalis</i>	Burn, abscess, wound, arthritis, respiratory tract/gut/ implant/surgical site infection, catheter-associated urinary tract infection, periodontitis, osteomyelitis

**FIG 4** Comparative visualization of biofilm-attributed human infections and classes of major vertebrate and nonvertebrate models developed. This is not an extensive list, but presentation of the bacterial strains that are most commonly encountered in biofilm-related research studies is included.



survival rates despite the wealth of microscopy and molecular methodologies that are often employed as surrogates for intensive interrogation.

*Drosophila* is extensively used to model wound or epithelial infections by Gram-negative bacteria, and comprehensive methodology exists for modeling persistent colonization and for assays of persister cell formation (271–273). For the adult fly, the infection methodology includes (i) needle pricking (mimicking wound infection), (ii) feeding (mimicking oral infection methods), and (iii) injection pumping (mimicking a systemic infection similar to bloodstream infection in mammals). Larvae are less commonly infected than adults with either the feeding or injection pumping method (271–273).

Innate host responses in *Drosophila* against *P. aeruginosa* are largely conserved in humans (274–276). It was also demonstrated that there is a remarkable conservation in the virulence factors used by bacteria to infect both *Drosophila* and mammals (277, 278). *Drosophila* models remain valuable tools for exploring biofilm molecular determinants; two adherence factors required for *in vivo* virulence of *Pseudomonas fluorescens* are (i) *gmd*, encoding the enzyme GDP-mannose dehydratase, involved in the synthesis of A-band-O-antigen-containing lipopolysaccharide (LPS); and (ii) a *fadL* homologue involved in long-chain-fatty-acid transport (279). *D. melanogaster* has served as a model for the study of the functional correlation of the paraoxonase family members with biofilm formation and QS *in vivo*. This correlation has shown the protective role of the human enzyme paraoxonase 1 (PON1) in innate immunity (280). Finally, *Drosophila* as an infection model of *P. aeruginosa* biofilms has provided a direct or indirect model of virulence and pathogenesis determinants through comprehensive analysis of the molecular responses of hyper- and low-biofilm-forming strains (281).

The fly has also proven valuable for modeling of biofilm formation by *Providencia* spp.; it was identified that *Providencia sneebia* is lethal while propagating in the fly but elicits a mild immune response (282). Moreover, a chronic gut *Yersinia pestis* infection was established in the anterior fly larva midgut to mimic and dissect the relationships between biofilm-associated genes (PhoP, GmhA, and OxyR), the gut immune system, and antimicrobial peptides (283).

*Galleria mellonella*, a worm with a complex immune system, provides a competitively advantageous alternative to other hosts regarding size and amenability for the evaluation of antimicrobial treatments (284). The infection development model employs larval caterpillars (third- or final-instar stage) that are injected with bacteria in the hemocoel via the last left proleg (285). The wax moth has (i) facilitated screening of a U.S. Food and Drug Administration-approved library to identify antibiofilm compounds against *Francisella novicida* (286); (ii) been used to model biofilm formation by *Acinetobacter baumannii*, *Burkholderia cepacia*, *Burkholderia multivorans*, *Campylobacter* spp., and species in polymicrobial infections, such as the *P. aeruginosa* Liverpool epidemic strain and oral streptococci (287–292); and (iii) been applied for evaluation of the antibacterial and antibiofilm activities of alternative therapeutic strategies against a multitude of pathogens, including *S. aureus*, MSSA, MRSA, and *Acinetobacter baumannii* (293–295).

The free-living nematode *C. elegans* has been used to model infections by most Gram-negative bacteria, including *E. coli*, *Burkholderia pseudomallei*, *B. cepacia* complex (BCC), *P. aeruginosa*, and *Yersinia pseudotuberculosis*, through the feeding methodology (296–300). The *C. elegans*-BCC interaction studies provided insights into the identification of the roles of specific biofilm-related virulence factors, including (i) the autoinducer-dependent acyl-homoserine lactone (*aidA*), (ii) the phenazine biosynthesis regulator (*pbr*), and (iii) the host factor phage Q (*hfq*) surface-associated lipoproteins (261, 301–307).

A few reports involve less common invertebrate hosts for modeling of biofilm infections, such as (i) the ciliated protozoan *Tetrahymena pyriformis* for *Legionella* sp. and *K. pneumoniae* biofilms, (ii) the amoebae *Acanthamoeba* spp. for *Legionella* sp. and nontuberculous mycobacterium (NTM) biofilms, and (iii) the soil-living amoeba *Dictyostelium discoideum* for *A. baumannii*, *Legionella* sp., *P. aeruginosa*, and *S. aureus* biofilms

(308–314). There have been attempts to employ plants, such as the duckweed *Lemna minor* and the wounded alfalfa *Medicago sativa*, to allow biofilm growth of *Burkholderia cenocepacia* and *S. enterica* (315–317). *Arabidopsis thaliana* (thale cress) is a popular tool in plant molecular biology that has been utilized as a host system to study *B. subtilis* and *P. aeruginosa* biofilm formation (318, 319).

### Vertebrate Animal Models

Vertebrate animal models have been used extensively to mimic human biofilm infections and to test antimicrobial efficacy (320, 321). Localized mammalian animal models may refer to skin and soft tissue infections experimentally studied by use of infected excisional wounds, partial-thickness abrasions, scratches, burns, abscesses, and surgical sites. Apart from the pathogen of interest, experimental variation can also include the mammalian host by alteration of its immunological state (5, 266, 321–338). Here we include some examples from the literature which underline the recent efforts and achievements in the field of vertebrate-based biofilm formation and evaluation.

The optically clear zebrafish, *Danio rerio*, has been applied for *P. aeruginosa* biofilm imaging and for biofilm formation quantification of the bacterial fish pathogen *Edwardsiella tarda* and the pig pathogen *Streptococcus suis* (339–342). Zebrafish has also been used to study *Mycobacterium haemophilum* and to evaluate oral pathogen adhesion in a vertebrate orointestinal model (343, 344).

Mouse model biofilm formation has been described for (i) a multidrug-persistent *A. baumannii* murine wound infection to evaluate therapeutic solutions against trauma and surgical infections in hospitalized patients (345) and (ii) BALB/c and C3H/HeN mice to study chronic *P. aeruginosa* wound infection establishment after a third-degree burn with skin necrosis (346).

Reports for *in vivo* porcine skin infection models are surprisingly scarce given, for example, the MRSA-associated skin wound model that examines the effective bacterial load reductions of various methods of debridement (hydrosurgery and plasma-mediated bipolar radiofrequency ablation) (347). Antimicrobial photodynamic therapy (aPDT) has been applied against a variety of pathogens implicated in acute and chronic biofilm-associated infections. In order to test the efficacy of photosensitization, various animal models have been applied. Mouse, rat, and pig wound, osteomyelitis, and arthritis models as well as dog dental infection models revealed the therapeutic potential of PDT against pathogens, including streptococci, MSSA, MRSA, *P. aeruginosa*, *A. baumannii*, *P. gingivalis*, and *Fusobacterium nucleatum* (322–327).

Rat models are in constant use due to their amenability to wound and infection site colonization without the requirement of disturbing factors (foreign bodies or diabetes mellitus induction), allowing a correlation with rat age, location of the wound, and size of the inoculum (348). Mouse models employing tissue cages and catheter infection can provide information about the antimicrobial efficacy of biomaterial coatings and host-pathogen interactions (349, 350). In the field of implanted device-associated infections, a major model involves totally implantable venous access ports (TIVAPs) implanted in rats. This model allows monitoring of bacterial biofilm development, physiology, and prevention strategies by use of inocula of four bioluminescent pathogens, including *S. aureus*, *S. epidermidis*, *E. coli*, and *P. aeruginosa* (351). Along with rat models, rabbits have also been used in prospective animal studies to investigate, for example, the effect of a 60- $\mu$ A implantable direct-current fusion stimulator on the implant-related infection rates in a postoperative spinal wound infection model. All sites were inoculated with MSSA, but no significant difference was observed for the implant and bone infection rates and the bacterial load (352). Another observation found by use of an indwelling device rat model was the inhibitory effect of QS disruption via RNAIII-inhibiting peptide (RIP) on *S. epidermidis* infections (333).

Titanium implants have been used to examine the inhibitory and prophylactic effects of gentamicin coatings on titanium oxide surfaces (bioactive TiOB) (353). Likewise, murine osteomyelitis models have been developed to monitor immune responses occurring during *S. aureus* infection and healing (interleukin-4 [IL-4] and

gamma interferon) following implant placement after bone fractures. A fracture fixation murine model employed skeletally mature C57BL/6 mice that were treated with Ti fracture fixation plates and screws after femur osteotomy (354). A rat model of acute foreign-body osteomyelitis was used to evaluate the role of the *E. faecalis ahrC* and *eep* genes in biofilm formation and virulence. Stainless steel orthopedic wires were inoculated with *E. faecalis* OG1RF  $\Omega$ *ahrC* and  $\Delta$ *eep* isogenic mutants and implanted into the proximal tibiae of rats (355). In an *S. aureus*-associated murine osteomyelitis model, a fixation plate was employed for debridement of the fracture during a revision surgery, followed by the placement of a vancomycin-laden implant. Infection monitoring was achieved via bioluminescence imaging, X-ray, and micro-computed tomography ( $\mu$ CT) for the evaluation of both osteolysis and bone formation (328).

An implantable-cage MRSA infection model using male albino guinea pigs was developed, and treatment efficacy against planktonic and biofilm infections was evaluated for the most commonly prescribed antimicrobial agents. Antimicrobial testing concluded with an optimal combination of fosfomycin and rifampin against implant-associated MRSA infections (356). Rabbits have also been used in models of spinal implant *S. aureus* infections to assess the antimicrobial potential of modified Ti pedicle screw coatings as well as the efficacy of front-line antistaphylococcal drugs (357, 358).

The majority of models developed for the study of gastrointestinal colonization and biofilm formation are murine, with an emphasis on colitis. One of these mouse models identified the importance of the stringent response regulator DksA for *Salmonella* pathogenicity, virulence, and biofilm formation. During early stages of *S. Typhimurium* infection, DksA is induced at the murine midcecum and is required for systemic infection (359). Likewise, the contribution of other bacterial species to early GI colonization was proved by use of a *Clostridium difficile* colon and cecum mucus mouse model with FISH application (360). A notable reported intestinal model involves evaluation of *Shigella flexneri* adhesiveness in the guinea pig gut. Deficient LPS inner core biosynthesis presented by the  $\Delta$ *rfaC* mutant resulted in enhanced biofilm formation on and adhesion and invasiveness to human epithelial cells, an observation that could be utilized for the development of new therapeutics. It was also concluded that fitness gains through host adhesion and strong biofilm formation did not replace the effect of fitness loss due to LPS deletion on survival rates (361).

Mouse models have also been applied to mimic biofilm-associated UTIs as well as to evaluate the correlation between host immune systems and local defense factors, the attributed infection (nephron obstruction and pyelonephritis), and treatment (362). Future UTI models may utilize human-mouse chimeras based on severe combined immunodeficient (SCID)-hu mice in order to achieve a better match with human conditions (321).

*P. aeruginosa* is of utmost importance in chronic lung infection, and efforts to reveal the relationships between the vertebrate host and virulence factors are long-standing (329). A murine inhalation model was developed to connect chronic *P. aeruginosa* nasopharyngeal carriage with lung infection, which complicates and increases resistance to therapeutic agents (363). In a *P. aeruginosa* and *S. aureus* coinfection mouse CF model, *P. aeruginosa* isolates were found to outcompete *S. aureus* at early stages of chronic infection (364). Moreover, the therapeutic potential of inhaled liposomal amikacin was tested in a *P. aeruginosa* rat lung infection model (330). *P. aeruginosa* biofilms formed on murine tumors have also been used to examine the efficacy of ciprofloxacin, colistin, tobramycin, and their combinations (331).

Oral biofilms are a major chapter in biofilm-related literature, and the quest for animal models in closer proximity to humans leads to the exploitation of primates. In a screening effort to identify an optimal host for monitoring *Aggregatibacter actinomycetemcomitans*, the leading cause of periodontitis in humans, *Macaca mulatta* (rhesus [Rh] monkeys) ranked as the first choice. Rh monkeys provide an established oral habitat to validate *A. actinomycetemcomitans*-mediated periodontitis (365). Rh monkeys have also been tested for age-mediated apoptosis gene expression in oral mucosal tissues. The transcriptomic analysis of apoptotic gene expression reflects

decreased apoptotic phenomena in the oral mucosa of aging animals that consequently may increase dysregulation in anti-inflammatory responses and induce disease (366).

A murine periodontitis model combined with genomics and quantitative PCR was used to examine the role of host factors in persistent subgingival biofilms (336). Likewise, a rat model of *A. actinomycetemcomitans*-induced periodontitis was combined with RT-PCR for versatile applications, ranging from genetic reduction to therapeutic efficacy evaluation according to exopolysaccharide variations (367). Another rat model, the *in vivo* extraradicular biofilm model, is more inclusive, as it may facilitate identification and quantification of biofilm-forming bacteria by use of real-time PCR (rt-PCR) and micro-computed tomography (368). Chinchillas (*Chinchilla lanigera*) have been employed for study of middle ear infections in an attempt to establish realistic infection models, to overcome limitations in biofilm analysis, and to correlate the sequence of events in polymicrobial infections with the host immune system. A chinchilla otitis media model involving an NTHi 86-028NP isolate and an isogenic phosphorylcholine (PCho) transferase (*licD*) mutant was deployed to show that PCho facilitates biofilm stability and alleviates the host immune response, promoting NTHi infection and increased persistence (369).

Biofilm treatment efficacy testing is a field that demands available surfaces and assays, and rabbits and guinea pigs have been tested toward this end. A rabbit otitis model examined the efficacy of a nanoporous middle ear implant coating releasing ciprofloxacin against *P. aeruginosa* (370). In another study, a guinea pig animal model combined with otoendoscopy, histology, and bone CT was used to examine the inhibitory effect of a vancomycin-eluting nanofiber mat against MRSA biofilms formed on ossicular prostheses and middle ear infections (371).

Animal models offer insight into the interplay of basic biofilm features and host defense mechanisms (372). However, the risk of coincidental assessment of the experimental conditions is high, and most mammalian models are considered not identical in effectively reproducing the major infectious entities within the human host (Fig. 4).

### IN VIVO IMAGING TOOLS

Bioluminescence imaging takes advantage of bacterial cloning vectors optimized to allow for the expression of luciferin in different bacterial cells (373). As a result, these microbial cells “glow in the dark,” and a sensitive imaging camera is able to capture images of small animals, revealing both the location and intensity of the infecting microorganisms in real time, in a noninvasive manner. This technology has dramatically reduced the number of animals needed to obtain statistically significant data on antimicrobial therapeutics (374). Previously, animals were generally sacrificed at discrete time points, followed by tissue removal, homogenization, and CFU culture and enumeration. This has often left unanswered the question of what happens at later times, as many antimicrobial treatments are highly effective at early time points but the microbial cells regrow when the initial antimicrobial action has ceased (351, 375). Scarce protocols examine the dynamic processes of biofilm formation, bacterial load, infection physiology, and response to treatment for *in situ* models of implantable devices. Bioluminescence combined with a totally implantable venous access port model has been used to assess localized and systemic infections related to CVC in rats, reproducing clinically significant situations of foreign body-associated infections (351). These models have been valuable in the investigation of aPDT, which involves photosensitizing dyes topically applied to the infection site and subsequent harmless visible light illumination and reactive oxygen species (ROS) generation (324, 376). Bioluminescence imaging of localized infections not only is well suited for monitoring the effectiveness of experimental antimicrobial therapeutics but also has a major role in the study of microbial virulence and pathogenicity. A virulence-specific study of an oral mouse infection model that employed a multiplexed biophotonic imaging-based inducible luciferase reporter was used to track individual species temporally and spatially in polymicrobial biofilms (377). Bioluminescence technology has expanded to

include imaging in three dimensions for biofilm infections that would otherwise be challenging to monitor and treat (378–382).

Near-infrared fluorescence molecular probes have been delivered by local injection and used to visualize inflammation as well as implant-related biofilm infections in a rapid and minimally invasive manner, therefore aiming at detecting orthopedic-related infections (383). The hydro-sulfo-Cy5 probe detects ROS generation following bacterium-free or biofilm-containing implant application. On the other hand, diamino-cyanine sulfonate was used to detect *ad hoc* biofilm-associated nitric oxide production (384).

The dye C-SNARF-4 coupled with ratiometric imaging allowed 3D visualization in real time of the extracellular pH variation in the growth of dental biofilms (385). Ligand-targeted ultrasound contrast agents (UCAs) coupled with optical and high-frequency acoustic microscopy have facilitated detection, visualization, and quantification of *S. aureus* biofilm matrices in both test tube and animal model adjusted surface cultures (386). Noninvasive 3D OCT can be used to identify as well as visualize, in real time, *in vivo* bacterial microcommunities involved in biofilm-associated otitis media (387). OCT has been coupled with low-coherence interferometry to image the biofilm layer on the sensitive, ultrathin tympanic membrane in the middle ear (388). Another optical technique, intraoral cross-polarization swept-source OCT (CP-OCT), provided an additional tool to visualize the *in vivo* density of the biofilm formed between the enamel and the interface (389). Spatially resolved MRI was used to study structures within dynamic physical and chemical material systems, and also in biological systems, with a limited number of biofilm applications (390). In an analogous fashion, micro-positron electron tomography coupled with the radioactive probe [<sup>18</sup>F]fluorodeoxyglucose was used to monitor *S. aureus* biofilm infections and antimicrobial therapy in a mouse model (391).

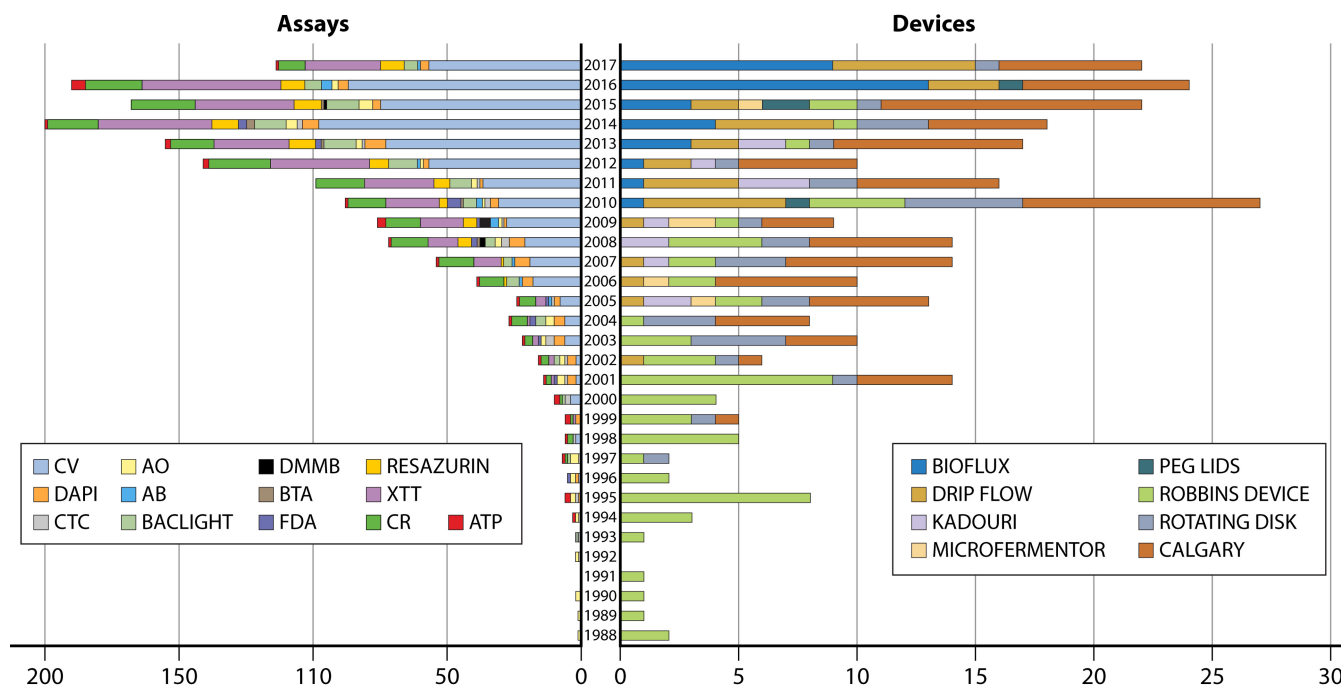
Optical, radiographic, and  $\mu$ CT imaging modalities have been used as tools to monitor orthopedic implant biofilm infections longitudinally, to assess the bacterial load, and to detect osteolysis (392). Multiresolution imaging coupled with *in vivo* labeling uncovered the supplemental tasks of the matrix components of *V. cholerae* biofilms (393). Maltodextrin-based imaging probes (MDPs), a family of light-emitting contrast agents chaperoned with maltohexaose, enable *in vivo* bacterial detection with paramount responsiveness through a cell-specific mechanism. MDPs are rapidly internalized through the maltodextrin transport pathway and selectively accumulate within bacteria at low concentrations, with enhanced specificity over that for mammalian cells (394).

Finally, a bioluminescence-fluorescence combination containing a naturally light-emitting bioluminescent *S. aureus* strain and fluorescent neutrophils from an enhanced green fluorescent protein (EGFP)-expressing mouse strain (LysEGFP) was applied for visualization of a surgical site infection in the knee joint in a mouse model. *In vivo* bioluminescence imaging was used to quantify the microbial burden. Accordingly, *in vivo* fluorescence imaging was used to assess the neutrophil inflammatory response. In the same mice, bioluminescence and fluorescence optical imaging combined with  $\mu$ CT imaging allowed for visualization of 3D anatomical details. This triple imaging combination was proposed to simultaneously track bone biofilm infections, including inflammatory responses and local anatomical modifications, in a noninvasive manner (381).

## SHAPING UP THE METHODOLOGICAL PIPELINE

### Literature Search on Method Implementation

Extensive electronic literature searches provided additional information on the current methodological landscape of biofilm research. Queries were conducted to search the literature from the first biofilm report in October 1988 through August 2017 by using the keywords “biofilm(s) and/or assay” (particularly involving the colorimetric assays applied in the lab) and “biofilm(s) and/or device” separately (Fig. 5). Two specialized exceptions, for “microfluidics” (“bioflux” and “microfluidic device”) and “Calgary” (“MBEC device” and “MBEC HT”), were introduced to the query search. Articles



**FIG 5** Illustrative quantitative and time-dependent representation of biofilm-based methodology publications for currently used devices and assays. CV, crystal violet; DAPI, 4',6-diamidino-2-phenylindole; CTC, oxidized 5-cyano-2,3-ditoyl tetrazolium chloride; AO, acridine orange; AB, alamarBlue; DMMB, dimethylmethylene blue; BTM, biotimer assay; FDA, fluorescein diacetate; XTT, 2,3-bis(2-methoxy-4-nitro-5-sulphophenyl)-5-[(phenylamino)carbonyl]-2H-tetrazolium hydroxide; CR, Congo red.

without an abstract or in a language other than English and papers with irrelevant content were excluded from the search process.

What we deduce from the graphical representation of biofilm-based methodology publications is that the number of research articles for assays is higher than that for devices, with an average ratio of 7 assay publications to 3 device publications and a statistically significant difference ( $P < 10^{-4}$ ). It is also evident that in the approximately 30-year timeline of the query, methodologies are irregularly distributed, indicating a lack of consistency and approval. Figure 5 reveals that (i) the peg lid CBD-MBEC and microfluidics-based devices stand out, with a dynamic presence and increasing rates of use; (ii) the drip-flow cell reactors and rotating-disk reactors might be occasional choices for biofilm growth; (iii) the Kadouri system has remained an interesting alternative in the past decade; (iv) CV, XTT, Congo red, Live/Dead BacLight, and resazurin assays show continuously increasing rates of use; and (v) DAPI appears to be a less popular yet solid choice that never acquired a dynamic rate similar to those of the five major assays for biofilm viability assessment. Another interesting observation is that significant development of different technologies for both assays and devices took place between 2008 and 2015 (up to 12 different assays and 7 different devices). Although an exponentially growing number of assays and devices were developed and applied, only a few have prevailed. More specifically, CV, XTT, and Congo red assays were the predominant methodologies among assays, while the Bioflux, Calgary, and drip-flow technologies dominated among devices over the past 6 years. This observation leads us to the conclusion that experimentation in developing novel methodologies in the biofilm research area is declining and that most of the methods have been abandoned by the research community.

Through implementation of the same search criteria, 4.9% of the publication fraction is dedicated to biofilm techniques over biofilm research (1,839/37,833 publications). This percentage is extremely low, taking into consideration the gap in studying multispecies biofilms under realistic environmental or clinical conditions. In order to strengthen our result that the percentage of publications regarding biofilm techniques

over biofilm research is low, we attempted to evaluate the publication fraction of another research area's methodological achievements. Genome editing is a large and promising area of research, leading the way toward exploring the potential of new developments by implementing a wide range of novel tools and techniques (395). Interestingly, the methodologies applied in the study of genome editing, until September 2017, amounted to 23.4% (2,355/10,062 publications) of publications, with the following keywords used as queries in PubMed searches: ("genome editing" or "chromosomal editing" or "genome inversions" or "chromosomal inversions" or "genome translocation" or "chromosomal translocation" or "structural variations" or "engineered nucleases" or "nucleotide repeats" or "DNA repeats") and ("double-strand breaks" or "DSBs" or "zinc-finger nuclease" or "ZFN" or "transcription activator-like effector nuclease" or "TALEN" or "clustered regularly interspaced short palindromic repeats" or "CRISPR" or "CRISPR-associated protein 9" or "Cas9" or "RNA-guided engineered nuclease" or "RGEN").

The field of biofilm research has proved that the establishment and definition of a "perfect method" comprise a rather precarious generalization. Taking for granted the uniqueness of bacterial biofilms as vivid microcommunities, the approach of a "one-size-fits-all" methodology would abolish any attempt at a thorough understanding. Pluralism in available methodologies is instrumental in order to address basic questions about biofilm formation, structure, adherence, physiology, kinetics, and interactions with the host.

### State-of-the-Art Methodologies in Biofilm Investigation

The majority of information that constitutes the current knowledge on biofilm formation patterns is based on *in vitro* studies. Combined technologies simulate biofilm growth and formation conditions. However, studying biofilms in the lab provides information which differs significantly from our experience in clinical practice. Such an observation defines the need for further experimental accuracy in order to link *in vitro* and *in vivo* outcomes. The host habitat, regarding immunity parameters as well as the components of the human body (tissues [acting as adherence surfaces] and body fluids, such as urine and blood), constitutes a challenging landscape for bacterial growth which differs from experimental conditions (396). Some state-of-the-art compositions and devices have already entered the market over the last decade (Table 4).

Biofilm growth detection based on molecular probes or staining agents enables direct observation, quantification, and topographical mapping of bacterial growth *in vivo* or on medical tool surfaces (397–402). A number of adherence assays exploit biofilm properties and detect biofilm formation and structure (403, 404). Indwelling medical devices carrying color change indicators integrated in substrates prone to degradation in the presence of bacteria mediate detection when applied *in vivo* (405, 406). Immunoassays and enzymatic methods certify biofilm presence and assist in quantification (407, 408). Other *in vivo* theranostic devices employ imaging and sensing tools enabling biofilm "fingerprint" detection through data collection and analysis of thickness, growth speed, and physicochemical properties (409–412).

Combinatorial application of older and conventional methodologies for both *in vitro* and *in vivo* biofilm investigation constitutes a significant resource for the launch of cutting-edge tools. Enhancement of techniques by use of sensing modules, bioinformatics, and the inspirational introduction of biomaterials in surface construction have provided alternative insights into biofilm research. Where lies the difference between research lab methodologies and inventions? What is the clinical significance of the innovation landscape? Sum-of-the-parts comparative analysis gives answers regarding the differences between conventional methodologies and innovative tools. Commercially exploited staining methods differ from those applied in the academic or clinical lab, including a wider variety of biocompatible dyes offering a speedy and easy way to detect results. In-host commercial theranostic devices allow real-time information on the applicability and success rate of the technique right from the bedside. Finally, computational and biosensing methods embedded in daily routines, even adjusted to

**TABLE 4** Innovative platforms for biofilm evaluation<sup>a</sup>

Patent no.	Method	Description	Reference(s)
US 8399649 B2	Molecular probes for biofilm-related protein expression	<i>mucE</i> and <i>algW</i> gene expression determination facilitates monitoring of biofilm formation initiation in human specimens and indwelling devices	397
US 20120322048 A1	Topographical detection on living tissues	Fluorescent staining agents (i.e., alcian blue and ruthenium red) topically react with extracellular matrix biofilm components found on wounds	398
EP 2537601 A1, EP 2634260 A1	Colorimetric detection assay	The detection kit contains a staining solution (i.e., aqueous solution of Coomassie blue, crystal violet, safranin, ruthenium red, rhodamine, or erythionine) and a rinsing solution (i.e., oxidizing or chelating agent) which identify the presence of biofilms on surfaces upon application	399, 400
US 7955818 B2	Microbial culture viscosity measurement	The motion of a charged particle driven by electrical, magnetic, or electromagnetic field application is indicative of biofilm presence in a microbial culture	401
US 20080176265 A1	Potassium permanganate staining solution	Potassium permanganate is applied as a slime matrix staining agent or contrast enhancer for biofilm microscopic visualization or quantification	402
US 20060275847 A1	Combinatorial automated structure analysis	Electromagnetic radiation and CLSM assays of fluorescent biofilm moieties are combined with computational image analysis to provide a multiplanar structure determination	403
US 20030177819 A1	Tools to validate clinical sterility	A flowchart of metabolic, imaging, and immunological assays can be used to certify the absence of biofilm formation on medical surfaces and devices (respirometry, Live/Dead staining, CLSM, SEM, AFM, FISH probing, ELISA)	404
US 20140356901 A1	Urine-detectable colorimetric assay	Indwelling device colonization is detected by the degradation of a polymeric substrate doped with a blood-soluble and urine-passable dye (i.e., methylene blue, $\beta$ -carotene, rifampin, Evan's blue, indocyanine green, or betanin)	405
US 20140352602 A1	Hydration/pH change indicator	Color change of a moisture indicator identifies biofilm presence on catheter surfaces	406
US 20100285496 A1	Lateral flow immunoassay	Labeled antibodies certify the presence of a biofilm-related target analyte	407
EP 1067385 B1	LAL assay	The reaction of LAL with bacterial endotoxins or lipopolysaccharides mediates surface-associated biofilm load quantification	408
WO 2014052449 A1	Photoacoustic flow cytometer	A photoacoustic flow cytometer is applied to blood and/or lymphatic circulation, and photoacoustic pulse analysis enables biofilm quantification	409
US 8697375 B2	MRI-based diagnosis	MRI scanning detects probes that are selectively bound to biofilm found either on mammalian tissues or on indwelling medical devices	410
US 8233957 B2	Electrochemical sensing system	pH and impedance sensor modules placed onto catheter surfaces calculate biofilm thickness, speed of growth, and chemical properties	411
US 20120295216 A1	Diagnostic ultrasonic toothbrush	An ultrasonic sensor detects biofilm thickness by temp, oximetry, proximity, and pH measurements	

<sup>a</sup>CLSM, confocal laser scanning microscopy; SEM, scanning electron microscopy; AFM, atomic force microscopy; FISH, fluorescence *in situ* hybridization; ELISA, enzyme-linked immunosorbent assay; LAL, *Limulus* amoebocyte lysate; MRI, magnetic resonance imaging.

the size of a toothbrush, set the road for the development of devices that will eventually enter clinical settings.

### Extending beyond Commonplace Platforms

Quartz tuning forks (QTFs) have been applied for *P. aeruginosa* biofilm growth monitoring and (bio)sensing (28, 413). The adhesion dynamics that determine biofilm development are monitored by use of piezoelectric tuning forks. QTFs also enable biomass growth detection as well as antibiotic testing and determination of nanomechanical surface properties (414).



A polyurethane-coated, magnetostrictive, ribbon-like sensor as part of a flow system connected to a bioreactor has been used to wirelessly monitor *P. aeruginosa* biofilm formation with the aid of magnetic field telemetry (415). Electromagnetic (EM) wave sensors offer a reliable, real-time, cost-effective methodological tool for *in situ* *P. aeruginosa* growth analysis. EM wave sensors mounted on a polymethyl-methacrylate microfluidic cell structure contributed to the early detection of biofilm growth upon excitation at microwave frequencies (416).

Chronicity due to AMR stems from the lack of detection methodologies for clinically relevant biofilms formed at an early stage. A shift in this reality would potentially support better treatment options. This concept was the foundation for development of a coupled optical and acoustic imaging technology that noninvasively detects and quantifies biofilm biomass. Ligand-targeted UCAs assessed the ability of *S. aureus* to form communities *in vitro* (386). High-frequency scanning acoustic microscopy (SAM) coupled with UCAs facilitated ultrasonic imaging and quantification of the mechano-elastic biofilm properties. This method was proven to be efficient, though the similarity of biofilm acoustic impedance (1.9 MRayl) and that of human soft tissues (1.35 to 1.85 MRayl) poses a serious limitation to *in vivo* imaging.

Bacterial aggregates require specific spatial distribution and environmental parameters to develop physicochemical properties that confer clinically relevant phenotypes (virulence factor production, AMR, and biofilm formation) contributing to strain-specific pathogenicity (417–419). The technical drawback of monitoring the behavior of these populations due to their small size ( $10^1$  to  $10^5$  cells) was recently overcome by use of a laser-based lithographic technology that provides microscopic printing of the 3D geometry of the bacterial aggregates, along with scanning electrochemical microscopy (SECM) enabling redox-active, biofilm-derived small-molecule quantification (for example, that of pyocyanin from *P. aeruginosa*) (420–422). Coupling of these two analytical tools achieves real-time quantitative monitoring of bacterial aggregate interplay and assesses the impacts of spatial organization and chemical signaling on sociomicrobiology.

Extending the use of 3D printing technologies, a novel material consisting of the broad-spectrum antibiotic nitrofurantoin and the biodegradable polymer poly(L-lactic acid) was manufactured to mimic catheters. The 3D-printed disks exhibited >85% biofilm inhibition; therefore, an antimicrobial option has emerged for medical device coatings (423). One of the most recent setups for real-time *E. coli* and *P. aeruginosa* biofilm biomass growth evaluation was achieved through a sensing microsystem in which a microfluidic flow reactor employs a surface acoustic wave (SAW) sensor and electrodes constituting a source for current signals. This electric field is coupled with the use of gentamicin, and therefore this integrated sensing platform serves for biofilm growth monitoring and biofilm elimination (424). A novel impedimetric sensing system based on the interdigitated microelectrode microsystem envisions paving the way for the development of smart biosensors for rapid implant-associated biofilm identification and removal. In short, this microsystem allows label-free *E. coli* biofilm growth detection in microfluidic channels by evaluating the fractional relative change in real time as well as monitoring the threshold-activated bioelectric effect on the *in situ* treatment process (425). A custom-made surface plasmon resonance (SPR) biosensor was recently applied for *E. coli* biofilm formation investigation on gold-plated glass disks. In particular, the angle-based SPR biosensor allowed real-time capture of the SPR curve as well as calculation of the refractive index change, thus offering a complete picture of the biofilm formation cycle (426).

## CONCLUDING REMARKS

It is evident that most experimental biofilm procedures provide descriptive and quantitative information, but combining tools and methods unravels more pieces of the puzzle. Most of the conclusions obtained here are derived from *in vitro* studies, yet their relevance to the processes and methodologies occurring *in vivo* are a subject for further consideration and experimentation. Recalcitrant and persistent biofilm-

associated diseases have raised the need for new therapeutic approaches and methods for reliably culturing mature biofilms and evaluating their chemical, structural, and physiological characteristics.

The lack of consistent and robust animal biofilm models is perhaps the most critical element missing from the equation. It appears that engineering-driven approaches give and will continue to give methods and tools transcending the current norm and status of biofilm analysis. This pool is still in the periphery of clinical knowledge. Thus, the fundamental questions remain partially answered. That is, how do we detect biofilm formation at the bedside, and what is the best course of action for eradication? Commercially available kits and the wealth of research information can educate but barely provide comprehensive and articulated answers. A more compelling set of answers may arise when the intersection of clinical and engineering approaches becomes relevant.

Advances regarding the microbiome and unculturable bacteria designate the imperative need for reliable tools for thorough investigation of host-biofilm interactions. Consequently, the establishment of robust biofilm susceptibility assays also remains a challenge for clinical entities. Information stemming from combinatorial assays may provide comprehensive and critical insights into any given biofilm-associated clinical query.

## ACKNOWLEDGMENTS

We thank Chengxue Lee for a critical review of the manuscript.

This work was supported by a General Secretariat for Research and Technology (GSRT)-Hellenic Foundation for Research and Innovation (HFRI) scholarship for doctoral studies (grant 164030/I2 to M.M.) and by academic development funds (grant APS 1-04-520-9211 to M.H.).

## REFERENCES

- Wimpenny J, Manz W, Szewzyk U. 2000. Heterogeneity in biofilms. *FEMS Microbiol Rev* 24:661–671. <https://doi.org/10.1111/j.1574-6976.2000.tb00565.x>.
- Monds RD, O'Toole GA. 2009. The developmental model of microbial biofilms: ten years of a paradigm up for review. *Trends Microbiol* 17:73–87. <https://doi.org/10.1016/j.tim.2008.11.001>.
- Stoodley P, Sauer K, Davies DG, Costerton JW. 2002. Biofilms as complex differentiated communities. *Annu Rev Microbiol* 56:187–209. <https://doi.org/10.1146/annurev.micro.56.012302.160705>.
- O'Toole G, Kaplan HB, Kolter R. 2000. Biofilm formation as microbial development. *Annu Rev Microbiol* 54:49–79. <https://doi.org/10.1146/annurev.micro.54.1.49>.
- Lebeaux D, Chauhan A, Rendueles O, Beloin C. 2013. From in vitro to in vivo models of bacterial biofilm-related infections. *Pathogens* 2:288–356. <https://doi.org/10.3390/pathogens2020288>.
- Roiling U, Balsalobre C. 2012. Biofilm infections, their resilience to therapy and innovative treatment strategies. *J Intern Med* 272:541–561. <https://doi.org/10.1111/joim.12004>.
- Wu H, Moser C, Wang HZ, Hoiby N, Song ZJ. 2015. Strategies for combating bacterial biofilm infections. *Int J Oral Sci* 7:1–7. <https://doi.org/10.1038/ijos.2014.65>.
- Bao K, Papadimitropoulos A, Akgul B, Belibasakis GN, Bostanci N. 2015. Establishment of an oral infection model resembling the periodontal pocket in a perfusion bioreactor system. *Virulence* 6:265–273. <https://doi.org/10.4161/21505594.2014.978721>.
- Belibasakis G, Thurnheer T, Bostanci N. 2014. Porphyromonas gingivalis: a heartfelt oral pathogen? *Virulence* 5:463–464. <https://doi.org/10.4161/viru.28930>.
- Bispo PJ, Haas W, Gilmore MS. 2015. Biofilms in infections of the eye. *Pathogens* 4:111–136. <https://doi.org/10.3390/pathogens4010111>.
- Mysorekar IU, Hultgren SJ. 2006. Mechanisms of uropathogenic Escherichia coli persistence and eradication from the urinary tract. *Proc Natl Acad Sci U S A* 103:14170–14175. <https://doi.org/10.1073/pnas.0602136103>.
- Percival SL, Hill KE, Williams DW, Hooper SJ, Thomas DW, Costerton JW. 2012. A review of the scientific evidence for biofilms in wounds. *Wound Repair Regen* 20:647–657. <https://doi.org/10.1111/j.1524-475X.2012.00836.x>.
- Percival SL, Suleman L, Vuotto C, Donelli G. 2015. Healthcare-associated infections, medical devices and biofilms: risk, tolerance and control. *J Med Microbiol* 64:323–334. <https://doi.org/10.1099/jmm.0.000032>.
- Costerton JW, Geesey GG, Cheng KJ. 1978. How bacteria stick. *Sci Am* 238:86–95. <https://doi.org/10.1038/scientificamerican0178-86>.
- Battin TJ, Sloan WT, Kjelleberg S, Daims H, Head IM, Curtis TP, Eberl L. 2007. Microbial landscapes: new paths to biofilm research. *Nat Rev Microbiol* 5:76–81. <https://doi.org/10.1038/nrmicro1556>.
- Auger JP, Chuzeville S, Roy D, Mathieu-Denoncourt A, Xu J, Grenier D, Gottschalk M. 2017. The bias of experimental design, including strain background, in the determination of critical Streptococcus suis serotype 2 virulence factors. *PLoS One* 12:e0181920. <https://doi.org/10.1371/journal.pone.0181920>.
- Jorge P, Lourenco A, Pereira MO. 2015. Data quality in biofilm high-throughput routine analysis: intralaboratory protocol adaptation and experiment reproducibility. *J AOAC Int* 98:1721–1727. <https://doi.org/10.5740/jaoacint.15-066>.
- Stewart PS. 2003. Diffusion in biofilms. *J Bacteriol* 185:1485–1491. <https://doi.org/10.1128/JB.185.5.1485-1491.2003>.
- Flemming HC, Wingender J. 2010. The biofilm matrix. *Nat Rev Microbiol* 8:623–633. <https://doi.org/10.1038/nrmicro2415>.
- Wozniak DJ, Wyckoff TJ, Starkey M, Keyser R, Azadi P, O'Toole GA, Parsek MR. 2003. Alginate is not a significant component of the extracellular polysaccharide matrix of PA14 and PAO1 Pseudomonas aeruginosa biofilms. *Proc Natl Acad Sci U S A* 100:7907–7912. <https://doi.org/10.1073/pnas.1231792100>.
- Hentzer M, Teitzel GM, Balzer GJ, Heydorn A, Molin S, Givskov M, Parsek MR. 2001. Alginate overproduction affects Pseudomonas aeruginosa biofilm structure and function. *J Bacteriol* 183:5395–5401. <https://doi.org/10.1128/JB.183.18.5395-5401.2001>.
- Hadjiifrangiskou M, Gu AP, Pinkner JS, Kostakioti M, Zhang EW, Greene SE, Hultgren SJ. 2012. Transposon mutagenesis identifies uropathogenic Escherichia coli biofilm factors. *J Bacteriol* 194:6195–6205. <https://doi.org/10.1128/JB.01012-12>.

23. Hung C, Zhou Y, Pinkner JS, Dodson KW, Crowley JR, Heuser J, Chapman MR, Hadjifrangiskou M, Henderson JP, Hultgren SJ. 2013. Escherichia coli biofilms have an organized and complex extracellular matrix structure. *mBio* 4:e00645-13. <https://doi.org/10.1128/mBio.00645-13>.
24. Floyd KA, Moore JL, Eberly AR, Good JA, Shaffer CL, Zaver H, Almqvist F, Skaar EP, Caprioli RM, Hadjifrangiskou M. 2015. Adhesive fiber stratification in uropathogenic Escherichia coli biofilms unveils oxygen-mediated control of type 1 pili. *PLoS Pathog* 11:e1004697. <https://doi.org/10.1371/journal.ppat.1004697>.
25. Chew SC, Kundukad B, Seviour T, van der Maarel JR, Yang L, Rice SA, Doyle P, Kjelleberg S. 2014. Dynamic remodeling of microbial biofilms by functionally distinct exopolysaccharides. *mBio* 5:e01536-14. <https://doi.org/10.1128/mBio.01536-14>.
26. Periasamy S, Nair HA, Lee KW, Ong J, Goh JQ, Kjelleberg S, Rice SA. 2015. Pseudomonas aeruginosa PAO1 exopolysaccharides are important for mixed species biofilm community development and stress tolerance. *Front Microbiol* 6:851. <https://doi.org/10.3389/fmicb.2015.00851>.
27. Donne J, Dewilde S. 2015. The challenging world of biofilm physiology. *Adv Microb Physiol* 67:235–292. <https://doi.org/10.1016/bs.ampbs.2015.09.003>.
28. Gula G, Waszczuk K, Olszak T, Majewska J, Sarowska J, Gotszalk T, Gutowicz J, Drulis-Kawa Z. 2012. Piezoelectric tuning fork based mass measurement method as a novel tool for determination of antibiotic activity on bacterial biofilm. *Sens Actuators B Chem* 175:34–39. <https://doi.org/10.1016/j.snb.2011.11.044>.
29. Koza A, Hallett PD, Moon CD, Spiers AJ. 2009. Characterization of a novel air-liquid interface biofilm of Pseudomonas fluorescens SBW25. *Microbiology* 155:1397–1406. <https://doi.org/10.1099/mic.0.025064-0>.
30. Ude S, Arnold DL, Moon CD, Timms-Wilson T, Spiers AJ. 2006. Biofilm formation and cellulose expression among diverse environmental Pseudomonas isolates. *Environ Microbiol* 8:1997–2011. <https://doi.org/10.1111/j.1462-2920.2006.01080.x>.
31. Anderson GG, Palermo JJ, Schilling JD, Roth R, Heuser J, Hultgren SJ. 2003. Intracellular bacterial biofilm-like pods in urinary tract infections. *Science* 301:105–107. <https://doi.org/10.1126/science.1084550>.
32. Justice SS, Hung C, Theriot JA, Fletcher DA, Anderson GG, Footer MJ, Hultgren SJ. 2004. Differentiation and developmental pathways of uropathogenic Escherichia coli in urinary tract pathogenesis. *Proc Natl Acad Sci U S A* 101:1333–1338. <https://doi.org/10.1073/pnas.0308125100>.
33. Rosen DA, Pinkner JS, Jones JM, Walker JN, Clegg S, Hultgren SJ. 2008. Utilization of an intracellular bacterial community pathway in Klebsiella pneumoniae urinary tract infection and the effects of FimK on type 1 pilus expression. *Infect Immun* 76:3337–3345. <https://doi.org/10.1128/IAI.00090-08>.
34. Mihai MM, Holban AM, Giurcaneanu C, Popa LG, Oanea RM, Lazar V, Chifriuc MC, Popa M, Popa MI. 2015. Microbial biofilms: impact on the pathogenesis of periodontitis, cystic fibrosis, chronic wounds and medical device-related infections. *Curr Top Med Chem* 15:1552–1576. <https://doi.org/10.2174/1568026615666150414123800>.
35. Fagerlind MG, Webb JS, Barraud N, McDougald D, Jansson A, Nilsson P, Harlen M, Kjelleberg S, Rice SA. 2012. Dynamic modelling of cell death during biofilm development. *J Theor Biol* 295:23–36. <https://doi.org/10.1016/j.jtbi.2011.10.007>.
36. Leiman SA, May JM, Lebar MD, Kahne D, Kolter R, Losick R. 2013. D-Amino acids indirectly inhibit biofilm formation in Bacillus subtilis by interfering with protein synthesis. *J Bacteriol* 195:5391–5395. <https://doi.org/10.1128/JB.00975-13>.
37. Kolodkin-Gal I, Romero D, Cao S, Clardy J, Kolter R, Losick R. 2010. D-Amino acids trigger biofilm disassembly. *Science* 328:627–629. <https://doi.org/10.1126/science.1188628>.
38. Simm R, Morr M, Kader A, Nimtz M, Romling U. 2004. GGDEF and EAL domains inversely regulate cyclic di-GMP levels and transition from sessility to motility. *Mol Microbiol* 53:1123–1134. <https://doi.org/10.1111/j.1365-2958.2004.04206.x>.
39. Tischler AD, Camilli A. 2004. Cyclic diguanylate (c-di-GMP) regulates Vibrio cholerae biofilm formation. *Mol Microbiol* 53:857–869. <https://doi.org/10.1111/j.1365-2958.2004.04155.x>.
40. Karaolis DK, Rashid MH, Chythanya R, Luo W, Hyodo M, Hayakawa Y. 2005. c-di-GMP (3'-5'-cyclic diguanylic acid) inhibits Staphylococcus aureus cell-cell interactions and biofilm formation. *Antimicrob Agents Chemother* 49:1029–1038. <https://doi.org/10.1128/AAC.49.3.1029-1038.2005>.
41. Chua SL, Tan SY, Rybtke MT, Chen Y, Rice SA, Kjelleberg S, Tolker-Nielsen T, Yang L, Givskov M. 2013. Bis-(3'-5')-cyclic dimeric GMP regulates antimicrobial peptide resistance in Pseudomonas aeruginosa. *Antimicrob Agents Chemother* 57:2066–2075. <https://doi.org/10.1128/AAC.02499-12>.
42. Serra DO, Hengge R. 2014. Stress responses go three dimensional—the spatial order of physiological differentiation in bacterial macrocolony biofilms. *Environ Microbiol* 16:1455–1471. <https://doi.org/10.1111/1462-2920.12483>.
43. Mikkelsen H, Duck Z, Lilley KS, Welch M. 2007. Interrelationships between colonies, biofilms, and planktonic cells of Pseudomonas aeruginosa. *J Bacteriol* 189:2411–2416. <https://doi.org/10.1128/JB.101687-06>.
44. Muller S, Strack SN, Ryan SE, Kearns DB, Kirby JR. 2015. Predation by Myxococcus xanthus induces Bacillus subtilis to form spore-filled megastructures. *Appl Environ Microbiol* 81:203–210. <https://doi.org/10.1128/AEM.02448-14>.
45. DePas WH, Hufnagel DA, Lee JS, Blanco LP, Bernstein HC, Fisher ST, James GA, Stewart PS, Chapman MR. 2013. Iron induces bimodal population development by Escherichia coli. *Proc Natl Acad Sci U S A* 110:2629–2634. <https://doi.org/10.1073/pnas.1218703110>.
46. Yildiz FH, Visick KL. 2009. Vibrio biofilms: so much the same yet so different. *Trends Microbiol* 17:109–118. <https://doi.org/10.1016/j.tim.2008.12.004>.
47. Teschler JK, Zamorano-Sanchez D, Utada AS, Warner CJ, Wong GC, Linington RG, Yildiz FH. 2015. Living in the matrix: assembly and control of Vibrio cholerae biofilms. *Nat Rev Microbiol* 13:255–268. <https://doi.org/10.1038/nrmicro3433>.
48. Morohashi M, Ohashi Y, Tani S, Ishii K, Itaya M, Nanamiya H, Kawamura F, Tomita M, Soga T. 2007. Model-based definition of population heterogeneity and its effects on metabolism in sporulating Bacillus subtilis. *J Biochem* 142:183–191. <https://doi.org/10.1093/jb/mvm121>.
49. Bischofs IB, Hug JA, Liu AW, Wolf DM, Arkin AP. 2009. Complexity in bacterial cell-cell communication: quorum signal integration and subpopulation signaling in the Bacillus subtilis phosphorelay. *Proc Natl Acad Sci U S A* 106:6459–6464. <https://doi.org/10.1073/pnas.0810878106>.
50. Liu WT, Yang YL, Xu Y, Lamsa A, Haste NM, Yang JY, Ng J, Gonzalez D, Ellermeier CD, Straight PD, Pevzner PA, Pogliano J, Nizet V, Pogliano K, Dorrestein PC. 2010. Imaging mass spectrometry of intraspecies metabolic exchange revealed the cannibalistic factors of Bacillus subtilis. *Proc Natl Acad Sci U S A* 107:16286–16290. <https://doi.org/10.1073/pnas.1008368107>.
51. Donlan RM, Costerton JW. 2002. Biofilms: survival mechanisms of clinically relevant microorganisms. *Clin Microbiol Rev* 15:167–193. <https://doi.org/10.1128/CMR.15.2.167-193.2002>.
52. Veerachamy S, Yarlagadda T, Manivasagam G, Yarlagadda PK. 2014. Bacterial adherence and biofilm formation on medical implants: a review. *Proc Inst Mech Eng H* 228:1083–1099. <https://doi.org/10.1177/0954411914556137>.
53. Krol JE, Nguyen HD, Rogers LM, Beyenal H, Krone SM, Top EM. 2011. Increased transfer of a multidrug resistance plasmid in Escherichia coli biofilms at the air-liquid interface. *Appl Environ Microbiol* 77:5079–5088. <https://doi.org/10.1128/AEM.00090-11>.
54. Mehall JR, Saltzman DA, Jackson RJ, Smith SD. 2002. Fibrin sheath enhances central venous catheter infection. *Crit Care Med* 30:908–912. <https://doi.org/10.1097/00003246-200204000-00033>.
55. Prindle A, Liu J, Asally M, Ly S, Garcia-Ojalvo J, Suel GM. 2015. Ion channels enable electrical communication in bacterial communities. *Nature* 527:59–63. <https://doi.org/10.1038/nature15709>.
56. Liu J, Prindle A, Humphries J, Gabalda-Sagarra M, Asally M, Lee DY, Ly S, Garcia-Ojalvo J, Suel GM. 2015. Metabolic co-dependence gives rise to collective oscillations within biofilms. *Nature* 523:550–554. <https://doi.org/10.1038/nature14660>.
57. Zhou Y, Smith D, Leong BJ, Brannstrom K, Almqvist F, Chapman MR. 2012. Promiscuous cross-seeding between bacterial amyloids promotes interspecies biofilms. *J Biol Chem* 287:35092–35103. <https://doi.org/10.1074/jbc.M112.383737>.
58. Scher K, Romling U, Yaron S. 2005. Effect of heat, acidification, and chlorination on Salmonella enterica serovar Typhimurium cells in a biofilm formed at the air-liquid interface. *Appl Environ Microbiol* 71:1163–1168. <https://doi.org/10.1128/AEM.71.3.1163-1168.2005>.
59. Old DC, Corneil I, Gibson LF, Thomson AD, Duguid JP. 1968. Fimbriation, pellicle formation and the amount of growth of salmonellas in

- broth. *J Gen Microbiol* 51:1–16. <https://doi.org/10.1099/00221287-51-1-1>.
60. Spiers AJ, Arnold DL, Moon CD, Timms-Wilson TM. 2006. A survey of A-L biofilm formation and cellulose expression amongst soil and plant-associated *Pseudomonas* isolates, p 121–132. In Bailey MJ, Lilley AK, Timms-Wilson TM, Spencer-Phillips PTN (ed), *Microbial ecology of aerial plant surfaces*. CABI, Wallingford, United Kingdom.
  61. Branda SS, Vik S, Friedman L, Kolter R. 2005. Biofilms: the matrix revisited. *Trends Microbiol* 13:20–26. <https://doi.org/10.1016/j.tim.2004.11.006>.
  62. Diaz PI, Chalmers NI, Rickard AH, Kong C, Milburn CL, Palmer RJ, Jr, Kolenbrander PE. 2006. Molecular characterization of subject-specific oral microflora during initial colonization of enamel. *Appl Environ Microbiol* 72:2837–2848. <https://doi.org/10.1128/AEM.72.4.2837-2848.2006>.
  63. Marsh PD, Moter A, Devine DA. 2011. Dental plaque biofilms: communities, conflict and control. *Periodontol* 2000 55:16–35. <https://doi.org/10.1111/j.1600-0757.2009.00339.x>.
  64. Thomsen T, Hall-Stoodley L, Moser C, Stoodley P. 2011. The role of bacterial biofilms in infections of catheters and shunts, p 91–109. In Bjarnsholt T, Jensen PØ, Moser C, Høiby N (ed), *Biofilm infections*. Springer, New York, NY.
  65. Foxman B. 2014. Urinary tract infection syndromes: occurrence, recurrence, bacteriology, risk factors, and disease burden. *Infect Dis Clin North Am* 28:1–13. <https://doi.org/10.1016/j.idc.2013.09.003>.
  66. Flores-Mireles AL, Walker JN, Bauman TM, Potretzke AM, Schreiber HL, IV, Park AM, Pinkner JS, Caparon MG, Hultgren SJ, Desai A. 2016. Fibrinogen release and deposition on urinary catheters placed during urological procedures. *J Urol* 196:416–421. <https://doi.org/10.1016/j.juro.2016.01.100>.
  67. Hornemann JA, Codd SL, Fell RJ, Stewart PS, Seymour JD. 2009. Secondary flow mixing due to biofilm growth in capillaries of varying dimensions. *Biotechnol Bioeng* 103:353–360. <https://doi.org/10.1002/bit.22248>.
  68. Chifriuc MC, Banu O, Bleotu C, Lazar V. 2011. Interaction of bacteria isolated from clinical biofilms with cardiovascular prosthetic devices and eukaryotic cells. *Anaerobe* 17:419–421. <https://doi.org/10.1016/j.anaerobe.2011.04.016>.
  69. Kim MK, Drescher K, Pak OS, Bassler BL, Stone HA. 2014. Filaments in curved streamlines: rapid formation of *Staphylococcus aureus* biofilm streamers. *New J Phys* 16:065024. <https://doi.org/10.1088/1367-2630/16/6/065024>.
  70. Van Kerckhoven M, Hotterbeekx A, Lanckacker E, Moons P, Lammens C, Kerstens M, Ieven M, Delputte P, Jorens PG, Malhotra-Kumar S, Goossens H, Maes L, Cos P. 2016. Characterizing the in vitro biofilm phenotype of *Staphylococcus epidermidis* isolates from central venous catheters. *J Microbiol Methods* 127:95–101. <https://doi.org/10.1016/j.mimet.2016.05.009>.
  71. Kostakioti M, Hadjifrangiskou M, Hultgren SJ. 2013. Bacterial biofilms: development, dispersal, and therapeutic strategies in the dawn of the postantibiotic era. *Cold Spring Harb Perspect Med* 3:a010306. <https://doi.org/10.1101/cshperspect.a010306>.
  72. McDougald D, Rice SA, Barraud N, Steinberg PD, Kjelleberg S. 2011. Should we stay or should we go: mechanisms and ecological consequences for biofilm dispersal. *Nat Rev Microbiol* 10:39–50. <https://doi.org/10.1038/nrmicro2695>.
  73. Spoering AL, Lewis K. 2001. Biofilms and planktonic cells of *Pseudomonas aeruginosa* have similar resistance to killing by antimicrobials. *J Bacteriol* 183:6746–6751. <https://doi.org/10.1128/JB.183.23.6746-6751.2001>.
  74. Ryall B, Eydallin G, Ferenci T. 2012. Culture history and population heterogeneity as determinants of bacterial adaptation: the adaptomics of a single environmental transition. *Microbiol Mol Biol Rev* 76: 597–625. <https://doi.org/10.1128/MMBR.05028-11>.
  75. Fong JN, Yildiz FH. 2015. Biofilm matrix proteins. *Microbiol Spectr* 3:MB-0004-2014. <https://doi.org/10.1128/microbiolspec.MB-0004-2014>.
  76. Lewis K. 2010. Persister cells. *Annu Rev Microbiol* 64:357–372. <https://doi.org/10.1146/annurev.micro.112408.134306>.
  77. Lewis K. 2005. Persister cells and the riddle of biofilm survival. *Biochemistry (Mosc)* 70:267–274. <https://doi.org/10.1007/s10541-005-0111-6>.
  78. Luidalepp H, Joers A, Kaldalu N, Tenson T. 2011. Age of inoculum strongly influences persister frequency and can mask effects of mutations implicated in altered persistence. *J Bacteriol* 193:3598–3605. <https://doi.org/10.1128/JB.00085-11>.
  79. Norton JP, Mulvey MA. 2012. Toxin-antitoxin systems are important for niche-specific colonization and stress resistance of uropathogenic *Escherichia coli*. *PLoS Pathog* 8:e1002954. <https://doi.org/10.1371/journal.ppat.1002954>.
  80. Keren I, Kaldalu N, Spoering A, Wang Y, Lewis K. 2004. Persister cells and tolerance to antimicrobials. *FEMS Microbiol Lett* 230:13–18. [https://doi.org/10.1016/S0378-1097\(03\)00856-5](https://doi.org/10.1016/S0378-1097(03)00856-5).
  81. Keren I, Shah D, Spoering A, Kaldalu N, Lewis K. 2004. Specialized persister cells and the mechanism of multidrug tolerance in *Escherichia coli*. *J Bacteriol* 186:8172–8180. <https://doi.org/10.1128/JB.186.24.8172-8180.2004>.
  82. Tande AJ, Osmon DR, Greenwood-Quaintance KE, Mabry TM, Hanssen AD, Patel R. 2014. Clinical characteristics and outcomes of prosthetic joint infection caused by small colony variant staphylococci. *mBio* 5:e01910-14. <https://doi.org/10.1128/mBio.01910-14>.
  83. Mirani ZA, Aziz M, Khan SI. 2015. Small colony variants have a major role in stability and persistence of *Staphylococcus aureus* biofilms. *J Antibiot* 68:98–105. <https://doi.org/10.1038/ja.2014.115>.
  84. Short FL, Murdoch SL, Ryan RP. 2014. Polybacterial human disease: the ills of social networking. *Trends Microbiol* 22:508–516. <https://doi.org/10.1016/j.tim.2014.05.007>.
  85. Ghannoum M. 2016. Cooperative evolutionary strategy between the bacteriome and mycobiome. *mBio* 7:e01951-16. <https://doi.org/10.1128/mBio.01951-16>.
  86. Shirtliff ME, Peters BM, Jabra-Rizk MA. 2009. Cross-kingdom interactions: *Candida albicans* and bacteria. *FEMS Microbiol Lett* 299: 1–8. <https://doi.org/10.1111/j.1574-6968.2009.01668.x>.
  87. Ratner AJ, Lysenko ES, Paul MN, Weiser JN. 2005. Synergistic proinflammatory responses induced by polymicrobial colonization of epithelial surfaces. *Proc Natl Acad Sci U S A* 102:3429–3434. <https://doi.org/10.1073/pnas.0500599102>.
  88. Armbruster CE, Hong W, Pang B, Weimer KE, Juneau RA, Turner J, Swords WE. 2010. Indirect pathogenicity of *Haemophilus influenzae* and *Moraxella catarrhalis* in polymicrobial otitis media occurs via interspecies quorum signaling. *mBio* 1:e00102-10. <https://doi.org/10.1128/mBio.00102-10>.
  89. Fazli M, Bjarnsholt T, Kirketerp-Møller K, Jørgensen B, Andersen AS, Krogfelt KA, Givskov M, Tolker-Nielsen T. 2009. Nonrandom distribution of *Pseudomonas aeruginosa* and *Staphylococcus aureus* in chronic wounds. *J Clin Microbiol* 47:4084–4089. <https://doi.org/10.1128/JCM.01395-09>.
  90. Kline KA, Schwartz DJ, Gilbert NM, Hultgren SJ, Lewis AL. 2012. Immune modulation by group B *Streptococcus* influences host susceptibility to urinary tract infection by uropathogenic *Escherichia coli*. *Infect Immun* 80:4186–4194. <https://doi.org/10.1128/IAI.00684-12>.
  91. Orth RK, O'Brien-Simpson NM, Dashper SG, Reynolds EC. 2011. Synergistic virulence of *Porphyromonas gingivalis* and *Treponema denticola* in a murine periodontitis model. *Mol Oral Microbiol* 26:229–240. <https://doi.org/10.1111/j.2041-1014.2011.00612.x>.
  92. Murray JL, Connell JL, Stacy A, Turner KH, Whiteley M. 2014. Mechanisms of synergy in polymicrobial infections. *J Microbiol* 52:188–199. <https://doi.org/10.1007/s12275-014-4067-3>.
  93. Merritt JH, Kadouri DE, O'Toole GA. 2005. Growing and analyzing static biofilms. *Curr Protoc Microbiol* Chapter 1:Unit 1B.1. <https://doi.org/10.1002/9780471729259.mc01b01s00>.
  94. Christensen GD, Simpson WA, Younger JJ, Baddour LM, Barrett FF, Melton DM, Beachey EH. 1985. Adherence of coagulase-negative staphylococci to plastic tissue culture plates: a quantitative model for the adherence of staphylococci to medical devices. *J Clin Microbiol* 22: 996–1006.
  95. Wu S, Baum MM, Kerwin J, Guerrero D, Webster S, Schaudinn C, VanderVelde D, Webster P. 2014. Biofilm-specific extracellular matrix proteins of nontypeable *Haemophilus influenzae*. *Pathog Dis* 72: 143–160. <https://doi.org/10.1111/2049-632X.12195>.
  96. O'Toole GA, Kolter R. 1998. Initiation of biofilm formation in *Pseudomonas fluorescens* WCS365 proceeds via multiple, convergent signalling pathways: a genetic analysis. *Mol Microbiol* 28:449–461. <https://doi.org/10.1046/j.1365-2958.1998.00797.x>.
  97. Gomes LC, Moreira JM, Simoes M, Melo LF, Mergulhao FJ. 2014. Biofilm localization in the vertical wall of shaking 96-well plates. *Scientifica* 2014:231083. <https://doi.org/10.1155/2014/231083>.
  98. Gomes LC, Moreira JM, Miranda JM, Simoes M, Melo LF, Mergulhao FJ. 2013. Macroscale versus microscale methods for physiological analysis

- of biofilms formed in 96-well microtiter plates. *J Microbiol Methods* 95:342–349. <https://doi.org/10.1016/j.mimet.2013.10.002>.
99. Frank KL, Guiton PS, Barnes AM, Manias DA, Chuang-Smith ON, Kohler PL, Spaulding AR, Hultgren SJ, Schlievert PM, Dunny GM. 2013. AhrC and Eep are biofilm infection-associated virulence factors in *Enterococcus faecalis*. *Infect Immun* 81:1696–1708. <https://doi.org/10.1128/IAI.01210-12>.
  100. Guiton PS, Hung CS, Kline KA, Roth R, Kau AL, Hayes E, Heuser J, Dodson KW, Caparon MG, Hultgren SJ. 2009. Contribution of autolysin and sortase A during *Enterococcus faecalis* DNA-dependent biofilm development. *Infect Immun* 77:3626–3638. <https://doi.org/10.1128/IAI.00219-09>.
  101. O'Toole GA. 2011. Microtiter dish biofilm formation assay. *J Vis Exp* 2011:2437. <https://doi.org/10.3791/2437>.
  102. Kristich CJ, Li YH, Cvitkovitch DG, Dunny GM. 2004. Esp-independent biofilm formation by *Enterococcus faecalis*. *J Bacteriol* 186:154–163. <https://doi.org/10.1128/JB.186.1.154-163.2004>.
  103. Caiazza NC, O'Toole GA. 2004. SadB is required for the transition from reversible to irreversible attachment during biofilm formation by *Pseudomonas aeruginosa* PA14. *J Bacteriol* 186:4476–4485. <https://doi.org/10.1128/JB.186.14.4476-4485.2004>.
  104. Woodworth BA, Tamashiro E, Bhargava G, Cohen NA, Palmer JN. 2008. An in vitro model of *Pseudomonas aeruginosa* biofilms on viable airway epithelial cell monolayers. *Am J Rhinol* 22:235–238. <https://doi.org/10.2500/ajr.2008.22.3178>.
  105. Chavant P, Gaillard-Martinie B, Talon R, Hebraud M, Bernardi T. 2007. A new device for rapid evaluation of biofilm formation potential by bacteria. *J Microbiol Methods* 68:605–612. <https://doi.org/10.1016/j.mimet.2006.11.010>.
  106. Liesse Iyamba JM, Seil M, Devleeschouwer M, Takaisi Kikuni NB, Dehaye JP. 2011. Study of the formation of a biofilm by clinical strains of *Staphylococcus aureus*. *Biofouling* 27:811–821. <https://doi.org/10.1080/08927014.2011.604776>.
  107. Puig C, Domenech A, Garmendia J, Langereis JD, Mayer P, Calatayud L, Linares J, Ardanuy C, Marti S. 2014. Increased biofilm formation by nontypeable *Haemophilus influenzae* isolates from patients with invasive disease or otitis media versus strains recovered from cases of respiratory infections. *Appl Environ Microbiol* 80:7088–7095. <https://doi.org/10.1128/AEM.02544-14>.
  108. Olivares E, Badel-Berchoux S, Provot C, Jaulhac B, Prevost G, Bernardi T, Jehl F. 2016. The BioFilm Ring Test: a rapid method for routine analysis of *Pseudomonas aeruginosa* biofilm formation kinetics. *J Clin Microbiol* 54:657–661. <https://doi.org/10.1128/JCM.02938-15>.
  109. Valour F, Rasigade JP, Trouillet-Assant S, Gagnaire J, Bouaziz A, Karsenty J, Lacour C, Bes M, Lustig S, Benet T, Chidiac C, Etienne J, Vandenesch F, Ferry T, Laurent F. 2015. Delta-toxin production deficiency in *Staphylococcus aureus*: a diagnostic marker of bone and joint infection chronicity linked with osteoblast invasion and biofilm formation. *Clin Microbiol Infect* 21:568.e1–568.e11. <https://doi.org/10.1016/j.cmi.2015.01.026>.
  110. Valour F, Trouillet-Assant S, Rasigade JP, Lustig S, Chanard E, Meugnier H, Tigaud S, Vandenesch F, Etienne J, Ferry T, Laurent F. 2013. *Staphylococcus epidermidis* in orthopedic device infections: the role of bacterial internalization in human osteoblasts and biofilm formation. *PLoS One* 8:e67240. <https://doi.org/10.1371/journal.pone.0067240>.
  111. Tasse J, Croisier D, Badel-Berchoux S, Chavanet P, Bernardi T, Provot C, Laurent F. 2016. Preliminary results of a new antibiotic susceptibility test against biofilm installation in device-associated infections: the Antibiofilmogram(R). *Pathog Dis* 74:ftw057. <https://doi.org/10.1093/femspd/ftw057>.
  112. Starek M, Kolev KI, Berthiaume L, Yeung CW, Sleep BE, Wolfaardt GM, Hausner M. 2011. A flow cell simulating a subsurface rock fracture for investigations of groundwater-derived biofilms. *Int Microbiol* 14:163–171.
  113. Lopez D, Vlamakis H, Kolter R. 2010. Biofilms. *Cold Spring Harb Perspect Biol* 2:a000398. <https://doi.org/10.1101/cshperspect.a000398>.
  114. Cruz SA, Popat R, Rybtke MT, Camara M, Givskov M, Tolker-Nielsen T, Diggle SP, Williams P. 2012. Bursting the bubble on bacterial biofilms: a flow cell methodology. *Biofouling* 28:835–842. <https://doi.org/10.1080/08927014.2012.716044>.
  115. Wolfaardt GM, Lawrence JR, Roberts RD, Caldwell SJ, Caldwell DE. 1994. Multicellular organization in a degradative biofilm community. *Appl Environ Microbiol* 60:434–446.
  116. Jurgens DJ, Sattar SA, Mah TF. 2008. Chloraminated drinking water does not generate bacterial resistance to antibiotics in *Pseudomonas aeruginosa* biofilms. *Lett Appl Microbiol* 46:562–567. <https://doi.org/10.1111/j.1472-765X.2008.02354.x>.
  117. Goeres DM, Hamilton MA, Beck NA, Buckingham-Meyer K, Hilyard JD, Loetterle LR, Lorenz LA, Walker DK, Stewart PS. 2009. A method for growing a biofilm under low shear at the air-liquid interface using the drip flow biofilm reactor. *Nat Protoc* 4:783–788. <https://doi.org/10.1038/nprot.2009.59>.
  118. Curtin JJ, Donlan RM. July 2009. Inhibition of biofilm formation using bacteriophage. US patent 20090191254 A1.
  119. McCoy WF, Bryers JD, Robbins J, Costerton JW. 1981. Observations of fouling biofilm formation. *Can J Microbiol* 27:910–917. <https://doi.org/10.1139/m81-143>.
  120. Costerton L-S. 1989. Behavior of bacteria in biofilms. *ASM News* 55: 650–654.
  121. Kolenbrander PE, Palmer RJ, Jr, Periasamy S, Jakubovics NS. 2010. Oral multispecies biofilm development and the key role of cell-cell distance. *Nat Rev Microbiol* 8:471–480. <https://doi.org/10.1038/nrmicro2381>.
  122. Blanc V, Isabal S, Sanchez MC, Llama-Palacios A, Herrera D, Sanz M, Leon R. 2014. Characterization and application of a flow system for in vitro multispecies oral biofilm formation. *J Periodontol Res* 49:323–332. <https://doi.org/10.1111/jre.12110>.
  123. Coenye T, Honraet K, Rigole P, Nadal Jimenez P, Nelis HJ. 2007. In vitro inhibition of *Streptococcus mutans* biofilm formation on hydroxyapatite by subinhibitory concentrations of anthraquinones. *Antimicrob Agents Chemother* 51:1541–1544. <https://doi.org/10.1128/AAC.00999-06>.
  124. Hughes G, Walker JT, Sharp R, Hart A. July 2010. Bacteriophage for the treatment of bacterial biofilms. US patent 7758856 B2.
  125. Raad I, Sherertz RJ. November 1994. M-EDTA pharmaceutical preparations and uses thereof. US patent 5362754 A.
  126. Schwartz K, Stephenson R, Hernandez M, Jambang N, Boles BR. 2010. The use of drip flow and rotating disk reactors for *Staphylococcus aureus* biofilm analysis. *J Vis Exp* 2010:2470. <https://doi.org/10.3791/2470>.
  127. Rickard AH, McBain AJ, Stead AT, Gilbert P. 2004. Shear rate moderates community diversity in freshwater biofilms. *Appl Environ Microbiol* 70:7426–7435. <https://doi.org/10.1128/AEM.70.12.7426-7435.2004>.
  128. Kirisits MJ, Prost L, Starkey M, Parsek MR. 2005. Characterization of colony morphology variants isolated from *Pseudomonas aeruginosa* biofilms. *Appl Environ Microbiol* 71:4809–4821. <https://doi.org/10.1128/AEM.71.8.4809-4821.2005>.
  129. Chen L, Wen YM. 2011. The role of bacterial biofilm in persistent infections and control strategies. *Int J Oral Sci* 3:66–73. <https://doi.org/10.4248/IJOS11022>.
  130. Joo HS, Otto M. 2012. Molecular basis of in vivo biofilm formation by bacterial pathogens. *Chem Biol* 19:1503–1513. <https://doi.org/10.1016/j.chembiol.2012.10.022>.
  131. Hill D, Rose B, Pajkos A, Robinson M, Bye P, Bell S, Elkins M, Thompson B, Macleod C, Aaron SD, Harbour C. 2005. Antibiotic susceptibilities of *Pseudomonas aeruginosa* isolates derived from patients with cystic fibrosis under aerobic, anaerobic, and biofilm conditions. *J Clin Microbiol* 43:5085–5090. <https://doi.org/10.1128/JCM.43.10.5085-5090.2005>.
  132. Moskowitz SM, Foster JM, Emerson J, Burns JL. 2004. Clinically feasible biofilm susceptibility assay for isolates of *Pseudomonas aeruginosa* from patients with cystic fibrosis. *J Clin Microbiol* 42:1915–1922. <https://doi.org/10.1128/JCM.42.5.1915-1922.2004>.
  133. Garcia-Sanchez S, Aubert S, Iraqui I, Janbon G, Ghigo JM, d'Enfert C. 2004. *Candida albicans* biofilms: a developmental state associated with specific and stable gene expression patterns. *Eukaryot Cell* 3:536–545. <https://doi.org/10.1128/EC.3.2.536-545.2004>.
  134. Toledo-Arana A, Merino N, Vergara-Irigaray M, Debarbouille M, Penades JR, Lasa I. 2005. *Staphylococcus aureus* develops an alternative, ica-independent biofilm in the absence of the *arlRS* two-component system. *J Bacteriol* 187:5318–5329. <https://doi.org/10.1128/JB.187.15.5318-5329.2005>.
  135. Vergara-Irigaray M, Valle J, Merino N, Latasa C, Garcia B, Ruiz de Los Mozos I, Solano C, Toledo-Arana A, Penades JR, Lasa I. 2009. Relevant role of fibronectin-binding proteins in *Staphylococcus aureus* biofilm-associated foreign-body infections. *Infect Immun* 77:3978–3991. <https://doi.org/10.1128/IAI.00616-09>.
  136. Benoit MR, Conant CG, Ionescu-Zanetti C, Schwartz M, Matin A. 2010. New device for high-throughput viability screening of flow biofilms.

- Appl Environ Microbiol 76:4136–4142. <https://doi.org/10.1128/AEM.03065-09>.
137. Tremblay YD, Vogeeler P, Jacques M, Harel J. 2015. High-throughput microfluidic method to study biofilm formation and host-pathogen interactions in pathogenic *Escherichia coli*. *Appl Environ Microbiol* 81:2827–2840. <https://doi.org/10.1128/AEM.04208-14>.
  138. Kim J, Hegde M, Jayaraman A. 2010. Microfluidic co-culture of epithelial cells and bacteria for investigating soluble signal-mediated interactions. *J Vis Exp* 2010:1749. <https://doi.org/10.3791/1749>.
  139. Lee JH, Wang H, Kaplan JB, Lee WY. 2010. Effects of *Staphylococcus epidermidis* on osteoblast cell adhesion and viability on a Ti alloy surface in a microfluidic co-culture environment. *Acta Biomater* 6:4422–4429. <https://doi.org/10.1016/j.actbio.2010.05.021>.
  140. Moreau-Marquis S, Redelman CV, Stanton BA, Anderson GG. 2010. Co-culture models of *Pseudomonas aeruginosa* biofilms grown on live human airway cells. *J Vis Exp* 2010:2186. <https://doi.org/10.3791/2186>.
  141. Anderson GG, Moreau-Marquis S, Stanton BA, O'Toole GA. 2008. In vitro analysis of tobramycin-treated *Pseudomonas aeruginosa* biofilms on cystic fibrosis-derived airway epithelial cells. *Infect Immun* 76:1423–1433. <https://doi.org/10.1128/IAI.01373-07>.
  142. Roussel L, Rousseau S. 2017. Exposure of airway epithelial cells to *Pseudomonas aeruginosa* biofilm-derived quorum sensing molecules decrease the activity of the anti-oxidant response element bound by NRF2. *Biochem Biophys Res Commun* 483:829–833. <https://doi.org/10.1016/j.bbrc.2017.01.009>.
  143. Millhouse E, Jose A, Sherry L, Lappin DF, Patel N, Middleton AM, Pratten J, Culshaw S, Ramage G. 2014. Development of an in vitro periodontal biofilm model for assessing antimicrobial and host modulatory effects of bioactive molecules. *BMC Oral Health* 14:80. <https://doi.org/10.1186/1472-6831-14-80>.
  144. Stephen AS, Millhouse E, Sherry L, Aduse-Opoku J, Culshaw S, Ramage G, Bradshaw DJ, Burnett GR, Allaker RP. 2016. In vitro effect of *Porphyromonas gingivalis* methionine gamma lyase on biofilm composition and oral inflammatory response. *PLoS One* 11:e0169157. <https://doi.org/10.1371/journal.pone.0169157>.
  145. Puttamreddy S, Minion FC. 2011. Linkage between cellular adherence and biofilm formation in *Escherichia coli* O157:H7 EDL933. *FEMS Microbiol Lett* 315:46–53. <https://doi.org/10.1111/j.1574-6968.2010.02173.x>.
  146. Zaatreh S, Haffner D, Strauss M, Dauben T, Zamponi C, Mittelmeier W, Quandt E, Kreikemeyer B, Bader R. 2017. Thin magnesium layer confirmed as an antibacterial and biocompatible implant coating in a coculture model. *Mol Med Rep* 15:1624–1630. <https://doi.org/10.3892/mmr.2017.6218>.
  147. Welch K, Cai Y, Stromme M. 2012. A method for quantitative determination of biofilm viability. *J Funct Biomater* 3:418–431. <https://doi.org/10.3390/jfb3020418>.
  148. Costerton W, Veeh R, Shirtliff M, Pasmore M, Post C, Ehrlich G. 2003. The application of biofilm science to the study and control of chronic bacterial infections. *J Clin Invest* 112:1466–1477. <https://doi.org/10.1172/JCI200320365>.
  149. Reichhardt C, Jacobson AN, Maher MC, Uang J, McCrate OA, Eckart M, Cegelski L. 2015. Congo red interactions with curli-producing *E. coli* and native curli amyloid fibers. *PLoS One* 10:e0140388. <https://doi.org/10.1371/journal.pone.0140388>.
  150. Serra DO, Richter AM, Hengge R. 2013. Cellulose as an architectural element in spatially structured *Escherichia coli* biofilms. *J Bacteriol* 195:5540–5554. <https://doi.org/10.1128/JB.00946-13>.
  151. Zhou Y, Blanco LP, Smith DR, Chapman MR. 2012. Bacterial amyloids. *Methods Mol Biol* 849:303–320. [https://doi.org/10.1007/978-1-61779-551-0\\_21](https://doi.org/10.1007/978-1-61779-551-0_21).
  152. Freeman DJ, Falkner FR, Keane CT. 1989. New method for detecting slime production by coagulase negative staphylococci. *J Clin Pathol* 42:872–874. <https://doi.org/10.1136/jcp.42.8.872>.
  153. Mann EE, Wozniak DJ. 2012. *Pseudomonas* biofilm matrix composition and niche biology. *FEMS Microbiol Rev* 36:893–916. <https://doi.org/10.1111/j.1574-6976.2011.00322.x>.
  154. Tote K, Vanden Berghe D, Maes L, Cos P. 2008. A new colorimetric microtitre model for the detection of *Staphylococcus aureus* biofilms. *Lett Appl Microbiol* 46:249–254. <https://doi.org/10.1111/j.1472-765X.2007.02298.x>.
  155. Stiefel P, Schmidt-Emrich S, Maniura-Weber K, Ren Q. 2015. Critical aspects of using bacterial cell viability assays with the fluorophores SYTO9 and propidium iodide. *BMC Microbiol* 15:36. <https://doi.org/10.1186/s12866-015-0376-x>.
  156. Ambriz-Avina V, Contreras-Garduno JA, Pedraza-Reyes M. 2014. Applications of flow cytometry to characterize bacterial physiological responses. *Biomed Res Int* 2014:461941. <https://doi.org/10.1155/2014/461941>.
  157. Stiefel P, Rosenberg U, Schneider J, Mauerhofer S, Maniura-Weber K, Ren Q. 2016. Is biofilm removal properly assessed? Comparison of different quantification methods in a 96-well plate system. *Appl Microbiol Biotechnol* 100:4135–4145. <https://doi.org/10.1007/s00253-016-7396-9>.
  158. Ohta T, Tokishita S, Yamagata H. 2001. Ethidium bromide and SYBR Green I enhance the genotoxicity of UV-irradiation and chemical mutagens in *E. coli*. *Mutat Res* 492:91–97. [https://doi.org/10.1016/S1383-5718\(01\)00155-3](https://doi.org/10.1016/S1383-5718(01)00155-3).
  159. Singer VL, Lawlor TE, Yue S. 1999. Comparison of SYBR Green I nucleic acid gel stain mutagenicity and ethidium bromide mutagenicity in the *Salmonella*/mammalian microsome reverse mutation assay (Ames test). *Mutat Res* 439:37–47. [https://doi.org/10.1016/S1383-5718\(98\)00172-7](https://doi.org/10.1016/S1383-5718(98)00172-7).
  160. Shapiro HM, Perlmutter NG. 2001. Violet laser diodes as light sources for cytometry. *Cytometry* 44:133–136. [https://doi.org/10.1002/1097-0320\(20010601\)44:2<133::AID-CYTO1092>3.0.CO;2-S](https://doi.org/10.1002/1097-0320(20010601)44:2<133::AID-CYTO1092>3.0.CO;2-S).
  161. Marshall JM, Flechtner AD, La Perle KM, Gunn JS. 2014. Visualization of extracellular matrix components within sectioned *Salmonella* biofilms on the surface of human gallstones. *PLoS One* 9:e89243. <https://doi.org/10.1371/journal.pone.0089243>.
  162. Pantanella F, Valenti P, Natalizi T, Passeri D, Berlutti F. 2013. Analytical techniques to study microbial biofilm on abiotic surfaces: pros and cons of the main techniques currently in use. *Ann Ig* 25:31–42. <https://doi.org/10.7416/ai.2013.1904>.
  163. Doll K, Jongstaphongpun KL, Stumpp NS, Winkel A, Stiesch M. 2016. Quantifying implant-associated biofilms: comparison of microscopic, microbiologic and biochemical methods. *J Microbiol Methods* 130:61–68. <https://doi.org/10.1016/j.mimet.2016.07.016>.
  164. Vandecandelaere I, Van Acker H, Coenye T. 2016. A microplate-based system as in vitro model of biofilm growth and quantification. *Methods Mol Biol* 1333:53–66. [https://doi.org/10.1007/978-1-4939-2854-5\\_5](https://doi.org/10.1007/978-1-4939-2854-5_5).
  165. Besnard V, Federighi M, Cappelier J. 2000. Evidence of viable but non-culturable state in *Listeria monocytogenes* by direct viable count and CTC-DAPI double staining. *Food Microbiol* 17:697–704. <https://doi.org/10.1006/fmic.2000.0366>.
  166. Rodriguez GG, Phipps D, Ishiguro K, Ridgway HF. 1992. Use of a fluorescent redox probe for direct visualization of actively respiring bacteria. *Appl Environ Microbiol* 58:1801–1808.
  167. Pantanella F, Valenti P, Frioni A, Natalizi T, Coltella L, Berlutti F. 2008. BioTimer assay, a new method for counting *Staphylococcus* spp. in biofilm without sample manipulation applied to evaluate antibiotic susceptibility of biofilm. *J Microbiol Methods* 75:478–484. <https://doi.org/10.1016/j.mimet.2008.07.027>.
  168. Honraet K, Goetghebeur E, Nelis HJ. 2005. Comparison of three assays for the quantification of *Candida* biomass in suspension and CDC reactor grown biofilms. *J Microbiol Methods* 63:287–295. <https://doi.org/10.1016/j.mimet.2005.03.014>.
  169. Cercado B, Chazaro-Ruiz LF, Ruiz V, Lopez-Prieto Ide J, Buitron G, Razo-Flores E. 2013. Biotic and abiotic characterization of bioanodes formed on oxidized carbon electrodes as a basis to predict their performance. *Biosens Bioelectron* 50:373–381. <https://doi.org/10.1016/j.bios.2013.06.051>.
  170. Cho SH, Naber K, Hacker J, Ziebuhr W. 2002. Detection of the *icaADBC* gene cluster and biofilm formation in *Staphylococcus epidermidis* isolates from catheter-related urinary tract infections. *Int J Antimicrob Agents* 19:570–575. [https://doi.org/10.1016/S0924-8579\(02\)00101-2](https://doi.org/10.1016/S0924-8579(02)00101-2).
  171. Conlon KM, Humphreys H, O'Gara JP. 2004. Inactivations of *rsbU* and *sarA* by IS256 represent novel mechanisms of biofilm phenotypic variation in *Staphylococcus epidermidis*. *J Bacteriol* 186:6208–6219. <https://doi.org/10.1128/JB.186.18.6208-6219.2004>.
  172. Bradford R, Abdul Manan R, Daley AJ, Pearce C, Ramalingam A, D'Mello D, Mueller Y, Uahwatanasakul W, Qu Y, Grando D, Garland S, Deighton M. 2006. Coagulase-negative staphylococci in very-low-birth-weight infants: inability of genetic markers to distinguish invasive strains from blood culture contaminants. *Eur J Clin Microbiol Infect Dis* 25:283–290. <https://doi.org/10.1007/s10096-006-0130-2>.
  173. Hennig S, Ziebuhr W. 2008. A transposase-independent mechanism gives rise to precise excision of IS256 from insertion sites in *Staphylo-*

- coccus epidermidis. *J Bacteriol* 190:1488–1490. <https://doi.org/10.1128/JB.01290-07>.
174. Beceiro A, Tomas M, Bou G. 2013. Antimicrobial resistance and virulence: a successful or deleterious association in the bacterial world? *Clin Microbiol Rev* 26:185–230. <https://doi.org/10.1128/CMR.00059-12>.
  175. Manos J, Arthur J, Rose B, Bell S, Tingpej P, Hu H, Webb J, Kjelleberg S, Gorrell MD, Bye P, Harbour C. 2009. Gene expression characteristics of a cystic fibrosis epidemic strain of *Pseudomonas aeruginosa* during biofilm and planktonic growth. *FEMS Microbiol Lett* 292:107–114. <https://doi.org/10.1111/j.1574-6968.2008.01472.x>.
  176. Schembri MA, Kjaergaard K, Klemm P. 2003. Global gene expression in *Escherichia coli* biofilms. *Mol Microbiol* 48:253–267. <https://doi.org/10.1046/j.1365-2958.2003.03432.x>.
  177. Cazares-Dominguez V, Ochoa SA, Cruz-Cordova A, Rodea GE, Escalona G, Olivares AL, Olivares-Trejo JJ, Velazquez-Guadarrama N, Xicohtencatl-Cortes J. 2015. Vancomycin modifies the expression of the agr system in multidrug-resistant *Staphylococcus aureus* clinical isolates. *Front Microbiol* 6:369. <https://doi.org/10.3389/fmicb.2015.00369>.
  178. Tsalik EL, Jones D, Nicholson B, Waring L, Liesenfeld O, Park LP, Glickman SW, Caram LB, Langley RJ, van Velkinburgh JC, Cairns CB, Rivers EP, Otero RM, Kingsmore SF, Lalani T, Fowler VG, Woods CW. 2010. Multiplex PCR to diagnose bloodstream infections in patients admitted from the emergency department with sepsis. *J Clin Microbiol* 48:26–33. <https://doi.org/10.1128/JCM.01447-09>.
  179. Iorio NL, Azevedo MB, Frazao VH, Barcellos AG, Barros EM, Pereira EM, de Mattos CS, dos Santos KR. 2011. Methicillin-resistant *Staphylococcus epidermidis* carrying biofilm formation genes: detection of clinical isolates by multiplex PCR. *Int Microbiol* 14:13–17.
  180. Duran-Pinedo AE, Yost S, Frias-Lopez J. 2015. Small RNA transcriptome of the oral microbiome during periodontitis progression. *Appl Environ Microbiol* 81:6688–6699. <https://doi.org/10.1128/AEM.01782-15>.
  181. Yadav MK, Chae SW, Go YY, Im GJ, Song JJ. 2017. In vitro multi-species biofilms of methicillin-resistant *Staphylococcus aureus* and *Pseudomonas aeruginosa* and their host interaction during in vivo colonization of an otitis media rat model. *Front Cell Infect Microbiol* 7:125. <https://doi.org/10.3389/fcimb.2017.00125>.
  182. Seneviratne CJ, Suriyanarayanan T, Swarup S, Chia KHB, Nagarajan N, Zhang C. 2017. Transcriptomics analysis reveals putative genes involved in biofilm formation and biofilm-associated drug resistance of *Enterococcus faecalis*. *J Endod* 43:949–955. <https://doi.org/10.1016/j.joen.2017.01.020>.
  183. Carvalhais V, Franca A, Cerca F, Vitorino R, Pier GB, Vilanova M, Cerca N. 2014. Dormancy within *Staphylococcus epidermidis* biofilms: a transcriptomic analysis by RNA-seq. *Appl Microbiol Biotechnol* 98:2585–2596. <https://doi.org/10.1007/s00253-014-5548-3>.
  184. Jagathrakshakan SN, Sethumadhava RJ, Mehta DT, Ramanathan A. 2015. 16S rRNA gene-based metagenomic analysis identifies a novel bacterial co-prevalence pattern in dental caries. *Eur J Dent* 9:127–132. <https://doi.org/10.4103/1305-7456.149661>.
  185. Pobre V, Arraiano CM. 2015. Next generation sequencing analysis reveals that the ribonucleases RNase II, RNase R and PNPase affect bacterial motility and biofilm formation in *E. coli*. *BMC Genomics* 16:72. <https://doi.org/10.1186/s12864-015-1237-6>.
  186. Yost S, Duran-Pinedo AE, Teles R, Krishnan K, Frias-Lopez J. 2015. Functional signatures of oral dysbiosis during periodontitis progression revealed by microbial metatranscriptome analysis. *Genome Med* 7:27. <https://doi.org/10.1186/s13073-015-0153-3>.
  187. Seneviratne CJ, Wang Y, Jin L, Wong SS, Herath TD, Samaranyake LP. 2012. Unraveling the resistance of microbial biofilms: has proteomics been helpful? *Proteomics* 12:651–665. <https://doi.org/10.1002/pmic.201100356>.
  188. Perez-Llarena FJ, Bou G. 2016. Proteomics as a tool for studying bacterial virulence and antimicrobial resistance. *Front Microbiol* 7:410. <https://doi.org/10.3389/fmicb.2016.00410>.
  189. Chen B, Zhang D, Wang X, Ma W, Deng S, Zhang P, Zhu H, Xu N, Liang S. 2017. Proteomics progresses in microbial physiology and clinical antimicrobial therapy. *Eur J Clin Microbiol Infect Dis* 36:403–413. <https://doi.org/10.1007/s10096-016-2816-4>.
  190. Kuboniwa M, Tribble GD, Hendrickson EL, Amano A, Lamont RJ, Hackett M. 2012. Insights into the virulence of oral biofilms: discoveries from proteomics. *Expert Rev Proteomics* 9:311–323. <https://doi.org/10.1586/ep.12.16>.
  191. Soufi Y, Soufi B. 2016. Mass spectrometry-based bacterial proteomics: focus on dermatologic microbial pathogens. *Front Microbiol* 7:181. <https://doi.org/10.3389/fmicb.2016.00181>.
  192. Grassl N, Kulak NA, Pichler G, Geyer PE, Jung J, Schubert S, Sinitcyn P, Cox J, Mann M. 2016. Ultra-deep and quantitative saliva proteome reveals dynamics of the oral microbiome. *Genome Med* 8:44. <https://doi.org/10.1186/s13073-016-0293-0>.
  193. Herschend J, Damholt ZBV, Marquard AM, Svensson B, Sorensen SJ, Hagglund P, Burmolle M. 2017. A meta-proteomics approach to study the interspecies interactions affecting microbial biofilm development in a model community. *Sci Rep* 7:16483. <https://doi.org/10.1038/s41598-017-16633-6>.
  194. Mallick H, Ma S, Franzosa EA, Vatanen T, Morgan XC, Huttenhower C. 2017. Experimental design and quantitative analysis of microbial community multiomics. *Genome Biol* 18:228. <https://doi.org/10.1186/s13059-017-1359-z>.
  195. Ammons MC, Triplet BP, Carlson RP, Kirker KR, Gross MA, Stanisch JJ, Copie V. 2014. Quantitative NMR metabolite profiling of methicillin-resistant and methicillin-susceptible *Staphylococcus aureus* discriminates between biofilm and planktonic phenotypes. *J Proteome Res* 13:2973–2985. <https://doi.org/10.1021/pr500120c>.
  196. Cegelski L. 2015. Bottom-up and top-down solid-state NMR approaches for bacterial biofilm matrix composition. *J Magn Reson* 253:91–97. <https://doi.org/10.1016/j.jmr.2015.01.014>.
  197. Reichhardt C, Fong JC, Yildiz F, Cegelski L. 2015. Characterization of the *Vibrio cholerae* extracellular matrix: a top-down solid-state NMR approach. *Biochim Biophys Acta* 1848:378–383. <https://doi.org/10.1016/j.bbame.2014.05.030>.
  198. Ngo JT, Babin BM, Champion JA, Schuman EM, Tirrell DA. 2012. State-selective metabolic labeling of cellular proteins. *ACS Chem Biol* 7:1326–1330. <https://doi.org/10.1021/cb300238w>.
  199. Wagstaff JL, Sadvokaya I, Vinogradov E, Jabbouri S, Howard MJ. 2008. Poly-N-acetylglucosamine and poly(glycerol phosphate) teichoic acid identification from staphylococcal biofilm extracts using excitation sculptured TOCSY NMR. *Mol Biosyst* 4:170–174. <https://doi.org/10.1039/B715242F>.
  200. Almeida C, Azevedo NF, Santos S, Keevil CW, Vieira MJ. 2011. Discriminating multi-species populations in biofilms with peptide nucleic acid fluorescence in situ hybridization (PNA FISH). *PLoS One* 6:e14786. <https://doi.org/10.1371/journal.pone.0014786>.
  201. Malic S, Hill KE, Hayes A, Percival SL, Thomas DW, Williams DW. 2009. Detection and identification of specific bacteria in wound biofilms using peptide nucleic acid fluorescent in situ hybridization (PNA FISH). *Microbiology* 155:2603–2611. <https://doi.org/10.1099/mic.0.028712-0>.
  202. Bjarnsholt T, Nielsen XC, Johansen U, Norgaard L, Hoiby N. 2011. Methods to classify bacterial pathogens in cystic fibrosis. *Methods Mol Biol* 742:143–171. [https://doi.org/10.1007/978-1-61779-120-8\\_9](https://doi.org/10.1007/978-1-61779-120-8_9).
  203. Shakes DC, Miller DM, III, Nonet ML. 2012. Immunofluorescence microscopy. *Methods Cell Biol* 107:35–66. <https://doi.org/10.1016/B978-0-12-394620-1.00002-3>.
  204. Lawrence JR, Swerhone GD, Leppard GG, Araki T, Zhang X, West MM, Hitchcock AP. 2003. Scanning transmission X-ray, laser scanning, and transmission electron microscopy mapping of the exopolymeric matrix of microbial biofilms. *Appl Environ Microbiol* 69:5543–5554. <https://doi.org/10.1128/AEM.69.9.5543-5554.2003>.
  205. McLoon AL, Kolodkin-Gal I, Rubinstein SM, Kolter R, Losick R. 2011. Spatial regulation of histidine kinases governing biofilm formation in *Bacillus subtilis*. *J Bacteriol* 193:679–685. <https://doi.org/10.1128/JB.01186-10>.
  206. Zhang Z, Nadezhina E, Wilkinson KJ. 2011. Quantifying diffusion in a biofilm of *Streptococcus mutans*. *Antimicrob Agents Chemother* 55:1075–1081. <https://doi.org/10.1128/AAC.01329-10>.
  207. Drago L, Agrappi S, Bortolin M, Toscano M, Romano CL, De Vecchi E. 2016. How to study biofilms after microbial colonization of materials used in orthopaedic implants. *Int J Mol Sci* 17:293. <https://doi.org/10.3390/ijms17030293>.
  208. Khajotia SS, Smart KH, Pilula M, Thompson DM. 2013. Concurrent quantification of cellular and extracellular components of biofilms. *J Vis Exp* 2013:e50639. <https://doi.org/10.3791/50639>.
  209. Neu TR, Lawrence JR. 2015. Innovative techniques, sensors, and approaches for imaging biofilms at different scales. *Trends Microbiol* 23:233–242. <https://doi.org/10.1016/j.tim.2014.12.010>.
  210. Gustafsson MG. 2005. Nonlinear structured-illumination microscopy: wide-field fluorescence imaging with theoretically unlimited resolu-

- tion. *Proc Natl Acad Sci U S A* 102:13081–13086. <https://doi.org/10.1073/pnas.0406877102>.
211. Shao L, Kner P, Rego EH, Gustafsson MG. 2011. Super-resolution 3D microscopy of live whole cells using structured illumination. *Nat Methods* 8:1044–1046. <https://doi.org/10.1038/nmeth.1734>.
  212. Fernandez-Suarez M, Ting AY. 2008. Fluorescent probes for super-resolution imaging in living cells. *Nat Rev Mol Cell Biol* 9:929–943. <https://doi.org/10.1038/nrm2531>.
  213. Schermelleh L, Heintzmann R, Leonhardt H. 2010. A guide to super-resolution fluorescence microscopy. *J Cell Biol* 190:165–175. <https://doi.org/10.1083/jcb.201002018>.
  214. Nguyen CT, Robinson SR, Jung W, Novak MA, Boppart SA, Allen JB. 2013. Investigation of bacterial biofilm in the human middle ear using optical coherence tomography and acoustic measurements. *Hear Res* 301:193–200. <https://doi.org/10.1016/j.heares.2013.04.001>.
  215. Chen R, Rudney J, Aparicio C, Fok A, Jones RS. 2012. Quantifying dental biofilm growth using cross-polarization optical coherence tomography. *Lett Appl Microbiol* 54:537–542. <https://doi.org/10.1111/j.1472-765X.2012.03243.x>.
  216. Xi C, Marks D, Schlachter S, Luo W, Boppart SA. 2006. High-resolution three-dimensional imaging of biofilm development using optical coherence tomography. *J Biomed Opt* 11:34001. <https://doi.org/10.1117/1.2209962>.
  217. Priester JH, Horst AM, Van de Werfhorst LC, Saleta JL, Mertes LA, Holden PA. 2007. Enhanced visualization of microbial biofilms by staining and environmental scanning electron microscopy. *J Microbiol Methods* 68:577–587. <https://doi.org/10.1016/j.mimet.2006.10.018>.
  218. Gahukamble AD, McDowell A, Post V, Salavarieta Varela J, Rochford ET, Richards RG, Patrick S, Moriarty TF. 2014. Propionibacterium acnes and Staphylococcus lugdunensis cause pyogenic osteomyelitis in an intramedullary nail model in rabbits. *J Clin Microbiol* 52:1595–1606. <https://doi.org/10.1128/JCM.03197-13>.
  219. Holling N, Dedi C, Jones CE, Hawthorne JA, Hanlon GW, Salvage JP, Patel BA, Barnes LM, Jones BV. 2014. Evaluation of environmental scanning electron microscopy for analysis of Proteus mirabilis crystalline biofilms in situ on urinary catheters. *FEMS Microbiol Lett* 355:20–27. <https://doi.org/10.1111/1574-6968.12451>.
  220. Walther P, Ziegler A. 2002. Freeze substitution of high-pressure frozen samples: the visibility of biological membranes is improved when the substitution medium contains water. *J Microsc* 208:3–10. <https://doi.org/10.1046/j.1365-2818.2002.01064.x>.
  221. Oates A, Bowling FL, Boulton AJ, Bowler PG, Metcalf DG, McBain AJ. 2014. The visualization of biofilms in chronic diabetic foot wounds using routine diagnostic microscopy methods. *J Diabetes Res* 2014:153586. <https://doi.org/10.1155/2014/153586>.
  222. Asahi Y, Miura J, Tsuda T, Kuwabata S, Tsunashima K, Noiri Y, Sakata T, Ebisu S, Hayashi M. 2015. Simple observation of Streptococcus mutans biofilm by scanning electron microscopy using ionic liquids. *AMB Express* 5:6. <https://doi.org/10.1186/s13568-015-0097-4>.
  223. Sugimoto S, Okuda K, Miyakawa R, Sato M, Arita-Morioka K, Chiba A, Yamanaka K, Ogura T, Mizunoe Y, Sato C. 2016. Imaging of bacterial multicellular behaviour in biofilms in liquid by atmospheric scanning electron microscopy. *Sci Rep* 6:25889. <https://doi.org/10.1038/srep25889>.
  224. Hunter RC, Hitchcock AP, Dynes JJ, Obst M, Beveridge TJ. 2008. Mapping the speciation of iron in Pseudomonas aeruginosa biofilms using scanning transmission X-ray microscopy. *Environ Sci Technol* 42:8766–8772. <https://doi.org/10.1021/es801642z>.
  225. Yang SI, George GN, Lawrence JR, Kaminskyj SG, Dynes JJ, Lai B, Pickering IJ. 2016. Multispecies biofilms transform selenium oxyanions into elemental selenium particles: studies using combined synchrotron X-ray fluorescence imaging and scanning transmission X-ray microscopy. *Environ Sci Technol* 50:10343–10350. <https://doi.org/10.1021/acs.est.5b04529>.
  226. Dynes JJ, Lawrence JR, Korber DR, Swerhone GD, Leppard GG, Hitchcock AP. 2009. Morphological and biochemical changes in Pseudomonas fluorescens biofilms induced by sub-inhibitory exposure to antimicrobial agents. *Can J Microbiol* 55:163–178. <https://doi.org/10.1139/W08-109>.
  227. Dufrene YF. 2002. Atomic force microscopy, a powerful tool in microbiology. *J Bacteriol* 184:5205–5213. <https://doi.org/10.1128/JB.184.19.5205-5213.2002>.
  228. Dufrene YF. 2014. Atomic force microscopy in microbiology: new structural and functional insights into the microbial cell surface. *mBio* 5:e01363-14. <https://doi.org/10.1128/mBio.01363-14>.
  229. Dufrene YF. 2001. Application of atomic force microscopy to microbial surfaces: from reconstituted cell surface layers to living cells. *Micron* 32:153–165. [https://doi.org/10.1016/S0968-4328\(99\)00106-7](https://doi.org/10.1016/S0968-4328(99)00106-7).
  230. Oh YJ, Lee NR, Jo W, Jung WK, Lim JS. 2009. Effects of substrates on biofilm formation observed by atomic force microscopy. *Ultramicroscopy* 109:874–880. <https://doi.org/10.1016/j.ultramic.2009.03.042>.
  231. Beier BD, Quivey RG, Berger AJ. 2010. Identification of different bacterial species in biofilms using confocal Raman microscopy. *J Biomed Opt* 15:066001. <https://doi.org/10.1117/1.3505010>.
  232. Watrous JD, Dorrestein PC. 2011. Imaging mass spectrometry in microbiology. *Nat Rev Microbiol* 9:683–694. <https://doi.org/10.1038/nrmicro2634>.
  233. Fang J, Dorrestein PC. 2014. Emerging mass spectrometry techniques for the direct analysis of microbial colonies. *Curr Opin Microbiol* 19:120–129. <https://doi.org/10.1016/j.mib.2014.06.014>.
  234. Lanni EJ, Masyuko RN, Driscoll CM, Aerts JT, Shrout JD, Bohn PW, Sweedler JV. 2014. MALDI-guided SIMS: multiscale imaging of metabolites in bacterial biofilms. *Anal Chem* 86:9139–9145. <https://doi.org/10.1021/ac5020222>.
  235. Lanni EJ, Masyuko RN, Driscoll CM, Dunham SJ, Shrout JD, Bohn PW, Sweedler JV. 2014. Correlated imaging with C60-SIMS and confocal Raman microscopy: visualization of cell-scale molecular distributions in bacterial biofilms. *Anal Chem* 86:10885–10891. <https://doi.org/10.1021/ac5030914>.
  236. Baig NF, Dunham SJ, Morales-Soto N, Shrout JD, Sweedler JV, Bohn PW. 2015. Multimodal chemical imaging of molecular messengers in emerging Pseudomonas aeruginosa bacterial communities. *Analyst* 140:6544–6552. <https://doi.org/10.1039/C5AN01149C>.
  237. Yang Q, Phillips PL, Sampson EM, Progulsk-Fox A, Jin S, Antonelli P, Schultz GS. 2013. Development of a novel ex vivo porcine skin explant model for the assessment of mature bacterial biofilms. *Wound Repair Regen* 21:704–714. <https://doi.org/10.1111/wrr.12074>.
  238. Al-Ishaq R, Armstrong J, Gregory M, O'Hara M, Phiri K, Harris LG, Rohde H, Siemssen N, Frommelt L, Mack D, Wilkinson TS. 2015. Effects of polysaccharide intercellular adhesin (PIA) in an ex vivo model of whole blood killing and in prosthetic joint infection (PJI): a role for C5a. *Int J Med Microbiol* 305:948–956. <https://doi.org/10.1016/j.ijmm.2015.08.005>.
  239. Ellington JK, Reilly SS, Ramp WK, Smeltzer MS, Kellam JF, Hudson MC. 1999. Mechanisms of Staphylococcus aureus invasion of cultured osteoblasts. *Microb Pathog* 26:317–323. <https://doi.org/10.1006/mpat.1999.0272>.
  240. Yang Q, Larose C, Della Porta AC, Schultz GS, Gibson DJ. 2017. A surfactant-based wound dressing can reduce bacterial biofilms in a porcine skin explant model. *Int Wound J* 14:408–413. <https://doi.org/10.1111/iwj.12619>.
  241. Wolcott RD, Rumbaugh KP, James G, Schultz G, Phillips P, Yang Q, Watters C, Stewart PS, Dowd SE. 2010. Biofilm maturity studies indicate sharp debridement opens a time-dependent therapeutic window. *J Wound Care* 19:320–328. <https://doi.org/10.12968/jowc.2010.19.8.77709>.
  242. Phillips PL, Yang Q, Schultz GS. 2013. The effect of negative pressure wound therapy with periodic instillation using antimicrobial solutions on Pseudomonas aeruginosa biofilm on porcine skin explants. *Int Wound J* 10(Suppl 1):S48–S55. <https://doi.org/10.1111/iwj.12180>.
  243. Alhusein N, Blagbrough IS, Beeton ML, Bolhuis A, De Bank PA. 2016. Electrospun Zein/PCL fibrous matrices release tetracycline in a controlled manner, killing Staphylococcus aureus both in biofilms and ex vivo on pig skin, and are compatible with human skin cells. *Pharm Res* 33:237–246. <https://doi.org/10.1007/s11095-015-1782-3>.
  244. John G, Becker J, Schwarz F. 2016. Effectivity of air-abrasive powder based on glycine and tricalcium phosphate in removal of initial biofilm on titanium and zirconium oxide surfaces in an ex vivo model. *Clin Oral Investig* 20:711–719. <https://doi.org/10.1007/s00784-015-1571-8>.
  245. Phillips PL, Yang Q, Davis S, Sampson EM, Azeke JI, Hamad A, Schultz GS. 2015. Antimicrobial dressing efficacy against mature Pseudomonas aeruginosa biofilm on porcine skin explants. *Int Wound J* 12:469–483. <https://doi.org/10.1111/iwj.12142>.
  246. Chuang-Smith ON, Wells CL, Henry-Stanley MJ, Dunny GM. 2010. Acceleration of Enterococcus faecalis biofilm formation by aggregation substance expression in an ex vivo model of cardiac valve colonization. *PLoS One* 5:e15798. <https://doi.org/10.1371/journal.pone.0015798>.
  247. Simmons WL, Dybvig K. 2009. Mycoplasma biofilms ex vivo and in vivo. *FEMS Microbiol Lett* 295:77–81. <https://doi.org/10.1111/j.1574-6968.2009.01592.x>.
  248. Harrison F, Diggle SP. 2016. An ex vivo lung model to study bronchioles



- infected with *Pseudomonas aeruginosa* biofilms. *Microbiology* 162: 1755–1760. <https://doi.org/10.1099/mic.0.000352>.
249. Vlastarakos PV, Nikolopoulos TP, Maragoudakis P, Tzagaroulakis A, Ferekidis E. 2007. Biofilms in ear, nose, and throat infections: how important are they? *Laryngoscope* 117:668–673. <https://doi.org/10.1097/MLG.0b013e318030e422>.
  250. Mehta AJ, Lee JC, Stevens GR, Antonelli PJ. 2006. Opening plugged tympanostomy tubes: effect of biofilm formation. *Otolaryngol Head Neck Surg* 134:121–125. <https://doi.org/10.1016/j.otohns.2005.10.017>.
  251. Leroy M, Cabral H, Figueira M, Bouchet V, Huot H, Ram S, Pelton SI, Goldstein R. 2007. Multiple consecutive lavage samplings reveal greater burden of disease and provide direct access to the nontypeable *Haemophilus influenzae* biofilm in experimental otitis media. *Infect Immun* 75:4158–4172. <https://doi.org/10.1128/IAI.00318-07>.
  252. Huang TY, Gulabivala K, Ng YL. 2008. A bio-molecular film ex-vivo model to evaluate the influence of canal dimensions and irrigation variables on the efficacy of irrigation. *Int Endod J* 41:60–71.
  253. McGill S, Gulabivala K, Mordan N, Ng YL. 2008. The efficacy of dynamic irrigation using a commercially available system (RinsEndo) determined by removal of a collagen 'bio-molecular film' from an ex vivo model. *Int Endod J* 41:602–608. <https://doi.org/10.1111/j.1365-2591.2008.01408.x>.
  254. Dos Santos PA, Pereira AC, Braga RL, Rosa AC, Freitas-Almeida AC. 2016. Adhesion and cytotoxicity of *Aeromonas caviae* to rabbit intestinal epithelium ex vivo. *Antonie Van Leeuwenhoek* 109:1261–1270. <https://doi.org/10.1007/s10482-016-0728-z>.
  255. Breshears LM, Edwards VL, Ravel J, Peterson ML. 2015. *Lactobacillus crispatus* inhibits growth of *Gardnerella vaginalis* and *Neisseria gonorrhoeae* on a porcine vaginal mucosa model. *BMC Microbiol* 15:276. <https://doi.org/10.1186/s12866-015-0608-0>.
  256. Fallon JP, Reeves EP, Kavanagh K. 2011. The *Aspergillus fumigatus* toxin fumagillin suppresses the immune response of *Galleria mellonella* larvae by inhibiting the action of haemocytes. *Microbiology* 157: 1481–1488. <https://doi.org/10.1099/mic.0.043786-0>.
  257. Lionakis MS. 2011. *Drosophila* and *Galleria* insect model hosts: new tools for the study of fungal virulence, pharmacology and immunology. *Virulence* 2:521–527. <https://doi.org/10.4161/viru.2.6.18520>.
  258. Abebe E, Abebe-Akele F, Morrison J, Cooper V, Thomas WK. 2011. An insect pathogenic symbiosis between a *Caenorhabditis* and *Serratia*. *Virulence* 2:158–161. <https://doi.org/10.4161/viru.2.2.15337>.
  259. Olsen RJ, Watkins ME, Cantu CC, Beres SB, Musser JM. 2011. Virulence of serotype M3 group A *Streptococcus* strains in wax worms (*Galleria mellonella* larvae). *Virulence* 2:111–119. <https://doi.org/10.4161/viru.2.2.14338>.
  260. Uehlinger S, Schwager S, Bernier SP, Riedel K, Nguyen DT, Sokol PA, Eberl L. 2009. Identification of specific and universal virulence factors in *Burkholderia cenocepacia* strains by using multiple infection hosts. *Infect Immun* 77:4102–4110. <https://doi.org/10.1128/IAI.00398-09>.
  261. Schwager S, Agnoli K, Kothe M, Feldmann F, Givskov M, Carlier A, Eberl L. 2013. Identification of *Burkholderia cenocepacia* strain H111 virulence factors using nonmammalian infection hosts. *Infect Immun* 81: 143–153. <https://doi.org/10.1128/IAI.00768-12>.
  262. Chuzel T, Sanchez V, Vandamme M, Martin S, Flety O, Pager A, Chabanel C, Magnier L, Foskolos M, Petit O, Rokbi B, Chereul E. 2015. Impact of anesthesia protocols on in vivo bioluminescent bacteria imaging results. *PLoS One* 10:e0134048. <https://doi.org/10.1371/journal.pone.0134048>.
  263. Sheps JA, Ralph S, Zhao Z, Baillie DL, Ling V. 2004. The ABC transporter gene family of *Caenorhabditis elegans* has implications for the evolutionary dynamics of multidrug resistance in eukaryotes. *Genome Biol* 5:R15. <https://doi.org/10.1186/gb-2004-5-3-r15>.
  264. James CE, Davey MW. 2009. Increased expression of ABC transport proteins is associated with ivermectin resistance in the model nematode *Caenorhabditis elegans*. *Int J Parasitol* 39:213–220. <https://doi.org/10.1016/j.ijpara.2008.06.009>.
  265. Swem LR, Swem DL, O'Loughlin CT, Gatmaitan R, Zhao B, Ulrich SM, Bassler BL. 2009. A quorum-sensing antagonist targets both membrane-bound and cytoplasmic receptors and controls bacterial pathogenicity. *Mol Cell* 35:143–153. <https://doi.org/10.1016/j.molcel.2009.05.029>.
  266. Brackman G, Cos P, Maes L, Nelis HJ, Coenye T. 2011. Quorum sensing inhibitors increase the susceptibility of bacterial biofilms to antibiotics in vitro and in vivo. *Antimicrob Agents Chemother* 55:2655–2661. <https://doi.org/10.1128/AAC.00045-11>.
  267. Zhang Y, Brackman G, Coenye T. 2017. Pitfalls associated with evaluating enzymatic quorum quenching activity: the case of MomL and its effect on *Pseudomonas aeruginosa* and *Acinetobacter baumannii* biofilms. *PeerJ* 5:e3251. <https://doi.org/10.7717/peerj.3251>.
  268. Schmid N, Suppiger A, Steiner E, Pessi G, Kaever V, Fazli M, Tolker-Nielsen T, Jenal U, Eberl L. 2017. High intracellular c-di-GMP levels antagonize quorum sensing and virulence gene expression in *Burkholderia cenocepacia* H111. *Microbiology* 163:754–764. <https://doi.org/10.1099/mic.0.000452>.
  269. Luo J, Dong B, Wang K, Cai S, Liu T, Cheng X, Lei D, Chen Y, Li Y, Kong J, Chen Y. 2017. Baicalin inhibits biofilm formation, attenuates the quorum sensing-controlled virulence and enhances *Pseudomonas aeruginosa* clearance in a mouse peritoneal infection model. *PLoS One* 12:e0176883. <https://doi.org/10.1371/journal.pone.0176883>.
  270. Husain FM, Ahmad I, Al-Thubiani AS, Abulreesh HH, AlHazza IM, Aqil F. 2017. Leaf extracts of *Mangifera indica* L. inhibit quorum sensing-regulated production of virulence factors and biofilm in test bacteria. *Front Microbiol* 8:727. <https://doi.org/10.3389/fmicb.2017.00727>.
  271. Salunkhe P, Smart CH, Morgan JA, Panagea S, Walshaw MJ, Hart CA, Geffers R, Tümmler B, Winstanley C. 2005. A cystic fibrosis epidemic strain of *Pseudomonas aeruginosa* displays enhanced virulence and antimicrobial resistance. *J Bacteriol* 187:4908–4920. <https://doi.org/10.1128/JB.187.14.4908-4920.2005>.
  272. Apidianakis Y, Rahme L. 2009. *Drosophila melanogaster* as a model host for studying *Pseudomonas aeruginosa* infection. *Nat Protoc* 4:1285–1294. <https://doi.org/10.1038/nprot.2009.124>.
  273. Scofield JA, Duan D, Zhu F, Wu H. 2017. A commensal streptococcus hijacks a *Pseudomonas aeruginosa* exopolysaccharide to promote biofilm formation. *PLoS Pathog* 13:e1006300. <https://doi.org/10.1371/journal.ppat.1006300>.
  274. Apidianakis Y, Mindrinos M, Xiao W, Lau G, Baldini R, Davis R, Rahme L. 2005. Profiling early infection responses: *Pseudomonas aeruginosa* eludes host defenses by suppressing antimicrobial peptide gene expression. *Proc Natl Acad Sci U S A* 102:2573–2578. <https://doi.org/10.1073/pnas.0409588102>.
  275. Apidianakis Y, Mindrinos M, Xiao W, Tegos G, Papisov M, Hamblin M, Davis R, Tompkins R, Rahme L. 2007. Involvement of skeletal muscle gene regulatory network in susceptibility to wound infection following trauma. *PLoS One* 2:e1356. <https://doi.org/10.1371/journal.pone.0001356>.
  276. Apidianakis Y, Que Y, Xu W, Tegos G, Zimniak P, Hamblin M, Tompkins R, Xiao W, Rahme L. 2012. Down-regulation of glutathione S-transferase  $\alpha$  4 (hGSTA4) in the muscle of thermally injured patients is indicative of susceptibility to bacterial infection. *FASEB J* 26:730–737. <https://doi.org/10.1096/fj.11-192484>.
  277. Lau G, Goumnerov B, Walendziewicz C, Hewitson J, Xiao W, Mahajan-Miklos S, Tompkins R, Perkins L, Rahme L. 2003. The *Drosophila melanogaster* Toll pathway participates in resistance to infection by the gram-negative human pathogen *Pseudomonas aeruginosa*. *Infect Immun* 71:4059–4066. <https://doi.org/10.1128/IAI.71.7.4059-4066.2003>.
  278. An D, Apidianakis Y, Boechat A, Baldini R, Goumnerov B, Rahme L. 2009. The pathogenic properties of a novel and conserved gene product, KerV, in proteobacteria. *PLoS One* 4:e7167. <https://doi.org/10.1371/journal.pone.0007167>.
  279. de Lima Pimenta A, Di Martino P, Le Boudier E, Hulen C, Blight MA. 2003. In vitro identification of two adherence factors required for in vivo virulence of *Pseudomonas fluorescens*. *Microbes Infect* 5:1177–1187. <https://doi.org/10.1016/j.micinf.2003.09.002>.
  280. Estin ML, Stoltz DA, Zabner J. 2010. Paraoxonase 1, quorum sensing, and *P. aeruginosa* infection: a novel model. *Adv Exp Med Biol* 660: 183–193. [https://doi.org/10.1007/978-1-60761-350-3\\_17](https://doi.org/10.1007/978-1-60761-350-3_17).
  281. Mulcahy H, Sibley CD, Surette MG, Lewenza S. 2011. *Drosophila melanogaster* as an animal model for the study of *Pseudomonas aeruginosa* biofilm infections in vivo. *PLoS Pathog* 7:e1002299. <https://doi.org/10.1371/journal.ppat.1002299>.
  282. Galac MR, Lazzaro BP. 2011. Comparative pathology of bacteria in the genus *Providencea* to a natural host, *Drosophila melanogaster*. *Microbes Infect* 13:673–683. <https://doi.org/10.1016/j.micinf.2011.02.005>.
  283. Earl SC, Rogers MT, Keen J, Bland DM, Houppert AS, Miller C, Temple I, Anderson DM, Marketon MM. 2015. Resistance to innate immunity contributes to colonization of the insect gut by *Yersinia pestis*. *PLoS One* 10:e0133318. <https://doi.org/10.1371/journal.pone.0133318>.
  284. Bokhari H, Ali A, Noreen Z, Thomson N, Wren BW. 2017. *Galleria mellonella* is low cost and suitable surrogate host for studying virulence of human pathogenic *Vibrio cholerae*. *Gene* 628:1–7. <https://doi.org/10.1016/j.gene.2017.07.019>.

285. Mylonakis E, Moreno R, El Khoury JB, Idnurm A, Heitman J, Calderwood SB, Ausubel FM, Diener A. 2005. *Galleria mellonella* as a model system to study *Cryptococcus neoformans* pathogenesis. *Infect Immun* 73:3842–3850. <https://doi.org/10.1128/IAI.73.7.3842-3850.2005>.
286. Dean SN, van Hoek ML. 2015. Screen of FDA-approved drug library identifies maprotiline, an antibiofilm and antivirulence compound with QseC sensor-kinase dependent activity in *Francisella novicida*. *Virulence* 6:487–503. <https://doi.org/10.1080/21505594.2015.1046029>.
287. Wand ME, Bock LJ, Turton JF, Nugent PG, Sutton JM. 2012. *Acinetobacter baumannii* virulence is enhanced in *Galleria mellonella* following biofilm adaptation. *J Med Microbiol* 61:470–477. <https://doi.org/10.1099/jmm.0.037523-0>.
288. Ibrahim M, Tang Q, Shi Y, Almoneafy A, Fang Y, Xu L, Li W, Li B, Xie GL. 2012. Diversity of potential pathogenicity and biofilm formation among *Burkholderia cepacia* complex water, clinical, and agricultural isolates in China. *World J Microbiol Biotechnol* 28:2113–2123. <https://doi.org/10.1007/s11274-012-1016-3>.
289. Denman CC, Robinson MT, Sass AM, Mahenthalingam E, Brown AR. 2014. Growth on mannitol-rich media elicits a genome-wide transcriptional response in *Burkholderia multivorans* that impacts on multiple virulence traits in an exopolysaccharide-independent manner. *Microbiology* 160:187–197. <https://doi.org/10.1099/mic.0.072975-0>.
290. Gundogdu O, Mills DC, Elmi A, Martin MJ, Wren BW, Dorrell N. 2011. The *Campylobacter jejuni* transcriptional regulator Cj1556 plays a role in the oxidative and aerobic stress response and is important for bacterial survival in vivo. *J Bacteriol* 193:4238–4249. <https://doi.org/10.1128/JB.05189-11>.
291. Cullen L, Weiser R, Olszak T, Maldonado RF, Moreira AS, Slachmuylders L, Brackman G, Paunova-Krasteva TS, Zarnowiec P, Czerwonka G, Reilly J, Drevinek P, Kaca W, Melter O, de Soyza A, Perry A, Winstanley C, Stoitsova SR, Lavigne R, Mahenthalingam E, Sa-Correia I, Coenye T, Drulis-Kawa Z, Augustyniak D, Valvano MA, McClean S. 2015. Phenotypic characterization of an international *Pseudomonas aeruginosa* reference panel: strains of cystic fibrosis (CF) origin show less in vivo virulence than non-CF strains. *Microbiology* 161:1961–1977. <https://doi.org/10.1099/mic.0.000155>.
292. Whiley RA, Sheikh NP, Mushtaq N, Hagi-Pavli E, Personne Y, Javaid D, Waite RD. 2014. Differential potentiation of the virulence of the *Pseudomonas aeruginosa* cystic fibrosis Liverpool epidemic strain by oral commensal streptococci. *J Infect Dis* 209:769–780. <https://doi.org/10.1093/infdis/jit568>.
293. Cruz-Muniz MY, Lopez-Jacome LE, Hernandez-Duran M, Franco-Cendejas R, Licona-Limon P, Ramos-Balderas JL, Martinez-Vazquez M, Belmont-Diaz JA, Wood TK, Garcia-Conteras R. 2017. Repurposing the anticancer drug mitomycin C for the treatment of persistent *Acinetobacter baumannii* infections. *Int J Antimicrob Agents* 49:88–92. <https://doi.org/10.1016/j.ijantimicag.2016.08.022>.
294. Sardi JCO, Polaquini CR, Freires IA, Galvao LCC, Lazarini JG, Torrezan GS, Regasini LO, Rosalen PL. 2017. Antibacterial activity of diacetylcurcumin against *Staphylococcus aureus* results in decreased biofilm and cellular adhesion. *J Med Microbiol* 66:816–824. <https://doi.org/10.1099/jmm.0.000494>.
295. Silva LN, Da Hora GCA, Soares TA, Bojer MS, Ingmer H, Macedo AJ, Trentin DS. 2017. Myricetin protects *Galleria mellonella* against *Staphylococcus aureus* infection and inhibits multiple virulence factors. *Sci Rep* 7:2823. <https://doi.org/10.1038/s41598-017-02712-1>.
296. Bhatt S, Anyanful A, Kalman D. 2011. CsrA and TnaB coregulate tryptophanase activity to promote exotoxin-induced killing of *Caenorhabditis elegans* by enteropathogenic *Escherichia coli*. *J Bacteriol* 193:4516–4522. <https://doi.org/10.1128/JB.05197-11>.
297. Lee SH, Ooi SK, Mahadi NM, Tan MW, Nathan S. 2011. Complete killing of *Caenorhabditis elegans* by *Burkholderia pseudomallei* is dependent on prolonged direct association with the viable pathogen. *PLoS One* 6:e16707. <https://doi.org/10.1371/journal.pone.0016707>.
298. O'Quinn AL, Wiegand EM, Jeddeloh JA. 2001. *Burkholderia pseudomallei* kills the nematode *Caenorhabditis elegans* using an endotoxin-mediated paralysis. *Cell Microbiol* 3:381–393. <https://doi.org/10.1046/j.1462-5822.2001.00118.x>.
299. Lee SH, Wong RR, Chin CY, Lim TY, Eng SA, Kong C, Ijap NA, Lau MS, Lim MP, Gan YH, He FL, Tan MW, Nathan S. 2013. *Burkholderia pseudomallei* suppresses *Caenorhabditis elegans* immunity by specific degradation of a GATA transcription factor. *Proc Natl Acad Sci U S A* 110:15067–15072. <https://doi.org/10.1073/pnas.1311725110>.
300. Joshua GW, Atkinson S, Goldstone RJ, Patrick HL, Stabler RA, Purves J, Camara M, Williams P, Wren BW. 2015. Genome-wide evaluation of the interplay between *Caenorhabditis elegans* and *Yersinia pseudotuberculosis* during in vivo biofilm formation. *Infect Immun* 83:17–27. <https://doi.org/10.1128/IAI.00110-14>.
301. Huber B, Feldmann F, Kothe M, Vandamme P, Wopperer J, Riedel K, Eberl L. 2004. Identification of a novel virulence factor in *Burkholderia cenocepacia* H111 required for efficient slow killing of *Caenorhabditis elegans*. *Infect Immun* 72:7220–7230. <https://doi.org/10.1128/IAI.72.12.7220-7230.2004>.
302. Sousa SA, Ramos CG, Leitao JH. 2011. *Burkholderia cepacia* complex: emerging multihost pathogens equipped with a wide range of virulence factors and determinants. *Int J Microbiol* 2011:607575. <https://doi.org/10.1155/2011/607575>.
303. Tegos GP, Haynes MK, Schweizer HP. 2012. Dissecting novel virulent determinants in the *Burkholderia cepacia* complex. *Virulence* 3:234–237. <https://doi.org/10.4161/viru.19844>.
304. O'Grady EP, Viteri DF, Sokol PA. 2012. A unique regulator contributes to quorum sensing and virulence in *Burkholderia cenocepacia*. *PLoS One* 7:e37611. <https://doi.org/10.1371/journal.pone.0037611>.
305. Cooper VS, Carlson WA, Lipuma JJ. 2009. Susceptibility of *Caenorhabditis elegans* to *Burkholderia* infection depends on prior diet and secreted bacterial attractants. *PLoS One* 4:e7961. <https://doi.org/10.1371/journal.pone.0007961>.
306. Springman AC, Jacobs JL, Somvanshi VS, Sundin GW, Mulks MH, Whittam TS, Viswanathan P, Gray RL, Lipuma JJ, Ciche TA. 2009. Genetic diversity and multihost pathogenicity of clinical and environmental strains of *Burkholderia cenocepacia*. *Appl Environ Microbiol* 75:5250–5260. <https://doi.org/10.1128/AEM.00877-09>.
307. Sousa SA, Ramos CG, Moreira LM, Leitao JH. 2010. The hfq gene is required for stress resistance and full virulence of *Burkholderia cepacia* to the nematode *Caenorhabditis elegans*. *Microbiology* 156:896–908. <https://doi.org/10.1099/mic.0.035139-0>.
308. Manz W, Amann R, Szewzyk R, Szewzyk U, Stenstrom TA, Hutzler P, Schleifer KH. 1995. In situ identification of Legionellaceae using 16S rRNA-targeted oligonucleotide probes and confocal laser scanning microscopy. *Microbiology* 141:29–39. <https://doi.org/10.1099/00221287-141-1-29>.
309. Benghezal M, Adam E, Lucas A, Burn C, Orchard MG, Deuschel C, Valentino E, Braillard S, Paccaud JP, Cosson P. 2007. Inhibitors of bacterial virulence identified in a surrogate host model. *Cell Microbiol* 9:1336–1342. <https://doi.org/10.1111/j.1462-5822.2006.00877.x>.
310. Lau HY, Ashbolt NJ. 2009. The role of biofilms and protozoa in Legionella pathogenesis: implications for drinking water. *J Appl Microbiol* 107:368–378. <https://doi.org/10.1111/j.1365-2672.2009.04208.x>.
311. Ovrutsky AR, Chan ED, Kartalija M, Bai X, Jackson M, Gibbs S, Falkinham JO, III, Iseman MD, Reynolds PR, McDonnell G, Thomas V. 2013. Cooccurrence of free-living amoebae and nontuberculous mycobacteria in hospital water networks, and preferential growth of *Mycobacterium avium* in *Acanthamoeba* lenticularia. *Appl Environ Microbiol* 79:3185–3192. <https://doi.org/10.1128/AEM.03823-12>.
312. Iwashkiw JA, Seper A, Weber BS, Scott NE, Vinogradov E, Stratilo C, Reiz B, Cordwell SJ, Whittall R, Schild S, Feldman MF. 2012. Identification of a general O-linked protein glycosylation system in *Acinetobacter baumannii* and its role in virulence and biofilm formation. *PLoS Pathog* 8:e1002758. <https://doi.org/10.1371/journal.ppat.1002758>.
313. Manske C, Hilbi H. 2014. Metabolism of the vacuolar pathogen *Legionella* and implications for virulence. *Front Cell Infect Microbiol* 4:125. <https://doi.org/10.3389/fcimb.2014.00125>.
314. Yang L, Liu Y, Markussen T, Hoiby N, Tolker-Nielsen T, Molin S. 2011. Pattern differentiation in co-culture biofilms formed by *Staphylococcus aureus* and *Pseudomonas aeruginosa*. *FEMS Immunol Med Microbiol* 62:339–347. <https://doi.org/10.1111/j.1574-695X.2011.00820.x>.
315. Zhang Y, Hu Y, Yang B, Ma F, Lu P, Li L, Wan C, Rayner S, Chen S. 2010. Duckweed (*Lemna minor*) as a model plant system for the study of human microbial pathogenesis. *PLoS One* 5:e13527. <https://doi.org/10.1371/journal.pone.0013527>.
316. Subramoni S, Nguyen DT, Sokol PA. 2011. *Burkholderia cenocepacia* ShvR-regulated genes that influence colony morphology, biofilm formation, and virulence. *Infect Immun* 79:2984–2997. <https://doi.org/10.1128/IAI.00170-11>.
317. Barak JD, Gorski L, Liang AS, Narm KE. 2009. Previously uncharacterized *Salmonella enterica* genes required for swarming play a role in seedling colonization. *Microbiology* 155:3701–3709. <https://doi.org/10.1099/mic.0.032029-0>.
318. Beauregard PB, Chai Y, Vlamakis H, Losick R, Kolter R. 2013. *Bacillus*

- subtilis biofilm induction by plant polysaccharides. *Proc Natl Acad Sci U S A* 110:E1621–E1630. <https://doi.org/10.1073/pnas.1218984110>.
319. Petrova OE, Sauer K. 2011. SagS contributes to the motile-sessile switch and acts in concert with BfiSR to enable *Pseudomonas aeruginosa* biofilm formation. *J Bacteriol* 193:6614–6628. <https://doi.org/10.1128/JB.00305-11>.
  320. Chan C, Hardin TC, Smart JI. 2015. A review of telavancin activity in vitro biofilms and animal models of biofilm-associated infections. *Future Microbiol* 10:1325–1338. <https://doi.org/10.2217/fmb.15.53>.
  321. Carey AJ, Tan CK, Ipe DS, Sullivan MJ, Cripps AW, Schembri MA, Ulett GC. 2016. Urinary tract infection of mice to model human disease: practicalities, implications and limitations. *Crit Rev Microbiol* 42: 780–799. <https://doi.org/10.3109/1040841X.2015.1028885>.
  322. Hamblin MR, Zahra T, Contag CH, McManus AT, Hasan T. 2003. Optical monitoring and treatment of potentially lethal wound infections in vivo. *J Infect Dis* 187:1717–1725. <https://doi.org/10.1086/375244>.
  323. Sharma SK, Dai T, Kharkwal GB, Huang YY, Huang L, De Arce VJ, Tegos GP, Hamblin MR. 2011. Drug discovery of antimicrobial photosensitizers using animal models. *Curr Pharm Des* 17:1303–1319. <https://doi.org/10.2174/138161211795703735>.
  324. Dai T, Huang YY, Hamblin MR. 2009. Photodynamic therapy for localized infections—state of the art. *Photodiagnosis Photodyn Ther* 6:170–188. <https://doi.org/10.1016/j.pdpdt.2009.10.008>.
  325. Dai T, Tegos GP, Zhiyentayev T, Mylonakis E, Hamblin MR. 2010. Photodynamic therapy for methicillin-resistant *Staphylococcus aureus* infection in a mouse skin abrasion model. *Lasers Surg Med* 42:38–44. <https://doi.org/10.1002/lsm.20887>.
  326. Tanaka M, Mroz P, Dai T, Huang L, Morimoto Y, Kinoshita M, Yoshihara Y, Nemoto K, Shinomiya N, Seki S, Hamblin MR. 2012. Photodynamic therapy can induce a protective innate immune response against murine bacterial arthritis via neutrophil accumulation. *PLoS One* 7:e39823. <https://doi.org/10.1371/journal.pone.0039823>.
  327. Goto B, Iriuchishima T, Horaguchi T, Tokuhashi Y, Nagai Y, Harada T, Saito A, Aizawa S. 2011. Therapeutic effect of photodynamic therapy using Na-pheophorbide A on osteomyelitis models in rats. *Photomed Laser Surg* 29:183–189. <https://doi.org/10.1089/pho.2010.2803>.
  328. Inzana JA, Schwarz EM, Kates SL, Awad HA. 2015. A novel murine model of established staphylococcal bone infection in the presence of a fracture fixation plate to study therapies utilizing antibiotic-laden spacers after revision surgery. *Bone* 72:128–136. <https://doi.org/10.1016/j.bone.2014.11.019>.
  329. Cash HA, Woods DE, McCullough B, Johanson WG, Jr, Bass JA. 1979. A rat model of chronic respiratory infection with *Pseudomonas aeruginosa*. *Am Rev Respir Dis* 119:453–459.
  330. Meers P, Neville M, Malinin V, Scotto AW, Sardaryan G, Kurumunda R, Mackinson C, James G, Fisher S, Perkins WR. 2008. Biofilm penetration, triggered release and in vivo activity of inhaled liposomal amikacin in chronic *Pseudomonas aeruginosa* lung infections. *J Antimicrob Chemother* 61:859–868. <https://doi.org/10.1093/jac/dkn059>.
  331. Pawar V, Komor U, Kasnitz N, Bielecki P, Pils MC, Gocht B, Moter A, Rohde M, Weiss S, Haussler S. 2015. In vivo efficacy of antimicrobials against biofilm-producing *Pseudomonas aeruginosa*. *Antimicrob Agents Chemother* 59:4974–4981. <https://doi.org/10.1128/AAC.00194-15>.
  332. Chen KM, Chiang MK, Wang M, Ho HC, Lu MC, Lai YC. 2014. The role of pgaC in *Klebsiella pneumoniae* virulence and biofilm formation. *Microb Pathog* 77:89–99. <https://doi.org/10.1016/j.micpath.2014.11.005>.
  333. Balaban N, Giacometti A, Cirioni O, Gov Y, Ghiselli R, Mocchegiani F, Viticchi C, Del Prete MS, Saba V, Scalise G, Dell'Acqua G. 2003. Use of the quorum-sensing inhibitor RNAIII-inhibiting peptide to prevent biofilm formation in vivo by drug-resistant *Staphylococcus epidermidis*. *J Infect Dis* 187:625–630. <https://doi.org/10.1086/345879>.
  334. Nakamoto DA, Rosenfield ML, Haaga JR, Merritt K, Sachs PB, Hutton MC, Graham RC, Rowland DY. 1994. Young investigator award. In vivo treatment of infected prosthetic graft material with urokinase: an animal model. *J Vasc Interv Radiol* 5:549–552.
  335. Garrison JR, Jr, Henke KP, Smith KR, Brittain KR, Lam TM, Peyton JC, Bergamini TM. 1997. In vitro and in vivo effects of rifampin on *Staphylococcus epidermidis* graft infections. *ASAIO J* 43:8–12.
  336. Sima C, Cheng Q, Rautava J, Levesque C, Sherman P, Glogauer M. 2016. Identification of quantitative trait loci influencing inflammation-mediated alveolar bone loss: insights into polygenic inheritance of host-biofilm disequilibria in periodontitis. *J Periodontol Res* 51: 237–249. <https://doi.org/10.1111/jre.12303>.
  337. Howlin RP, Fabbri S, Offin DG, Symonds N, Kiang KS, Knee RJ, Yoganantham DC, Webb JS, Birkin PR, Leighton TG, Stoodley P. 2015. Removal of dental biofilms with an ultrasonically activated water stream. *J Dent Res* 94:1303–1309. <https://doi.org/10.1177/0022034515589284>.
  338. Du T, Wang Z, Shen Y, Ma J, Cao Y, Haapasalo M. 2015. Combined antibacterial effect of sodium hypochlorite and root canal sealers against *Enterococcus faecalis* biofilms in dentin canals. *J Endod* 41: 1294–1298. <https://doi.org/10.1016/j.joen.2015.04.023>.
  339. Rocker AJ, Weiss AR, Lam JS, Van Raay TJ, Khursigara CM. 2015. Visualizing and quantifying *Pseudomonas aeruginosa* infection in the hindbrain ventricle of zebrafish using confocal laser scanning microscopy. *J Microbiol Methods* 117:85–94. <https://doi.org/10.1016/j.mimet.2015.07.013>.
  340. Dong X, Fan X, Wang B, Shi X, Zhang XH. 2013. Invasion of *Edwardsiella tarda* is essential for its haemolytic activity, biofilm formation and virulence towards fish. *J Appl Microbiol* 115:12–19. <https://doi.org/10.1111/jam.12198>.
  341. Zhang H, Ma Z, Li Y, Zheng J, Yi L, Fan H, Lu C. 2013. Identification of a novel collagen type capital I, Ukrainian-binding protein from *Streptococcus suis* serotype 2. *Vet J* 197:406–414. <https://doi.org/10.1016/j.tvjl.2013.01.030>.
  342. Ju CX, Gu HW, Lu CP. 2012. Characterization and functional analysis of atl, a novel gene encoding autolysin in *Streptococcus suis*. *J Bacteriol* 194:1464–1473. <https://doi.org/10.1128/JB.06231-11>.
  343. Whippes CM, Dougan ST, Kent ML. 2007. *Mycobacterium haemophilum* infections of zebrafish (*Danio rerio*) in research facilities. *FEMS Microbiol Lett* 270:21–26. <https://doi.org/10.1111/j.1574-6968.2007.00671.x>.
  344. Rendueles O, Ferrieres L, Fretaud M, Begaud E, Herbomel P, Levraud JP, Ghigo JM. 2012. A new zebrafish model of oro-intestinal pathogen colonization reveals a key role for adhesion in protection by probiotic bacteria. *PLoS Pathog* 8:e1002815. <https://doi.org/10.1371/journal.ppat.1002815>.
  345. Thompson MG, Black CC, Pavlicek RL, Honnold CL, Wise MC, Alameh YA, Moon JK, Kessler JL, Si Y, Williams R, Yildirim S, Kirkup BC, Jr, Green RK, Hall ER, Palys TJ, Zurawski DV. 2014. Validation of a novel murine wound model of *Acinetobacter baumannii* infection. *Antimicrob Agents Chemother* 58:1332–1342. <https://doi.org/10.1128/AAC.01944-13>.
  346. Trostrup H, Thomsen K, Christophersen LJ, Hougen HP, Bjarnsholt T, Jensen PO, Kirkby N, Calum H, Hoiby N, Moser C. 2013. *Pseudomonas aeruginosa* biofilm aggravates skin inflammatory response in BALB/c mice in a novel chronic wound model. *Wound Repair Regen* 21: 292–299. <https://doi.org/10.1111/wrr.12016>.
  347. Nusbaum AG, Gil J, Rippey MK, Warne B, Valdes J, Claro A, Davis SC. 2012. Effective method to remove wound bacteria: comparison of various debridement modalities in an in vivo porcine model. *J Surg Res* 176:701–707. <https://doi.org/10.1016/j.jss.2011.11.1040>.
  348. Asada M, Nakagami G, Minematsu T, Nagase T, Akase T, Huang L, Yoshimura K, Sanada H. 2012. Novel models for bacterial colonization and infection of full-thickness wounds in rats. *Wound Repair Regen* 20:601–610. <https://doi.org/10.1111/j.1524-475X.2012.00800.x>.
  349. Kuehl R, Brunetto PS, Woischnig AK, Varisco M, Rajacic Z, Vosbeck J, Terracciano L, Fromm KM, Khanna N. 2016. Preventing implant-associated infections by silver coating. *Antimicrob Agents Chemother* 60:2467–2475. <https://doi.org/10.1128/AAC.02934-15>.
  350. Jennings JA, Carpenter DP, Troxel KS, Beenken KE, Smeltzer MS, Courtney HS, Haggard WO. 2015. Novel antibiotic-loaded point-of-care implant coating inhibits biofilm. *Clin Orthop Relat Res* 473:2270–2282. <https://doi.org/10.1007/s11999-014-4130-8>.
  351. Chauhan A, Ghigo JM, Beloin C. 2016. Study of in vivo catheter biofilm infections using pediatric central venous catheter implanted in rat. *Nat Protoc* 11:525–541. <https://doi.org/10.1038/nprot.2016.033>.
  352. Paryavi E, Yanko M, Jaffe D, Nimmagadda N, Nouveau J, Schiavone J, Gilotra M, Gelb D, Ludwig SC. 2014. Implantable direct current spinal fusion stimulators do not decrease implant-related infections in a rabbit model. *Am J Orthop* 43:E98–E104.
  353. Diefenbeck M, Schrader C, Gras F, Muckley T, Schmidt J, Zankovych S, Bossert J, Jandt KD, Volpel A, Sigusch BW, Schubert H, Bischoff S, Pfister W, Edel B, Faucon M, Finger U. 2016. Gentamicin coating of plasma chemical oxidized titanium alloy prevents implant-related osteomyelitis in rats. *Biomaterials* 101:156–164. <https://doi.org/10.1016/j.biomaterials.2016.05.039>.
  354. Rochford ET, Sabate Bresco M, Zeiter S, Kluge K, Poulsson A, Ziegler M, Richards RG, O'Mahony L, Moriarty TF. 2016. Monitoring immune responses in a mouse model of fracture fixation with and without

- Staphylococcus aureus osteomyelitis. *Bone* 83:82–92. <https://doi.org/10.1016/j.bone.2015.10.014>.
355. Frank KL, Vergidis P, Brinkman CL, Greenwood Quintance KE, Barnes AM, Mandrekar JN, Schlievert PM, Dunny GM, Patel R. 2015. Evaluation of the *Enterococcus faecalis* biofilm-associated virulence factors AhrC and Eep in rat foreign body osteomyelitis and in vitro biofilm-associated antimicrobial resistance. *PLoS One* 10:e0130187. <https://doi.org/10.1371/journal.pone.0130187>.
  356. Mihailescu R, Furustrand Taffin U, Corvec S, Oliva A, Betrisey B, Borens O, Trampuz A. 2014. High activity of fosfomicin and rifampin against methicillin-resistant *Staphylococcus aureus* biofilm in vitro and in an experimental foreign-body infection model. *Antimicrob Agents Chemother* 58:2547–2553. <https://doi.org/10.1128/AAC.02420-12>.
  357. Liu G, Chen S, Fang J, Xu B, Li S, Hao Y, Al-Dhabi NA, Deng S, Duraipandian V. 2016. Vancomycin microspheres reduce postoperative spine infection in an in vivo rabbit model. *BMC Pharmacol Toxicol* 17:61. <https://doi.org/10.1186/s40360-016-0105-6>.
  358. Stavarakis AI, Loftin AH, Lord EL, Hu Y, Manegold JE, Dworsky EM, Scaduto AA, Bernthal NM. 2015. Current animal models of postoperative spine infection and potential future advances. *Front Med* 2:34. <https://doi.org/10.3389/fmed.2015.00034>.
  359. Azriel S, Goren A, Rahav G, Gal-Mor O. 2015. The stringent response regulator DksA is required for *Salmonella enterica* serovar Typhimurium growth in minimal medium, motility, biofilm formation, and intestinal colonization. *Infect Immun* 84:375–384. <https://doi.org/10.1128/IAI.01135-15>.
  360. Semenyuk EG, Poroyko VA, Johnston PF, Jones SE, Knight KL, Gerding DN, Driks A. 2015. Analysis of bacterial communities during *Clostridium difficile* infection in the mouse. *Infect Immun* 83:4383–4391. <https://doi.org/10.1128/IAI.00145-15>.
  361. Xu D, Zhang W, Zhang B, Liao C, Shao Y. 2016. Characterization of a biofilm-forming *Shigella flexneri* phenotype due to deficiency in Hep biosynthesis. *PeerJ* 4:e2178. <https://doi.org/10.7717/peerj.2178>.
  362. Melican K, Sandoval RM, Kader A, Josefsson L, Tanner GA, Molitoris BA, Richter-Dahlfors A. 2011. Uropathogenic *Escherichia coli* P and type 1 fimbriae act in synergy in a living host to facilitate renal colonization leading to nephron obstruction. *PLoS Pathog* 7:e1001298. <https://doi.org/10.1371/journal.ppat.1001298>.
  363. Fothergill JL, Neill DR, Loman N, Winstanley C, Kadioglu A. 2014. *Pseudomonas aeruginosa* adaptation in the nasopharyngeal reservoir leads to migration and persistence in the lungs. *Nat Commun* 5:4780. <https://doi.org/10.1038/ncomms5780>.
  364. Baldan R, Cigana C, Testa F, Bianconi I, De Simone M, Pellin D, Di Serio C, Bragonzi A, Cirillo DM. 2014. Adaptation of *Pseudomonas aeruginosa* in cystic fibrosis airways influences virulence of *Staphylococcus aureus* in vitro and murine models of co-infection. *PLoS One* 9:e89614. <https://doi.org/10.1371/journal.pone.0089614>.
  365. Fine DH, Karched M, Furgang D, Sampathkumar V, Velusamy S, Godbole D. 2015. Colonization and persistence of labeled and “foreign” strains of *Aggregatibacter actinomycetemcomitans* inoculated into the mouths of rhesus monkeys. *J Oral Biol* 2:10. <https://doi.org/10.13188/2377-987X.1000005>.
  366. Gonzalez OA, Novak MJ, Kirakodu S, Stromberg AJ, Shen S, Orraca L, Gonzalez-Martinez J, Ebersole JL. 2013. Effects of aging on apoptosis gene expression in oral mucosal tissues. *Apoptosis* 18:249–259. <https://doi.org/10.1007/s10495-013-0806-x>.
  367. Shanmugam M, Gopal P, El Abbar F, Schreiner HC, Kaplan JB, Fine DH, Ramasubbu N. 2015. Role of exopolysaccharide in *Aggregatibacter actinomycetemcomitans*-induced bone resorption in a rat model for periodontal disease. *PLoS One* 10:e0117487. <https://doi.org/10.1371/journal.pone.0117487>.
  368. Kuremoto K, Noiri Y, Ishimoto T, Yoneda N, Yamamoto R, Maezono H, Nakano T, Hayashi M, Ebisu S. 2014. Promotion of endodontic lesions in rats by a novel extraradicular biofilm model using obturation materials. *Appl Environ Microbiol* 80:3804–3810. <https://doi.org/10.1128/AEM.00421-14>.
  369. Hong W, Mason K, Jurcisek J, Novotny L, Bakaletz LO, Swords WE. 2007. Phosphorylcholine decreases early inflammation and promotes the establishment of stable biofilm communities of nontypeable *Haemophilus influenzae* strain 86-028NP in a chinchilla model of otitis media. *Infect Immun* 75:958–965. <https://doi.org/10.1128/IAI.01691-06>.
  370. Hesse D, Ehlert N, Luenhop T, Smoczek A, Glage S, Behrens P, Muller PP, Esser KH, Lenarz T, Stieve M, Bleich A, Prenzler NK. 2013. Nanoporous silica coatings as a drug delivery system for ciprofloxacin: outcome of variable release rates in the infected middle ear of rabbits. *Otol Neurotol* 34:1138–1145. <https://doi.org/10.1097/MAO.0b013e3182839671>.
  371. Jang CH, Cho YB, Jang YS, Kim MS, Kim GH. 2015. Antibacterial effect of electrospun polycaprolactone/polyethylene oxide/vancomycin nanofiber mat for prevention of periprosthetic infection and biofilm formation. *Int J Pediatr Otorhinolaryngol* 79:1299–1305. <https://doi.org/10.1016/j.ijporl.2015.05.037>.
  372. Roilides E, Simitsopoulou M, Katragkou A, Walsh TJ. 2015. How biofilms evade host defenses. *Microbiol Spectr* 3:MB-0012-2014. <https://doi.org/10.1128/microbiolspec.MB-0012-2014>.
  373. Dunlap P. 2014. Biochemistry and genetics of bacterial bioluminescence. *Adv Biochem Eng Biotechnol* 144:37–64. [https://doi.org/10.1007/978-3-662-43385-0\\_2](https://doi.org/10.1007/978-3-662-43385-0_2).
  374. Kadurugamuwa JL, Francis KP. 2008. Bioluminescent imaging of bacterial biofilm infections in vivo. *Methods Mol Biol* 431:225–239.
  375. Hamblin MR, O'Donnell DA, Murthy N, Contag CH, Hasan T. 2002. Rapid control of wound infections by targeted photodynamic therapy monitored by in vivo bioluminescence imaging. *Photochem Photobiol* 75: 51–57. [https://doi.org/10.1562/0031-8655\(2002\)075<0051:RCOWIB>2.0.CO;2](https://doi.org/10.1562/0031-8655(2002)075<0051:RCOWIB>2.0.CO;2).
  376. Rineh A, Dolla NK, Ball AR, Magana M, Bremner JB, Hamblin MR, Tegos GP, Kelso MJ. 2017. Attaching the NorA efflux pump inhibitor INF55 to methylene blue enhances antimicrobial photodynamic inactivation of methicillin-resistant *Staphylococcus aureus* in vitro and in vivo. *ACS Infect Dis* 3:756–766. <https://doi.org/10.1021/acinfecdis.7b00095>.
  377. Merritt J, Senpuku H, Kretz J. 2016. Let there be bioluminescence: development of a biophotonic imaging platform for in situ analyses of oral biofilms in animal models. *Environ Microbiol* 18:174–190. <https://doi.org/10.1111/1462-2920.12953>.
  378. Baban CK, Cronin M, Akin AR, O'Brien A, Gao X, Tabirca S, Francis KP, Tangney M. 2012. Bioluminescent bacterial imaging in vivo. *J Vis Exp* 2012:e4318. <https://doi.org/10.3791/4318>.
  379. Cronin M, Akin AR, Collins SA, Meganck J, Kim JB, Baban CK, Joyce SA, van Dam GM, Zhang N, van Sinderen D, O'Sullivan GC, Kasahara N, Gahan CG, Francis KP, Tangney M. 2012. High resolution in vivo bioluminescent imaging for the study of bacterial tumour targeting. *PLoS One* 7:e30940. <https://doi.org/10.1371/journal.pone.0030940>.
  380. Collins JW, Meganck JA, Kuo C, Francis KP, Frankel G. 2013. 4D multimodality imaging of *Citrobacter rodentium* infections in mice. *J Vis Exp* 2013:50450. <https://doi.org/10.3791/50450>.
  381. Bernthal NM, Taylor BN, Meganck JA, Wang Y, Shahbazian JH, Niska JA, Francis KP, Miller LS. 2014. Combined in vivo optical and microCT imaging to monitor infection, inflammation, and bone anatomy in an orthopaedic implant infection in mice. *J Vis Exp* 2014:e51612. <https://doi.org/10.3791/51612>.
  382. Walton KD, Lord A, Kendall LV, Dow SW. 2014. Comparison of 3 real-time, quantitative murine models of staphylococcal biofilm infection by using in vivo bioluminescent imaging. *Comp Med* 64:25–33.
  383. Tidwell JE, Dawson-Andoh B, Adedipe EO, Nkansah K, Dietz MJ. 2015. Can near-infrared spectroscopy detect and differentiate implant-associated biofilms? *Clin Orthop Relat Res* 473:3638–3646. <https://doi.org/10.1007/s11999-015-4497-1>.
  384. Suri S, Lehman SM, Selvam S, Reddie K, Maity S, Murthy N, Garcia AJ. 2015. In vivo fluorescence imaging of biomaterial-associated inflammation and infection in a minimally invasive manner. *J Biomed Mater Res A* 103:76–83. <https://doi.org/10.1002/jbm.a.35162>.
  385. Schlafer S, Garcia JE, Greve M, Raarup MK, Nyvad B, Dige I. 2015. Ratiometric imaging of extracellular pH in bacterial biofilms with C-SNARF-4. *Appl Environ Microbiol* 81:1267–1273. <https://doi.org/10.1128/AEM.02831-14>.
  386. Anastasiadis P, Mojica KD, Allen JS, Matter ML. 2014. Detection and quantification of bacterial biofilms combining high-frequency acoustic microscopy and targeted lipid microparticles. *J Nanobiotechnol* 12:24. <https://doi.org/10.1186/1477-3155-12-24>.
  387. Hubler Z, Shemonski ND, Shelton RL, Monroy GL, Nolan RM, Boppart SA. 2015. Real-time automated thickness measurement of the in vivo human tympanic membrane using optical coherence tomography. *Quant Imaging Med Surg* 5:69–77. <https://doi.org/10.3978/j.issn.2223-4292.2014.11.32>.
  388. Nguyen CT, Jung W, Kim J, Chaney EJ, Novak M, Stewart CN, Boppart SA. 2012. Noninvasive in vivo optical detection of biofilm in the human middle ear. *Proc Natl Acad Sci U S A* 109:9529–9534. <https://doi.org/10.1073/pnas.1201592109>.
  389. Lenton P, Rudney J, Chen R, Fok A, Aparicio C, Jones RS. 2012. Imaging

- in vivo secondary caries and ex vivo dental biofilms using cross-polarization optical coherence tomography. *Dent Mater* 28:792–800. <https://doi.org/10.1016/j.dental.2012.04.004>.
390. Feindel KW. 2016. Spatially resolved chemical reaction monitoring using magnetic resonance imaging. *Magn Reson Chem* 54:429–436. <https://doi.org/10.1002/mrc.4179>.
391. Garrido V, Collantes M, Barberan M, Penuelas I, Arbizu J, Amorena B, Grillo MJ. 2014. In vivo monitoring of *Staphylococcus aureus* biofilm infections and antimicrobial therapy by [<sup>18</sup>F]fluoro-deoxyglucose-microPET in a mouse model. *Antimicrob Agents Chemother* 58:6660–6667. <https://doi.org/10.1128/AAC.03138-14>.
392. Niska JA, Meganck JA, Pribaz JR, Shahbazian JH, Lim E, Zhang N, Rice BW, Akin A, Ramos RI, Bernthal NM, Francis KP, Miller LS. 2012. Monitoring bacterial burden, inflammation and bone damage longitudinally using optical and muCT imaging in an orthopaedic implant infection in mice. *PLoS One* 7:e47397. <https://doi.org/10.1371/journal.pone.0047397>.
393. Berk V, Fong JC, Dempsey GT, Develioglu ON, Zhuang X, Liphardt J, Yildiz FH, Chu S. 2012. Molecular architecture and assembly principles of *Vibrio cholerae* biofilms. *Science* 337:236–239. <https://doi.org/10.1126/science.1222981>.
394. Ning X, Lee S, Wang Z, Kim D, Stubblefield B, Gilbert E, Murthy N. 2011. Maltodextrin-based imaging probes detect bacteria in vivo with high sensitivity and specificity. *Nat Mater* 10:602–607. <https://doi.org/10.1038/nmat3074>.
395. Park CY, Sung JJ, Kim DW. 2016. Genome editing of structural variations: modeling and gene correction. *Trends Biotechnol* 34:548–561. <https://doi.org/10.1016/j.tibtech.2016.02.011>.
396. Roberts AE, Kragh KN, Bjarnsholt T, Diggle SP. 2015. The limitations of in vitro experimentation in understanding biofilms and chronic infection. *J Mol Biol* 427:3646–3661. <https://doi.org/10.1016/j.jmb.2015.09.002>.
397. Yu HD, Qiu D. March 2013. Methods of detecting and controlling mucoid *Pseudomonas* biofilm production. US patent 8399649 B2.
398. Schultz GS, Phillips PL, Sampson EM. December 2012. Materials and methods for assessing and mapping microbes and microbial biofilms on wounds. US patent 20120322048 A1.
399. Boels G, Blackman G, Calabozo A. December 2012. Biofilm detection kit and method. EP patent 2537601 A1.
400. Orihuel IE, Berto NR, Lorenzo CF, Lopez TC, San JSC, Orgaz MB. June 2014. Biofilm-marking composition and method for detection of same on surfaces. EP patent 2634260 A1.
401. Bernardi T, Bara N. June 2011. Method for detecting the formation of biofilms. US patent 7955818 B2.
402. Hall-Stoodley L, Stoodley P. July 2008. Biofilm preparation using potassium permanganate. US patent 20080176265 A1.
403. Goodyer I, Labarbe R, Ruehlmann D, Stubbs S. December 2006. Method for assessing biofilms. US patent 20060275847 A1.
404. Maale G. September 2003. Method of detecting biofilms and residues on medical implants and other devices. US patent 20030177819 A1.
405. Peppou GC, Manion MK, Austin BM, Millar BW, Barends BW. December 2014. Method and device for detecting device colonization. US patent 20140356901 A1.
406. Manion MK, Peppou GC. December 2014. Color change indicator of biofilm formation. US patent 20140352602 A1.
407. Leid JG, Vail TL, Kofonow JM, Shirtliff ME, Brady RA. November 2010. Methods and devices for the detection of biofilm. US patent 20100285496 A1.
408. Seipp HM. February 2003. Method for the quantification of the biofilm load on sample bodies. EP patent 1067385 B1.
409. Smeltzer MS, Zharov V, Galanzha E. April 2014. Device and method for in vivo photoacoustic diagnosis and photothermal purging of infected blood. WO patent 2014052449 A1.
410. Shirtliff ME, Brady RA, Leid JG, Vail TL, Kofonow JM. April 2014. In vivo biofilm infection diagnosis and treatment. US patent 8697375 B2.
411. Merz M, Ponomarev Y, Pijnenburg R. July 2012. Sensor module for a catheter. US patent 8233957 B2.
412. Dykes DE, Frommeyer AX, Curry AD. November 2012. Diagnostic oral health care implement and system. US patent 20120295216 A1.
413. Piasecki T, Guła G, Nitsch K, Waszczuk K, Drulis-Kawa Z, Gotszalk T. 2013. Evaluation of *Pseudomonas aeruginosa* biofilm formation using quartz tuning forks as impedance sensors. *Sens Actuators B Chem* 189:60–65. <https://doi.org/10.1016/j.snb.2012.12.087>.
414. Otero J, Banos R, Gonzalez L, Torrents E, Juarez A, Puig-Vidal M. 2013. Quartz tuning fork studies on the surface properties of *Pseudomonas aeruginosa* during early stages of biofilm formation. *Colloids Surf B Biointerfaces* 102:117–123. <https://doi.org/10.1016/j.colsurfb.2012.08.013>.
415. Pang P, Xiao X, Cai Q, Yao S, Grimes CA. 2008. A wireless magnetoelastic-sensing device for in situ evaluation of *Pseudomonas aeruginosa* biofilm formation. *Sens Actuators B Chem* 133:473–477. <https://doi.org/10.1016/j.snb.2008.03.009>.
416. Blakey R, Nakouti I, Korostynska O, Mason A, Al-Shamma'a A. 2013. Real-time monitoring of *Pseudomonas aeruginosa* concentration using a novel electromagnetic sensors microfluidic cell structure. *IEEE Trans Biomed Eng* 60:3291–3297. <https://doi.org/10.1109/TBME.2013.2268277>.
417. Hall-Stoodley L, Stoodley P. 2005. Biofilm formation and dispersal and the transmission of human pathogens. *Trends Microbiol* 13:7–10. <https://doi.org/10.1016/j.tim.2004.11.004>.
418. Horswill AR, Stoodley P, Stewart PS, Parsek MR. 2007. The effect of the chemical, biological, and physical environment on quorum sensing in structured microbial communities. *Anal Bioanal Chem* 387:371–380. <https://doi.org/10.1007/s00216-006-0720-y>.
419. Parsek MR, Greenberg EP. 2005. Sociomicrobiology: the connections between quorum sensing and biofilms. *Trends Microbiol* 13:27–33. <https://doi.org/10.1016/j.tim.2004.11.007>.
420. Connell JL, Kim J, Shear JB, Bard AJ, Whiteley M. 2014. Real-time monitoring of quorum sensing in 3D-printed bacterial aggregates using scanning electrochemical microscopy. *Proc Natl Acad Sci U S A* 111:18255–18260. <https://doi.org/10.1073/pnas.1421211111>.
421. Connell JL, Ritschdorff ET, Whiteley M, Shear JB. 2013. 3D printing of microscopic bacterial communities. *Proc Natl Acad Sci U S A* 110:18380–18385. <https://doi.org/10.1073/pnas.1309729110>.
422. Kim J, Connell JL, Whiteley M, Bard AJ. 2014. Development of a versatile in vitro platform for studying biological systems using micro-3D printing and scanning electrochemical microscopy. *Anal Chem* 86:12327–12333. <https://doi.org/10.1021/ac5036204>.
423. Sandler N, Salmela I, Fallarero A, Rosling A, Khajeheian M, Kolakovic R, Genina N, Nyman J, Vuorela P. 2014. Towards fabrication of 3D printed medical devices to prevent biofilm formation. *Int J Pharm* 459:62–64. <https://doi.org/10.1016/j.ijpharm.2013.11.001>.
424. Kim YW, Meyer MT, Berkovich A, Subramanian S, Iliadis AA, Bentley WE, Ghodssi R. 2016. A surface acoustic wave biofilm sensor integrated with a treatment method based on the bioelectric effect. *Sens Actuators A Phys* 238:140–149. <https://doi.org/10.1016/j.sna.2015.12.001>.
425. Subramanian S, Tolstaya EI, Winkler TE, Bentley WE, Ghodssi R. 2017. An integrated microsystem for real-time detection and threshold-activated treatment of bacterial biofilms. *ACS Appl Mater Interfaces* 9:31362–31371. <https://doi.org/10.1021/acsami.7b04828>.
426. Filion-Cote S, Melaine F, Kirk AG, Tabrizian M. 2017. Monitoring of bacterial film formation and its breakdown with an angular-based surface plasmon resonance biosensor. *Analyst* 142:2386–2394. <https://doi.org/10.1039/C7AN00068E>.
427. Palmer RJ, Jr. 2010. Supragingival and subgingival plaque: paradigm of biofilms. *Compend Contin Educ Dent* 31:104–106, 108, 110.
428. Bridier A, Le Coq D, Dubois-Brissonnet F, Thomas V, Aymerich S, Briand R. 2011. The spatial architecture of *Bacillus subtilis* biofilms deciphered using a surface-associated model and in situ imaging. *PLoS One* 6:e16177. <https://doi.org/10.1371/journal.pone.0016177>.
429. Marti S, Nait Chabane Y, Alexandre S, Coquet L, Vila J, Jouenne T, De E. 2011. Growth of *Acinetobacter baumannii* in pellicle enhanced the expression of potential virulence factors. *PLoS One* 6:e26030. <https://doi.org/10.1371/journal.pone.0026030>.
430. Mitra A, Palaniyandi S, Herren CD, Zhu X, Mukhopadhyay S. 2013. Pleiotropic roles of *uvrY* on biofilm formation, motility and virulence in uropathogenic *Escherichia coli* CFT073. *PLoS One* 8:e55492. <https://doi.org/10.1371/journal.pone.0055492>.
431. Bueno J. 2014. Anti-biofilm drug susceptibility testing methods: looking for new strategies against resistance mechanism. *J Microb Biochem Technol* 5:304.
432. Harrison JJ, Stremick CA, Turner RJ, Allan ND, Olson ME, Ceri H. 2010. Microtiter susceptibility testing of microbes growing on peg lids: a miniaturized biofilm model for high-throughput screening. *Nat Protoc* 5:1236–1254. <https://doi.org/10.1038/nprot.2010.71>.
433. Mikkelsen H, Hui K, Barraud N, Filloux A. 2013. The pathogenicity island encoded PvrSR/RcsCB regulatory network controls biofilm formation and dispersal in *Pseudomonas aeruginosa* PA14. *Mol Microbiol* 89:450–463. <https://doi.org/10.1111/mmi.12287>.

434. Jung GB, Nam SW, Choi S, Lee GJ, Park HK. 2014. Evaluation of antibiotic effects on *Pseudomonas aeruginosa* biofilm using Raman spectroscopy and multivariate analysis. *Biomed Opt Express* 5:3238–3251. <https://doi.org/10.1364/BOE.5.003238>.
435. Peterson SB, Irie Y, Borlee BR, Murakami K, Harrison JJ, Colvin KM, Parsek MR. 2011. Different methods for culturing biofilms in vitro, p 251–266. In Bjarnsholt T, Jensen PØ, Moser C, Høiby N (ed), *Biofilm infections*. Springer, New York, NY.
436. Macia MD, Rojo-Molinero E, Oliver A. 2014. Antimicrobial susceptibility testing in biofilm-growing bacteria. *Clin Microbiol Infect* 20:981–990. <https://doi.org/10.1111/1469-0691.12651>.
437. Peeters E, Nelis HJ, Coenye T. 2008. Comparison of multiple methods for quantification of microbial biofilms grown in microtiter plates. *J Microbiol Methods* 72:157–165. <https://doi.org/10.1016/j.mimet.2007.11.010>.
438. Hall-Stoodley L, Rayner JC, Stoodley P, Lappin-Scott HM. 1999. Establishment of experimental biofilms using the modified Robbins device and flow cells, p 307–319. In Edwards C (ed), *Environmental monitoring of bacteria*. Humana Press, Totowa, NJ.
439. Banin E, Brady KM, Greenberg EP. 2006. Chelator-induced dispersal and killing of *Pseudomonas aeruginosa* cells in a biofilm. *Appl Environ Microbiol* 72:2064–2069. <https://doi.org/10.1128/AEM.72.3.2064-2069.2006>.
440. Harrison JJ, Ceri H, Yerly J, Stremick CA, Hu Y, Martinuzzi R, Turner RJ. 2006. The use of microscopy and three-dimensional visualization to evaluate the structure of microbial biofilms cultivated in the Calgary biofilm device. *Biol Proced Online* 8:194–215. <https://doi.org/10.1251/bpo127>.
441. Valle J, Da Re S, Henry N, Fontaine T, Balestrino D, Latour-Lambert P, Ghigo JM. 2006. Broad-spectrum biofilm inhibition by a secreted bacterial polysaccharide. *Proc Natl Acad Sci U S A* 103:12558–12563. <https://doi.org/10.1073/pnas.0605399103>.
442. Kaiser TD, Pereira EM, Dos Santos KR, Maciel EL, Schuenck RP, Nunes AP. 2013. Modification of the Congo red agar method to detect biofilm production by *Staphylococcus epidermidis*. *Diagn Microbiol Infect Dis* 75:235–239. <https://doi.org/10.1016/j.diagmicrobio.2012.11.014>.
443. Boulos L, Prevost M, Barbeau B, Coallier J, Desjardins R. 1999. LIVE/DEAD BacLight: application of a new rapid staining method for direct enumeration of viable and total bacteria in drinking water. *J Microbiol Methods* 37:77–86. [https://doi.org/10.1016/S0167-7012\(99\)00048-2](https://doi.org/10.1016/S0167-7012(99)00048-2).
444. Esteban J, Molina-Manso D, Spiliopoulou I, Cordero-Ampuero J, Fernandez-Roblas R, Foka A, Gomez-Barena E. 2010. Biofilm development by clinical isolates of *Staphylococcus* spp. from retrieved orthopedic prostheses. *Acta Orthop* 81:674–679. <https://doi.org/10.3109/17453674.2010.537810>.
445. Liu K, Liu PC, Liu R, Wu X. 2015. Dual AO/EB staining to detect apoptosis in osteosarcoma cells compared with flow cytometry. *Med Sci Monit Basic Res* 21:15–20. <https://doi.org/10.12659/MSMBR.893327>.
446. Donlan RM, Piede JA, Heyes CD, Sani L, Murga R, Edmonds P, El-Sayed I, El-Sayed MA. 2004. Model system for growing and quantifying *Streptococcus pneumoniae* biofilms in situ and in real time. *Appl Environ Microbiol* 70:4980–4988. <https://doi.org/10.1128/AEM.70.8.4980-4988.2004>.
447. Pettit RK, Weber CA, Kean MJ, Hoffmann H, Pettit GR, Tan R, Franks KS, Horton ML. 2005. Microplate Alamar blue assay for *Staphylococcus epidermidis* biofilm susceptibility testing. *Antimicrob Agents Chemother* 49:2612–2617. <https://doi.org/10.1128/AAC.49.7.2612-2617.2005>.
448. Bauer J, Siala W, Tulkens PM, Van Bambeke F. 2013. A combined pharmacodynamic quantitative and qualitative model reveals the potent activity of daptomycin and delafloxacin against *Staphylococcus aureus* biofilms. *Antimicrob Agents Chemother* 57:2726–2737. <https://doi.org/10.1128/AAC.00181-13>.
449. Kim J, Pitts B, Stewart PS, Camper A, Yoon J. 2008. Comparison of the antimicrobial effects of chlorine, silver ion, and tobramycin on biofilm. *Antimicrob Agents Chemother* 52:1446–1453. <https://doi.org/10.1128/AAC.00054-07>.
450. Stewart PS, Franklin MJ. 2008. Physiological heterogeneity in biofilms. *Nat Rev Microbiol* 6:199–210. <https://doi.org/10.1038/nrmicro1838>.
451. Winkelstroter LK, Martinis EC. 2015. Different methods to quantify *Listeria monocytogenes* biofilms cells showed different profile in their viability. *Braz J Microbiol* 46:231–235. <https://doi.org/10.1590/S1517-838220131071>.
452. Berlutti F, Frioni A, Natalizi T, Pantanella F, Valenti P. 2014. Influence of sub-inhibitory antibiotics and flow condition on *Staphylococcus aureus* ATCC 6538 biofilm development and biofilm growth rate: BioTimer assay as a study model. *J Antibiot* 67:763–769. <https://doi.org/10.1038/ja.2014.66>.
453. Schneider DA, Gourse RL. 2004. Relationship between growth rate and ATP concentration in *Escherichia coli*: a bioassay for available cellular ATP. *J Biol Chem* 279:8262–8268. <https://doi.org/10.1074/jbc.M311996200>.
454. Franca A, Freitas AI, Henriques AF, Cerca N. 2012. Optimizing a qPCR gene expression quantification assay for *S. epidermidis* biofilms: a comparison between commercial kits and a customized protocol. *PLoS One* 7:e37480. <https://doi.org/10.1371/journal.pone.0037480>.
455. Guilbaud M, de Coppet P, Bourion F, Rachman C, Prevost H, Dousset X. 2005. Quantitative detection of *Listeria monocytogenes* in biofilms by real-time PCR. *Appl Environ Microbiol* 71:2190–2194. <https://doi.org/10.1128/AEM.71.4.2190-2194.2005>.
456. Cairns J, Thomas JG, Hooper SJ, Wise MP, Frost PJ, Wilson MJ, Lewis MA, Williams DW. 2011. Molecular analysis of microbial communities in endotracheal tube biofilms. *PLoS One* 6:e14759. <https://doi.org/10.1371/journal.pone.0014759>.
457. Brooks JL, Jefferson KK. 2014. Phase variation of poly-N-acetylglucosamine expression in *Staphylococcus aureus*. *PLoS Pathog* 10:e1004292. <https://doi.org/10.1371/journal.ppat.1004292>.
458. Zaura E. 2012. Next-generation sequencing approaches to understanding the oral microbiome. *Adv Dent Res* 24:81–85. <https://doi.org/10.1177/0022034512449466>.
459. Cerqueira L, Azevedo NF, Almeida C, Jardim T, Keevil CW, Vieira MJ. 2008. DNA mimics for the rapid identification of microorganisms by fluorescence in situ hybridization (FISH). *Int J Mol Sci* 9:1944–1960. <https://doi.org/10.3390/ijms9101944>.
460. Thurnheer T, Gmur R, Guggenheim B. 2004. Multiplex FISH analysis of a six-species bacterial biofilm. *J Microbiol Methods* 56:37–47. <https://doi.org/10.1016/j.mimet.2003.09.003>.
461. Gu F, Lux R, Du-Thumm L, Stokes I, Kreth J, Anderson MH, Wong DT, Wolinsky L, Sullivan R, Shi W. 2005. In situ and non-invasive detection of specific bacterial species in oral biofilms using fluorescently labeled monoclonal antibodies. *J Microbiol Methods* 62:145–160. <https://doi.org/10.1016/j.mimet.2005.02.013>.
462. Neu T, Swerhone GD, Lawrence JR. 2001. Assessment of lectin-binding analysis for in situ detection of glycoconjugates in biofilm systems. *Microbiology* 147:299–313. <https://doi.org/10.1099/00221287-147-2-299>.
463. Werner E, Roe F, Bugnicourt A, Franklin MJ, Heydorn A, Molin S, Pitts B, Stewart PS. 2004. Stratified growth in *Pseudomonas aeruginosa* biofilms. *Appl Environ Microbiol* 70:6188–6196. <https://doi.org/10.1128/AEM.70.10.6188-6196.2004>.
464. Fiolka R. 2014. Seeing more with structured illumination microscopy. *Methods Cell Biol* 123:295–313. <https://doi.org/10.1016/B978-0-12-420138-5.00016-1>.
465. Blauert F, Horn H, Wagner M. 2015. Time-resolved biofilm deformation measurements using optical coherence tomography. *Biotechnol Bioeng* 112:1893–1905. <https://doi.org/10.1002/bit.25590>.
466. Heidari AE, Moghaddam S, Truong KK, Chou L, Genberg C, Brenner M, Chen Z. 2015. Visualizing biofilm formation in endotracheal tubes using endoscopic three-dimensional optical coherence tomography. *J Biomed Opt* 20:126010. <https://doi.org/10.1117/1.JBO.20.12.126010>.
467. Rasmussen K, Reilly C, Li Y, Jones RS. 2016. Real-time imaging of anti-biofilm effects using CP-OCT. *Biotechnol Bioeng* 113:198–205. <https://doi.org/10.1002/bit.25701>.
468. Alvarez-Fraga L, Perez A, Rumbo-Feal S, Merino M, Vallejo JA, Ohneck EJ, Edelmann RE, Beceiro A, Vazquez-Ucha JC, Valle J, Actis LA, Bou G, Poza M. 2016. Analysis of the role of the LH92\_11085 gene of a biofilm hyper-producing *Acinetobacter baumannii* strain on biofilm formation and attachment to eukaryotic cells. *Virulence* 7:443–455. <https://doi.org/10.1080/21505594.2016.1145335>.
469. De Carlo S, Harris JR. 2011. Negative staining and cryo-negative staining of macromolecules and viruses for TEM. *Micron* 42:117–131. <https://doi.org/10.1016/j.micron.2010.06.003>.
470. Alhede M, Qvortrup K, Liebrechts R, Høiby N, Givskov M, Bjarnsholt T. 2012. Combination of microscopic techniques reveals a comprehensive visual impression of biofilm structure and composition. *FEMS Immunol Med Microbiol* 65:335–342. <https://doi.org/10.1111/j.1574-695X.2012.00956.x>.
471. Dufrene YF. 2003. Recent progress in the application of atomic force microscopy imaging and force spectroscopy to microbiology. *Curr Opin Microbiol* 6:317–323. [https://doi.org/10.1016/S1369-5274\(03\)00058-4](https://doi.org/10.1016/S1369-5274(03)00058-4).

472. Dynes JJ, Tylliszczak T, Araki T, Lawrence JR, Swerhone GD, Leppard GG, Hitchcock AP. 2006. Speciation and quantitative mapping of metal species in microbial biofilms using scanning transmission X-ray microscopy. *Environ Sci Technol* 40:1556–1565. <https://doi.org/10.1021/es0513638>.
473. Neu TR, Manz B, Volke F, Dynes JJ, Hitchcock AP, Lawrence JR. 2010. Advanced imaging techniques for assessment of structure, composition and function in biofilm systems. *FEMS Microbiol Ecol* 72:1–21. <https://doi.org/10.1111/j.1574-6941.2010.00837.x>.
474. Chatterjee S, Biswas N, Datta A, Dey R, Maiti P. 2014. Atomic force microscopy in biofilm study. *Microscopy* 63:269–278. <https://doi.org/10.1093/jmicro/dfu013>.
475. Jonas K, Tomenius H, Kader A, Normark S, Romling U, Belova LM, Melefors O. 2007. Roles of curli, cellulose and BapA in Salmonella biofilm morphology studied by atomic force microscopy. *BMC Microbiol* 7:70. <https://doi.org/10.1186/1471-2180-7-70>.
476. Zeng G, Vad BS, Dueholm MS, Christiansen G, Nilsson M, Tolker-Nielsen T, Nielsen PH, Meyer RL, Otzen DE. 2015. Functional bacterial amyloid increases *Pseudomonas* biofilm hydrophobicity and stiffness. *Front Microbiol* 6:1099. <https://doi.org/10.3389/fmicb.2015.01099>.
477. Masyuko RN, Lanni EJ, Driscoll CM, Shrout JD, Sweedler JV, Bohn PW. 2014. Spatial organization of *Pseudomonas aeruginosa* biofilms probed by combined matrix-assisted laser desorption ionization mass spectrometry and confocal Raman microscopy. *Analyst* 139:5700–5708. <https://doi.org/10.1039/C4AN00435C>.
478. Javanbakht T, Laurent S, Stanicki D, Wilkinson KJ. 2016. Relating the surface properties of superparamagnetic iron oxide nanoparticles (SPIONs) to their bactericidal effect towards a biofilm of *Streptococcus mutans*. *PLoS One* 11:e0154445. <https://doi.org/10.1371/journal.pone.0154445>.
479. Arciola CR, Campoccia D, Montanaro L. 2002. Detection of biofilm-forming strains of *Staphylococcus epidermidis* and *S. aureus*. *Expert Rev Mol Diagn* 2:478–484. <https://doi.org/10.1586/14737159.2.5.478>.
480. Mirzaee M, Najar-Peerayeh S, Behmanesh M, Moghadam MF. 2015. Relationship between adhesion genes and biofilm formation in vancomycin-intermediate *Staphylococcus aureus* clinical isolates. *Curr Microbiol* 70:665–670. <https://doi.org/10.1007/s00284-014-0771-9>.
481. Zuniga E, Melville PA, Saidenberg AB, Laes MA, Gonsales FF, Salaberry SR, Gregori F, Brandao PE, dos Santos FG, Lincopan NE, Benites NR. 2015. Occurrence of genes coding for MSCRAMM and biofilm-associated protein Bap in *Staphylococcus* spp. isolated from bovine subclinical mastitis and relationship with somatic cell counts. *Microb Pathog* 89:1–6. <https://doi.org/10.1016/j.micpath.2015.08.014>.
482. Heikens E, Bonten MJ, Willems RJ. 2007. Enterococcal surface protein Esp is important for biofilm formation of *Enterococcus faecium* E1162. *J Bacteriol* 189:8233–8240. <https://doi.org/10.1128/JB.01205-07>.
483. Lopez-Salas P, Llaca-Díaz J, Morfin-Otero R, Tinoco JC, Rodriguez-Noriega E, Salcido-Gutierrez L, Gonzalez GM, Mendoza-Olazarán S, Garza-Gonzalez E. 2013. Virulence and antibiotic resistance of *Enterococcus faecalis* clinical isolates recovered from three states of Mexico. Detection of linezolid resistance. *Arch Med Res* 44:422–428. <https://doi.org/10.1016/j.arcmed.2013.07.003>.
484. Almoahamad S, Somarajan SR, Singh KV, Nallapareddy SR, Murray BE. 2014. Influence of isolate origin and presence of various genes on biofilm formation by *Enterococcus faecium*. *FEMS Microbiol Lett* 353:151–156. <https://doi.org/10.1111/1574-6968.12418>.
485. Fattahi S, Kafil HS, Nahai MR, Asgharzadeh M, Nori R, Aghazadeh M. 2015. Relationship of biofilm formation and different virulence genes in uropathogenic *Escherichia coli* isolates from Northwest Iran. *GMS Hyg Infect Control* 10:Doc11. <https://doi.org/10.3205/dgkh000254>.
486. Seixas R, Machado J, Bernardo F, Vilela C, Oliveira M. 2014. Biofilm formation by *Salmonella enterica* serovar 1,4,[5],12:i:- Portuguese isolates: a phenotypic, genotypic, and socio-geographic analysis. *Curr Microbiol* 68:670–677. <https://doi.org/10.1007/s00284-014-0523-x>.
487. Dong H, Peng D, Jiao X, Zhang X, Geng S, Liu X. 2011. Roles of the *spiA* gene from *Salmonella enteritidis* in biofilm formation and virulence. *Microbiology* 157:1798–1805. <https://doi.org/10.1099/mic.0.046185-0>.
488. Rao RS, Karthika RU, Singh SP, Shashikala P, Kanungo R, Jayachandran S, Prashanth K. 2008. Correlation between biofilm production and multiple drug resistance in imipenem resistant clinical isolates of *Acinetobacter baumannii*. *Indian J Med Microbiol* 26:333–337. <https://doi.org/10.4103/0255-0857.43566>.
489. Badmasti F, Siadat SD, Bouzari S, Ajdari S, Shahcheraghi F. 2015. Molecular detection of genes related to biofilm formation in multidrug-resistant *Acinetobacter baumannii* isolated from clinical settings. *J Med Microbiol* 64:559–564. <https://doi.org/10.1099/jmm.0.000058>.
490. Jackson KD, Starkey M, Kremer S, Parsek MR, Wozniak DJ. 2004. Identification of *psl*, a locus encoding a potential exopolysaccharide that is essential for *Pseudomonas aeruginosa* PAO1 biofilm formation. *J Bacteriol* 186:4466–4475. <https://doi.org/10.1128/JB.186.14.4466-4475.2004>.
491. Cabrol S, Olliver A, Pier GB, Andremont A, Ruimy R. 2003. Transcription of quorum-sensing system genes in clinical and environmental isolates of *Pseudomonas aeruginosa*. *J Bacteriol* 185:7222–7230. <https://doi.org/10.1128/JB.185.24.7222-7230.2003>.
492. Hemati S, Azizi-Jalilian F, Pakzad I, Taherikalani M, Maleki A, Karimi S, Monjezei A, Mahdavi Z, Fadavi MR, Sayehmiri K, Sadeghifard N. 2014. The correlation between the presence of quorum sensing, toxin-antitoxin system genes and MIC values with ability of biofilm formation in clinical isolates of *Pseudomonas aeruginosa*. *Iran J Microbiol* 6:133–139.
493. Alcantar-Curiel MD, Blackburn D, Saldana Z, Gayosso-Vazquez C, Iovine NM, De la Cruz MA, Giron JA. 2013. Multi-functional analysis of *Klebsiella pneumoniae* fimbrial types in adherence and biofilm formation. *Virulence* 4:129–138. <https://doi.org/10.4161/viru.22974>.
494. Vidiava NA, Eroshenko GA, Kukleva LM, Shavina N, Kuznetsov OS, Kutyrev VV. 2010. The biofilm formation in *Yersinia pestis* strains isolated in Astrakhan region. *Zh Mikrobiol Epidemiol Immunobiol* 2010:3–7. (In Russian.)
495. Oggioni MR, Trappetti C, Kadioglu A, Cassone M, Iannelli F, Ricci S, Andrew PW, Pozzi G. 2006. Switch from planktonic to sessile life: a major event in pneumococcal pathogenesis. *Mol Microbiol* 61:1196–1210. <https://doi.org/10.1111/j.1365-2958.2006.05310.x>.
496. Shemesh M, Tam A, Steinberg D. 2007. Differential gene expression profiling of *Streptococcus mutans* cultured under biofilm and planktonic conditions. *Microbiology* 153:1307–1317. <https://doi.org/10.1099/mic.0.2006/002030-0>.
497. Xiang J, Sun Z, Song F, Huan JN. 2011. Expressions of *pgaABC* gene clusters and changes in biofilm phenotype of *Acinetobacter baumannii* in burn patients. *Zhonghua Shao Shang Za Zhi* 27:100–103.
498. Sun YC, Guo XP, Hinnebusch BJ, Darby C. 2012. The *Yersinia pestis* Rcs phosphorelay inhibits biofilm formation by repressing transcription of the diguanylate cyclase gene *hmsT*. *J Bacteriol* 194:2020–2026. <https://doi.org/10.1128/JB.06243-11>.
499. Ji Y, Li W, Zhang Y, Chen L, Zhang Y, Zheng X, Huang X, Ni B. 2017. QseB mediates biofilm formation and invasion in *Salmonella enterica* serovar Typhi. *Microb Pathog* 104:6–11. <https://doi.org/10.1016/j.micpath.2017.01.010>.
500. Mastronardi CC, Ramirez-Arcos S. 2007. Quantitative PCR for detection and discrimination of the bloodborne pathogen *Staphylococcus epidermidis* in platelet preparations using *divIVA* and *icaA* as target genes. *Can J Microbiol* 53:1222–1231. <https://doi.org/10.1139/w07-091>.
501. Frebourg NB, Lefebvre S, Baert S, Lemeland JF. 2000. PCR-based assay for discrimination between invasive and contaminating *Staphylococcus epidermidis* strains. *J Clin Microbiol* 38:877–880.
502. Cha JO, Yoo JI, Yoo JS, Chung HS, Park SH, Kim HS, Lee YS, Chung GT. 2013. Investigation of biofilm formation and its association with the molecular and clinical characteristics of methicillin-resistant *Staphylococcus aureus*. *Osong Public Health Res Perspect* 4:225–232. <https://doi.org/10.1016/j.phrp.2013.09.001>.
503. Thomas VC, Thurlow LR, Boyle D, Hancock LE. 2008. Regulation of autolysis-dependent extracellular DNA release by *Enterococcus faecalis* extracellular proteases influences biofilm development. *J Bacteriol* 190:5690–5698. <https://doi.org/10.1128/JB.00314-08>.
504. Wu Y, Wang J, Xu T, Liu J, Yu W, Lou Q, Zhu T, He N, Ben H, Hu J, Gotz F, Qu D. 2012. The two-component signal transduction system *ArlRS* regulates *Staphylococcus epidermidis* biofilm formation in an *ica*-dependent manner. *PLoS One* 7:e40041. <https://doi.org/10.1371/journal.pone.0040041>.
505. Atshan SS, Shamsudin MN, Karunanidhi A, van Belkum A, Lung LT, Sekawi Z, Nathan JJ, Ling KH, Seng JS, Ali AM, Abduljaleel SA, Hamat RA. 2013. Quantitative PCR analysis of genes expressed during biofilm development of methicillin resistant *Staphylococcus aureus* (MRSA). *Infect Genet Evol* 18:106–112. <https://doi.org/10.1016/j.meegid.2013.05.002>.
506. Lazenby JJ, Griffin PE, Kyd J, Whitchurch CB, Cooley MA. 2013. A quadruple knockout of *lasIR* and *rhlIR* of *Pseudomonas aeruginosa*

PAO1 that retains wild-type twitching motility has equivalent infectivity and persistence to PAO1 in a mouse model of lung infection. *PLoS One* 8:e60973. <https://doi.org/10.1371/journal.pone.0060973>.  
507. Mangwani N, Kumari S, Das S. 2015. Involvement of quorum sensing

genes in biofilm development and degradation of polycyclic aromatic hydrocarbons by a marine bacterium *Pseudomonas aeruginosa* N6P6. *Appl Microbiol Biotechnol* 99:10283–10297. <https://doi.org/10.1007/s00253-015-6868-7>.

**Maria Magana, R.N., M.Sc.**, graduated from her R.N. program (2013) and received her master's degree (2016) from the Department of Nursing at the University of Peloponnese. Currently, she is a Ph.D. student at the Medical School of Athens University, studying drug design in the era of antimicrobial resistance. Since 2010, she has received scholarships for her undergraduate, postgraduate, and doctoral studies from the State Scholarships Foundation, the Lilian Voudouri Greek Public Benefit Foundation, and the General Secretariat for Research and Technology (GSRT)-Hellenic Foundation for Research and Innovation (HFRI), respectively. During her undergraduate studies (2009 to 2013), she trained in the Basic Sciences Laboratory of the Department of Nursing and actively participated in research programs in the field of molecular biology. Since 2013, she has been a scientific collaborator in the Microbiology Laboratory of Aeginition Hospital, and she recently entered the area of publications in peer-reviewed journals, with 10 articles regarding host-pathogen interactions, alternative therapeutic options against multidrug-resistant staphylococcal infections, and the role of nanomaterials in diverse applications over conventional therapeutic approaches. Her broad research interests focus on bacteriology, with special emphasis on antimicrobial resistance mechanisms, therapeutic repurposing of nonantibiotic compounds, and understanding natural compound antimicrobial identities.



**Christina Sereti, M.D.**, graduated from the Medical School of Ioannina in 2008 and in 2016 finished her residency in the Medical Biopathology Department of Thriassio General Hospital, Athens, Greece. During her residency, she trained in the topics of hematology, microbiology, biochemistry, and internal medicine. She works as a specialized biopathologist doctor in the Blood Donation Department of Thriassio General Hospital. For the last 2 years, she has been a Ph.D. student in the Microbiology Department of Aeginition Hospital of Athens, studying the bacterial biofilm mode of growth and its relevance to chronic infections. She has been a member of the Hellenic Microbiology Society for the last 6 years.



**Anastasios Ioannidis, B.Sc., M.D., Ph.D.**, is Assistant Professor of Microbiology in the Department of Nursing, University of Peloponnese, and a medical biopathologist. He graduated from the Department of Biology (1997) and the Medical School (2007) of the University of Athens. His Ph.D. thesis referred to the molecular epidemiology of *Campylobacter jejuni*. His fields of interest include genetic association and gene expression studies, recombinant DNA technology, microbial biofilms, microbial virulence, and seroepidemiology. His scientific activity includes 46 publications in peer-reviewed international journals, and he is a reviewer for 8 peer-reviewed scientific journals. He cooperated in the following three research projects: (i) "Genetic Epidemiology of the Metabolic Syndrome" (Greek Ministry of Health), (ii) "PYTHAGORAS II: Development of a Database with Genotypic and Phenotypic Characteristics of Clinical Isolates of *Campylobacter jejuni* Strains from Greece," and (iii) "IRAKLEITOS: Molecular Epidemiology of *Campylobacter jejuni* Strains from Clinical Isolates."



**Courtney A. Mitchell, Ph.D.**, graduated from Hampton University with a B.S. in chemical engineering in 2011 and from Vanderbilt University with a Ph.D. in chemical and biomolecular engineering in 2016. She serves as a resident engineer in the lab of Maria Hadjifrangiskou in the Pathology, Microbiology, and Immunology Department at Vanderbilt University. Her research focuses on using phototherapy as an antibacterial treatment, including methods to prevent biofilm formation implicated in the pathogenic cascade of uropathogenic *Escherichia coli*. Specifically, her work investigates the mechanisms of blue light irradiation-induced growth reduction of pathogenic *E. coli*.



**Anthony R. Ball, B.Sc., NRCM**, holds bachelor of sciences and graduate research degrees from Northeastern University, where he trained as a molecular microbiologist at the Antimicrobial Discovery Center under supervisor Kim Lewis. His research and scientific interests focus on multidrug efflux systems and nontraditional discovery strategies, including prodrugs, anti-infectives, dual-action antimicrobials, and photodynamic inactivation of microorganisms. He is currently a Chief Scientific Officer at GAMA Therapeutics LLC and a Study Director at Toxikon Inc. (Bedford, MA), a preclinical bioanalytical research organization. He was the founder of Gliese 623b, LLC (Mendon, MA), a consulting firm providing product development support and biocompatibility/safety validation services in the areas of medical devices, material manufacture, and molecular drugs and discovery. He has published 6 peer-reviewed articles, 1 book chapter, and 2 conference proceedings and serves as a reviewer for *Photochemistry and Photobiology*.





**Emmanouil Magiorkinis**, M.D., Ph.D., B.Sc., Path. (CCT), is a specialized medical biopathologist. He studied medicine and biology at Athens University and holds a Ph.D. in microbiology (molecular virology) from the Athens University Medical School. He currently works as a specialist at the Metaxas Memorial Anticancer Hospital in Piraeus, Greece, in the Department of Clinical Microbiology, and he is a postdoctoral research associate at Athens University Medical School, in the Department of Hygiene, Epidemiology and Medical Statistics. His current interests focus on molecular microbiology and virology, an exciting and rapidly evolving research field, and especially on microbial genomics. He has been actively involved in research since 1997, having published 84 articles in peer-reviewed international scientific journals, with over 1,200 citations.



**Stylianos Chatzipanagiotou**, M.D., Ph.D., is Associate Professor of Microbiology in the Social Medicine Sector, Psychiatry and Neurology, of Athens Medical School and a medical biopathologist-clinical microbiologist in the Microbiology Laboratory of Aeginition Hospital. He is a member of the Secretary Board of the Hellenic Society for Microbiology and a Greek Delegate in the European Union of Medical Specialists-UEMS Section of Medical Biopathology/Laboratory Medicine. His 25 years of teaching experience includes teaching medical students and residents in medical and clinical microbiology, hygiene and public health, immunology, and medical biochemistry. Dr. Chatzipanagiotou's special fields of interest include clinical microbiology and travel medicine. His scientific activity includes more than 79 publications in peer-reviewed international journals and other scientific journals, and he is a reviewer for 5 scientific journals.



**Michael R. Hamblin**, Ph.D., is a Principal Investigator at the Wellman Center for Photomedicine at Massachusetts General Hospital, an Associate Professor of Dermatology at Harvard Medical School, and a member of the affiliated faculty of the Harvard-MIT Division of Health Science and Technology. He was trained as a synthetic organic chemist and received his Ph.D. from Trent University in England. His research interests lie in the areas of photodynamic therapy (PDT) for infections, cancer, and heart disease and in low-level light therapy (LLLT) for wound healing, arthritis, traumatic brain injury, and hair regrowth. His research program is supported by the NIH, CDMRP, and CIMIT, among other funding agencies. He has published 158 peer-reviewed articles, over 150 conference proceedings, book chapters, and international abstracts and holds 8 patents. He is Associate Editor for 3 journals and serves on NIH Study Sections. For the past 7 years, Dr. Hamblin has chaired an annual conference at SPIE Photonics West, entitled "Mechanisms for Low-Level Light Therapy," and he has coedited the six proceedings volumes together with two other textbooks.



**Maria Hadjifrangiskou**, Ph.D., is Assistant Professor in the Department of Pathology, Microbiology and Immunology at the Vanderbilt University School of Medicine. She obtained her B.Sc. in molecular biology and biotechnology from Clarion University, PA, and her Ph.D. in microbiology and molecular genetics from the University of Texas Health Science Center and the M. D. Anderson Cancer Center, Houston, TX, and she performed her postdoctoral training at the Washington University School of Medicine in St. Louis, MO. Dr. Hadjifrangiskou is the author of 22 publications in peer-reviewed journals, mainly on uropathogenic *Escherichia coli* (UPEC) forming biofilm-like intracellular bacterial communities (IBCs). Her lab is interested in identifying factors and mechanisms that regulate UPEC biofilm formation and that may serve as new drug targets and in understanding the mechanism by which rationally designed small molecules act against UPEC pathogenesis.



**George P. Tegos**, Ph.D., is a Research Director at GAMA Therapeutics LLC. He received his Ph.D. from the University of Ioannina, Greece. He was a Director at Gliese LLC, a Visiting Scientist at the Wellman Center for Photomedicine at Massachusetts General Hospital, Harvard Medical School (2010 to 2016), an Instructor of Medicine at Harvard Medical School (2006 to 2009), and Assistant Professor (Research) at the Department of Pathology School of Medicine at the University of New Mexico (2010 to 2014). His research interests focus on drug discovery, with an emphasis on multidrug efflux systems, photodynamic therapy, and localized infections, and he has published over 75 peer-reviewed articles. His research program has been supported by the National Institutes of Health and the Department of Defense (DOD-DTRA). He has been an EU Marie Curie fellow in biotechnology and a recipient of the Massachusetts Technology Transfer Center award in antimicrobials. Dr. Tegos served on the editorial board of *Photochemistry and Photobiology* and as a guest editor for *Current Opinion in Pharmacology* and *Frontiers in Pharmacology*.

